

**DOCTORAL THESIS**

**Development of Sensing Probes of Peptide Aptamers**

**by Incorporation of Non-Natural Amino Acids**

**K.C. Tara Bahadur**

**Department of Biological Sciences**

**Tokyo Metropolitan University**

**2018**

# TABLE OF CONTENTS

ABSTRACT.....	4
List of Abbreviations.....	6
CHAPTER 1: GENERAL INTRODUCTION.....	8
1. INTRODUCTION.....	9
2. APTAMER SELECTION.....	12
2.1 Phage Display.....	15
2.2 Ribosome Display.....	16
3. APPLICATIONS OF APTAMERS.....	21
3.1 Diagnosis Application.....	22
3.2 Therapeutic Application.....	24
3.3 Other Applications.....	27
4. REFERENCES.....	28
CHAPTER 2: WASH-FREE AND SELECTIVE IMAGING OF EPITHELIAL CELL ADHESION MOLECULE (EPCAM) EXPRESSING CELLS WITH FLUOROGENIC PEPTIDE LIGANDS.....	40
1. INTRODUCTION.....	41
2. MATERIALS AND METHODS.....	44
2.1 Chemical Synthesis.....	44
2.3 Solubility Test.....	47
2.4 Preparation of Cells for Imaging.....	47
2.5 Image Analysis to Obtain Fluorescence Intensity.....	48
3. RESULTS AND DISCUSSION.....	50
3.1 Fluorogenic Functionalization of an EpCAM-Binding Peptide.....	50
3.2 Solubility.....	51
3.3 Cell Imaging and Image Analysis to Obtain Fluorescence Intensity.....	52
4. CONCLUSION.....	55
5. REFERENCES.....	56
CHAPTER 3: IN VITRO SELECTION OF ELECTROCHEMICAL PEPTIDE PROBES USING BIOORTHOGONAL tRNA FOR INFLUENZA VIRUS DETECTION.....	60
1. INTRODUCTION.....	60
2. MATERIALS AND METHODS.....	63
2.1 Synthesis of EDOT-Aminophenylalanyl-tRNA.....	63
2.2 <i>In Vitro</i> Selection of an Electrosensitive Peptide Ligand.....	64
2.3 Preparation of EDOT Aminophenylalanine.....	67

2.3 Synthesis and Purification of Peptide Sequences. ....	70
2.4 Evaluation of Peptide Binding Affinity.....	71
2.5 Biological Specificity.....	72
2.6 Electropolymerization of EDOT-Conjugated Peptide Ligand.....	72
2.7 Electrochemical Detection of Influenza Virus.....	75
2.8 Interference of Microorganism on Electrochemical Detection System.....	76
3. RESULTS AND DISCUSSION.....	76
3.1 Selection of Electrosensitive Peptides.....	76
3.2 Affinity and Selectivity Analysis.....	78
3.3 Electrochemical Analysis.....	81
4. CONCLUSION.....	90
5. REFERENCES.....	91
CHAPTER 4: CONCLUSION.....	97
CONCLUSION.....	98
ACKNOWLEDGMENTS.....	100
APPENDIX.....	102
LIST OF PUBLICATIONS.....	113

**Dedicated to my Father**

**Gopal Bahadur Kunwar**

## ABSTRACT

Aptamers are experimentally-selected oligonucleotides (RNA, ssDNA) or peptide ligands that bind to specific target molecules. Although the primary function of aptamers is specific binding to targets, the incorporation of functional compounds in the aptamers can advance their functions for various applications. In this thesis, I tried to prepare two types of aptamer-based sensing probe by incorporation of functional compounds: a fluorogenic probe by modification of a previously selected aptamer with an environmental sensitive dye conjugated amino acid and an electrochemically sensing probe by selecting such aptamer from a peptide library containing electrochemically active amino acid.

As the first project, I aimed to prepare a fluorogenic probe. Specifically, I modified a previously selected peptide aptamer (Ep114) for a marker of circulating tumor cell (CTC), epithelial cell adhesion molecule (EpCAM), with an environment sensitive dye, 7-nitro-2,1,3-benzoxadiazole (NBD) coupled aminophenylalanine. For the modification of some amino acids in the aptamer with NBD-coupled aminophenylalanine one-by-one, I chose the less important amino acids in the aptamer to bind to the EpCAM. Among the six synthesized peptides, I have found that two peptides retained the Ep114's binding ability and specifically marked EpCAM-expressing cells by just adding these peptides to the cultivation medium. These wash-free, fluorogenic peptide ligands could be useful to capture CTCs without damage to the cell viability which is difficult from the current cell search technique. Thus, I believe that the technique boosts the development of the next-generation devices for CTC diagnoses.

In the second project, I aimed to construct an electrochemical detection system for influenza virus by employing electro-polymerization properties of 3,4-

ethylenedioxythiophene (EDOT). Here, the peptide aptamers were directly selected from the random sequence of a peptide library containing EDOT-coupled aminophenylalanine using the ribosomal display method. After six rounds of selection, sequences were analyzed using next-generation sequencing. The three highest frequency sequences were prepared using solid phase peptide synthesis method. I found that one of the peptides bound to the virus with a moderate affinity ( $EC_{50} = 9.6 \pm 2.3 \mu M$ ) and effective selectivity. As I expected, the aptamer, in the absence of virus was electrochemically polymerized via EDOT, although the polymerization was suppressed in the presence of virus presumably due to hindrance by the virus. As a result, the polymerized material deposited on the working electrode reduces the electric current with the decrease of virus concentration. The detection limit of this system was  $12.5 \mu g mL^{-1}$  ( $P < 0.05$ ) of the virus, which is comparable to the sensitivity of immunochromatography. This work represents the first example of the *in vitro* selection of an electro-sensitive peptide aptamer for the development of electrochemical biosensors.

## List of Abbreviations

BSA	Bovine serum albumin
CatE	Cathepsin E
CFU	Colony-forming unit
CTC	Circulating tumor cell
CV	Cyclic voltammetry
DNA	Deoxyribonucleic acid
EDOT	3,4-Ethylenedioxythiophene
ELISA	Enzyme-linked immunosorbent assay
EpCAM	Epithelial cell adhesion molecule
FT-IR	Fourier transform infrared
HER2	Human epidermal growth factor receptor 2
IDP	Intrinsically disordered proteins
LOD	Limit of detection
mRNA	Messenger ribonucleic acid
NBD	7-Nitro-2,1,3-benzoxadiazole
NBDaa	NBD labeled aminophenylalanine
NGS	Next generation sequencing
NMP	N-Methyl-2-pyrrolidone
PCR	Polymerase chain reaction
pdCpA	5'-O-phosphoryl-2'-deoxycytidylyl-(3'-5') adenosine
PDGF	Platelet-derived growth factor
PRM	Peptide-ribosome-mRNA
PVDF	Polyvinylidene fluoride
RBS	Ribosome binding site

Rmp	Rotation per minute
r.t.	Room temperature
RT-PCR	Reverse transcription polymerase chain reaction
SD	Shine-Dalgarno
SELEX	Systematic evolution of ligands by exponential enrichment
ssDNA	Single strand Deoxyribonucleic acid
tRNA	Transfer ribonucleic acid
USFDA	United State Food and Drug Administration
VEGF	Vascular endothelial growth factor

# **CHAPTER 1: GENERAL INTRODUCTION**

## 1. INTRODUCTION

The concept of aptamer started in 1990 when two prominent studies reported the generation of high-affinity molecules against respective targets using an *in vitro* selection method. Tuerk and Gold selected ribonucleic acid (RNA) ligands against T4 deoxyribonucleic acid (DNA) polymerase and introduced the term “Systematic Evolution of Ligands by Exponential Enrichment” (SELEX).<sup>1</sup> Similarly, Ellington and Szostak selected an RNA aptamer that binds to small organic dye and coined the term “aptamer” which was derived from the Latin word “aptus” (fit) and Greek word “meros” (part).<sup>2-4</sup> Since then, short RNA or single-stranded DNA (ssDNA) molecules selected against a specific target have been termed “nucleic acid aptamers”.<sup>5</sup> Six years later, Colas et al.<sup>6</sup> reported the construction of artificial combinatorial proteins that bind to human cyclin dependent kinase 2, and he defined the molecule as "peptide aptamers." Following his definition, peptide aptamers are combinatorial protein molecules in which a variable peptide sequence with the affinity for a given target protein is displayed on an inert, constant scaffold protein.<sup>4,6-9</sup> Now, aptamers are small oligonucleotides (RNA or ssDNA) of 20 - 100 residual or peptides of 8 - 20 amino acid residues that can bind to their respective targets with high affinity and specificity.<sup>10</sup>

Since the development of aptamer, they have gotten attention as a valuable substitute for antibodies in various applications such as medical diagnosis, therapeutic agents, and other basic researches<sup>10,11</sup>, because there are some limitations for the production and application of antibodies. For example, antibodies are produced biologically, it is difficult to scale up their production, quality control, chemically ligation with functional molecules and store them for long time in a shelf.<sup>12</sup> On the other hand, aptamers have much wider freedom than antibodies; for example, aptamers are selected and developed using *in vitro* system. Besides that, aptamers possess high specificity comparable to antibodies. For example, RNA aptamers selected against theophylline exhibited a >10,000-fold discrimination against caffeine, which

differs just by a methyl group<sup>13</sup>, and similarly, an anti-L-arginine RNA aptamer exhibited a 12,000-fold affinity for L-arginine than D-arginine<sup>14</sup> (Figure 1-1).

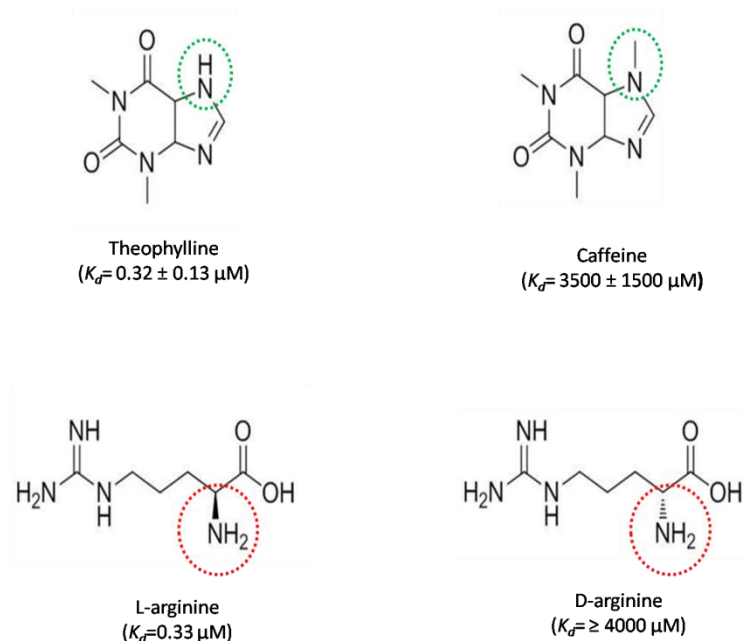


**Figure 1-1.** RNA aptamers affinity and selectivity against small molecules

In addition to the affinity and selectivity, aptamers have following advantages.<sup>10, 12</sup>

- Aptamers can be easily synthesized in a scalable process and no lot-to-lot variability.
- The production process is not prone to viral or bacterial contamination.
- Aptamers are small in size, and it is expected that they efficiently enter into biological compartments.
- Aptamers can be selected against any targets (including targets which cannot be used for immunization due to toxicity or less amount).
- Because aptamers are chemically stable, they can be easily modified with compounds including dyes or functional groups.
- Aptamers are low-immunogenic, low-toxic and they often exhibit good stability.

In this research, I developed two different kinds of aptamer-based biosensors for diagnostic applications. In the first approach (Chapter Two), I functionalized a previously selected peptide aptamer using an artificially prepared fluorogenic non-natural amino acid. The developed peptide biosensor exhibited an enhanced fluorescence in the presence of a target molecule (Figure 1-2)

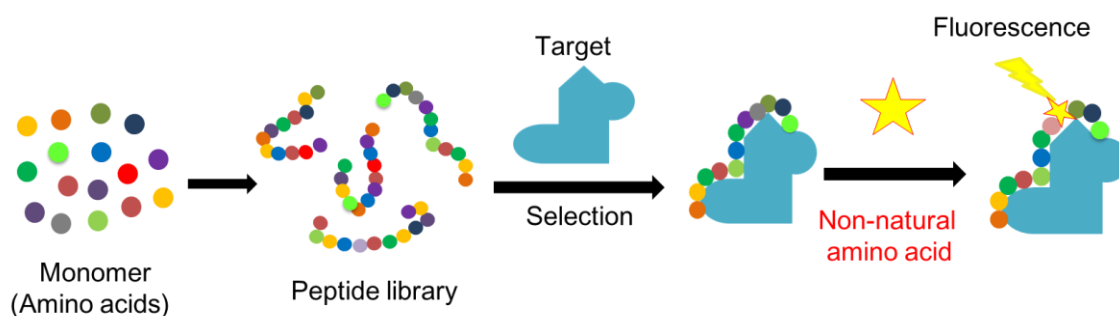


**Figure 1-2.** Functionalization of a peptide aptamer with functional amino acid

In the second approach (Chapter Three), I used a more advanced technique to develop peptide aptamer-based biosensor. Additionally, the modification of the selected aptamer with a signaling molecule sometimes leads to affinity loss with the target or weak signaling because of the hindrance to the target-recognizing domain or an unintended conformational change of the target-recognizing molecule. To realize an active role of the artificially introduced non-natural amino acid during peptide aptamers interaction, pre-incorporation of non-natural amino acid to the random peptide library was done. Specifically, a pool of random peptide library was prepared by using a bioorthogonal tRNA bearing functional non-natural amino acid, then the peptide aptamer containing functional non-natural amino acid was selected against the desired target molecule by *in vitro* selection method (Figure 1-3). Compared to post-selection modification, this selection method can exclude some peptide sequences, which have a weak affinity because of the functional molecule conjugation.

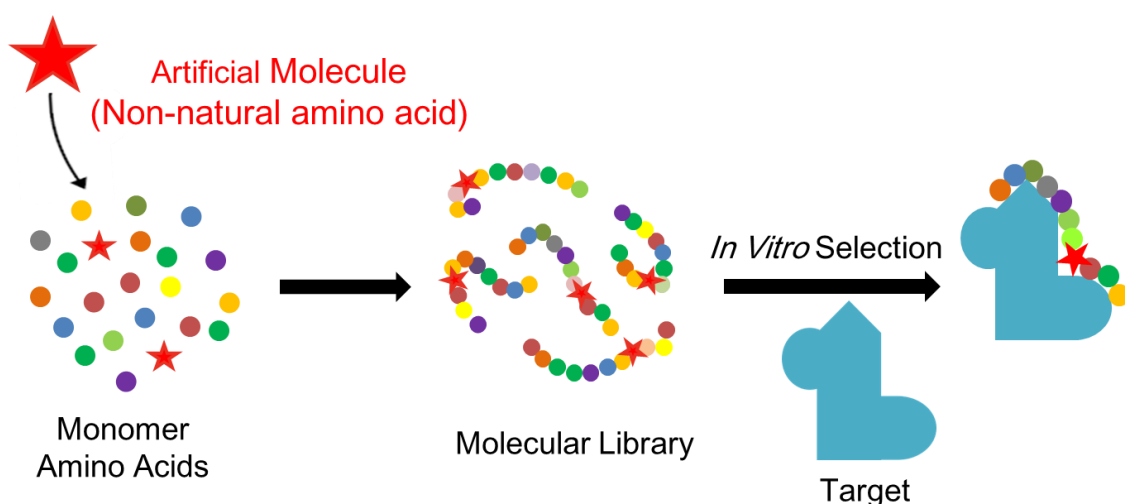


**Figure 1-3.** Incorporation of functional non-natural amino acids into randomized library prior to selection

## 2. APTAMER SELECTION

The basic principle of the aptamer selection is the use of combinatorial strategies to generate a pool of various candidates, run selection against a designated target, amplify the selected candidates, and repeat the selection process (Figure 1-4). The technique used for aptamer preparation merely resembles the Charles Darwin theory of natural selection, a key mechanism of the evolution described in "The Origin of Species" book.<sup>15</sup> So, the method can be simply compared with Darwin's selection process.

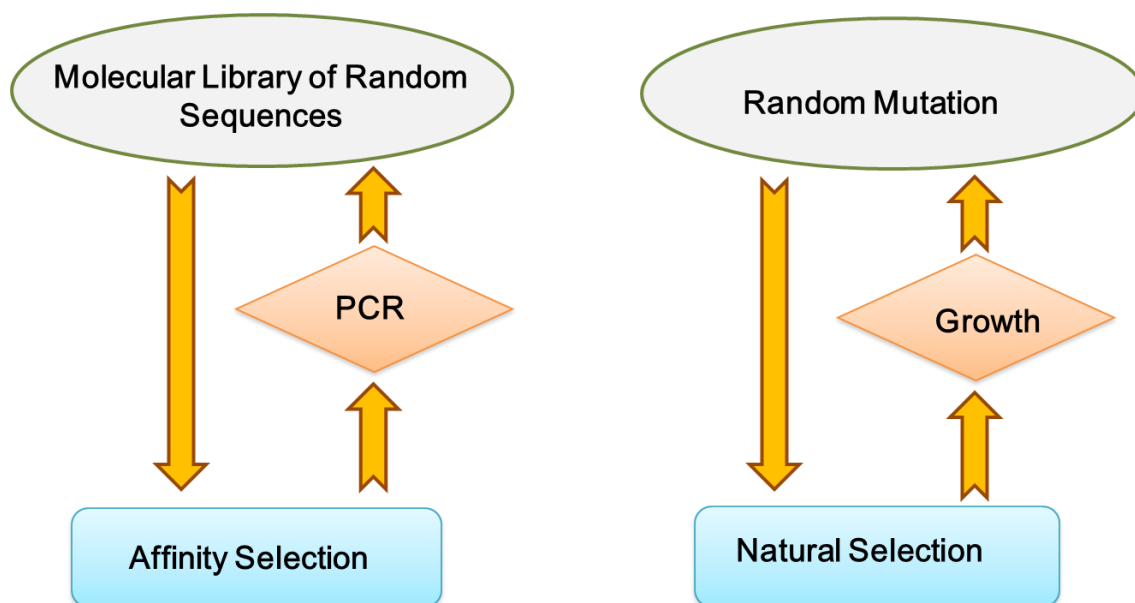


**Figure 1-4.** Comparison of *in vitro* aptamer selection with Darwinian evolution theory "natural selection."

However, from a specific technical point of view, the selection of aptamers is entirely different between the types of aptamers. For oligonucleotide aptamers, the selection process is carried out using SELEX technique. This is the most common technique because the wide range of targets (small molecules, proteins, viruses, bacteria, live cells, and even tissues) can be used directly for the selection.<sup>16,17</sup> The first step of the SELEX method is the preparation of a random sequence of oligonucleotides by synthesis. The primary libraries are prepared as single strand DNAs in length of 20-100 nucleotide.<sup>18</sup> The prepared libraries can be used directly for DNA aptamer selection. Whereas for RNA aptamer selection, single strand DNA libraries are transcribed to the libraries of RNA molecule, usually using T7 RNA polymerase by *in vitro* transcription system. For affinity selection, prepared libraries are exposed to the pre-immobilized target molecules. Washing removes unbound RNAs, and the bound RNAs are collected by elution. The collected RNAs are transcribed to cDNAs by reverse transcription and then perform polymerase chain reaction (PCR) to increase the copies of the

enriched sequences for the next round of the selection. Thus, the affinity-based selection is repeated to enrich desired DNA/RNA molecules.

For peptide aptamer selection, a prerequisite is the coupling of genotype (RNA, DNA) and phenotype (protein). A linkage between genotype and phenotype is essential for amplification of phenotypically selected combinatorial peptide molecules for enrichment as well to know the genetic information of the binding aptamer generated from the random library. The peptide aptamer selection can be run using either *in vivo* or *in vitro* display methods. In *in vivo* screening method, both target and ligand are produced in a living cell. The concept was originally introduced by Fields and Song, and an important feature of in cell selection is the lack of competition among the expressed peptide aptamers within a cell.<sup>19,20</sup>

The most common approach used for the selection of peptide aptamers is *in vitro* methods. In this approach, the selection of peptide aptamers carried out through the extracellular display technologies such as phage display<sup>21-23</sup>, yeast display<sup>24,25</sup>, bacterial surface display<sup>26</sup>, ribosome display<sup>27,28</sup>, mRNA display<sup>25,29-32</sup>, DNA display<sup>33-36</sup> and *in vitro* compartmentalization.<sup>37-40</sup> Because phage display, yeast display, bacterial surface displays are cell-based display technologies, their library sizes are limited due to the efficiency of DNA transformation into cells. Besides that, the toxicity of combinatorial library proteins to the host cells potentially a problem. This limitation is overcome in ribosomal display, mRNA display, DNA display and *in vitro* compartmentalization by employing a cell-free translation system. Although these display techniques can handle larger library than cell-based display techniques, these techniques have some concerns about the potential loss of peptide binders due to the expression of the peptide/protein outside of cell environment, which might lead to misfolding or post-translation modification. All these methods have their merit and demerits. Choice of a method depends on an individual objective, an employed target, and strategies going to apply for the peptide aptamers section. Here, I aimed to develop functional peptide

aptamers for diagnosis application. The desired peptide aptamers were selected by phage display in chapter two and ribosomal display method in chapter three.

## **2.1 Phage Display**

First-time phage display technique was used by Smith in 1985 to map epitope binding sites of immunoglobulins.<sup>41</sup> Now the phage display method is well established and widely used to develop peptide aptamers against the variety of targets including small molecules to large polymers, bacteria, cells, and even tissues.<sup>42-53</sup> In this technique, the random peptide libraries are fused with a bacteriophage coat protein and displayed on the surface of a virion. Then the displayed libraries are incubated with immobilized targets for affinity selection followed by extensive washing to remove nonbinding phages (Figure1-5). The peptide sequences bound to the target can be easily identified because the phages provide the physical link between phenotype (the displayed peptide) and genotype (the encoding DNA). Theoretically, one selection cycle would be enough to find the binding phages from the pool of phages.<sup>41,45</sup> But in practice, the selection is repeated several times to obtain aptamer candidates that exhibit higher affinity than the original library. Finally, peptide sequences that bind specifically to target molecules are identified by sequence analysis of individual clones.

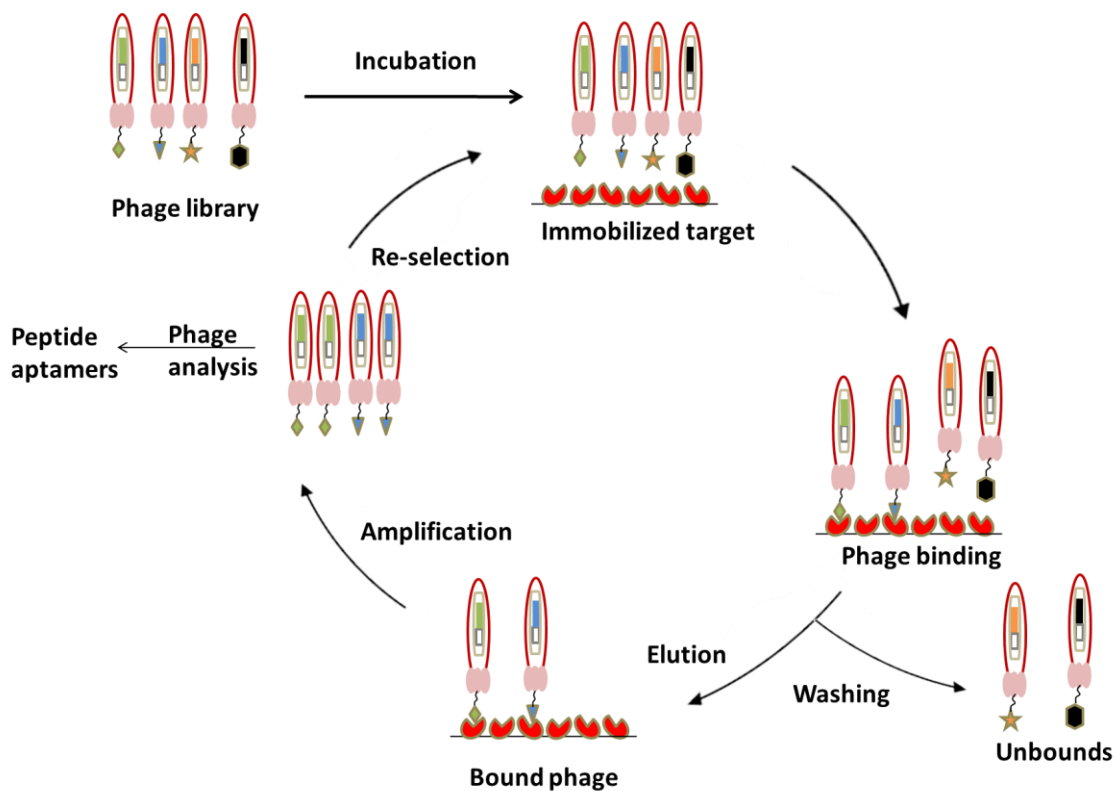


**Figure 1-5.** A schematic representation of the phage display technique

## 2.2 Ribosome Display

Ribosome display was introduced by Mattheakis et al. in 1994, and the method was subsequently adopted by Hanes and Pluckthun for selection of functional proteins.<sup>27, 28</sup> It has been widely used compared to other competing methods due to some advantages. Ribosomal display is performed entirely *in vitro* system. The diversity of the library is just limited by the number of ribosomes and mRNA molecules present in the system. Another important advantage of the ribosomal display is that random mutations can be introduced easily after each selection round, as no library must be transformed after any diversification step. These features made the ribosome display method an important technology to select high-affinity aptamers from diverse libraries of  $10^9$ - $10^{12}$  clones.<sup>54</sup> Thus, I choose ribosomal display technology to introduce a functional molecule into a peptide library prior to affinity selection.

The ribosomal complex is the place where translation process, conversion of the information in mRNA into protein occurred. A ribosome contains four binding sites: one for mRNA and other three for tRNA (the A- site, the P-site and the E-site). During protein biosynthesis, mRNA is translated from 5' to 3' direction, and the protein synthesis is initiated from N terminal, each new amino acid is added to the elongating protein in a repeating cycle having four major steps as shown in Figure 1-6.<sup>55</sup> Four step reaction cycles are repeated each time until to get the desired protein

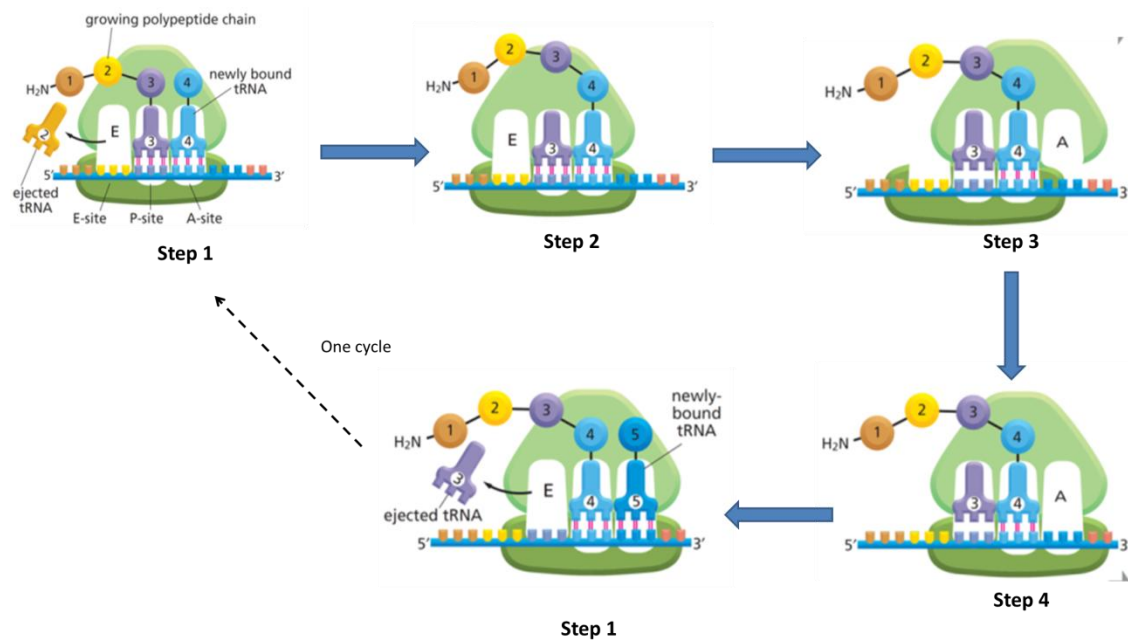


**Figure 1-6.** Translating an mRNA molecule into the ribosome. The protein synthesis process completed with four major steps. In step 1, tRNA carrying the next amino acid binds to a vacant, where the selection of the tRNA depends on the codon on mRNA in A site. In step 2, the most important reaction of the protein synthesis occurred; a new peptide bond is formed. The carboxyl end of the polypeptide chain is released from tRNA and joins to the free amino group of next amino acid linked to tRNA. In step 3, the large subunit of the ribosomal complex move towards the 3' of mRNA followed by the small subunit translocates carrying its

*mRNA distance of three nucleotides in step 4 to create an empty A site for the next aminoacyl-tRNA molecule to bind.*<sup>55</sup>

Finally, the release of the synthesized proteins from the ribosomal complex is signaled by the presence of stop codons on mRNA. A stop codon terminated the addition of further amino acids due to binding with release factor. The completed protein chain is immediately released (Figure 1-7)

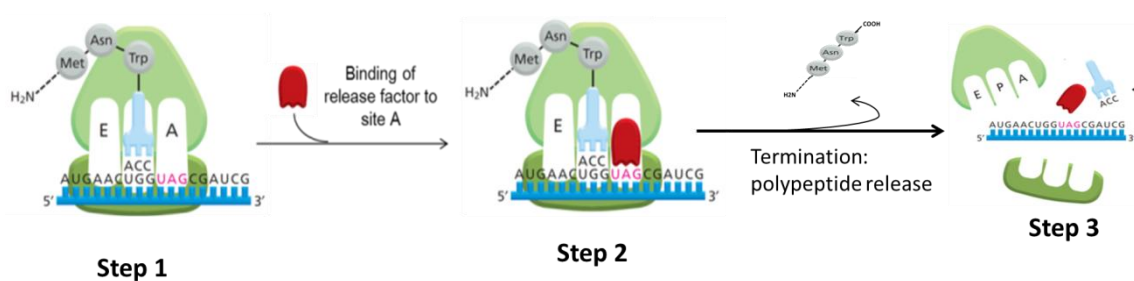


**Figure 1-7.** Termination of the polypeptide synthesis. Presence of stop codons are not recognized by tRNA, on A site of the ribosomal complex, a protein is known as release factor binds to stop codon. Where water molecule is added on the growing carboxylic end instead of next amino acyl-tRNA as a result terminated the addition of further amino acids.

But, the idea of the ribosome display accomplished with the formation of a stable ternary complex consisting of the ribosome, the mRNA and the correctly folded nascent polypeptide during *in vitro* translation. That can be archived by removing the stop codon on mRNA which prevents the release factor from binding and triggering the disassembly of the translation complex. As a result, mRNA stays physically attached to the ribosomal system with newly synthesized nascent protein. Thus the peptide libraries for the affinity selection are designed by removing the stop codon from the sequences (Figure 1- 8) to form a complex for affinity selection. The library sequence not only contains the randomized region but also

contains region like T7 promoter, ribosome binding site (RBS), a start codon (AUG), and spacer protein. T7 promoter that allows for mRNA synthesis, RBS base pair with ribosomal RNA and took the ribosome to the downstream start codon (AUG) where protein synthesis initiated. The translated protein of interest must be folded correctly into its three-dimensional structure to bind with the target molecule.<sup>56,57</sup> So the spacer protein facilitates the complete exit of display protein outside of the ribosome tunnel, a spacer protein required at least 23-30 amino acids length at C terminal to exit completely from the tunnel.<sup>58</sup> Ribosomal display construct should also contain 5' and 3' stem loops to stabilize the mRNA *in vivo* or *in vitro* system.



**Figure 1-8.** DNA construct for ribosomal display. (a) Construct for ribosomal display using *Escherichia coli* ribosomes (b) Construct for eukaryotic ribosome display. A translation initiation system may be Shine-Dalgarno sequence for *Escherichia coli* S30 extract or Kozak sequence for the eukaryotic system. This sequence is followed by open reading frame encoding the library of binding proteins followed by a spacer sequence fused in frame to the protein of interest

The basic principle of the ribosomal display selection method is shown in Figure 1-9. DNA constructs are converted to mRNA libraries by *in vitro* transcription. The obtained mRNAs are translated using a reconstructed cell-free translation system derived from typically *E. coli*, wheat germ or rabbit reticulocytes. Library sequences translations run to the end of mRNA due to the absence of stop codon. Ribosome itself serves as the connector to forms a ternary complex consists of the ribosome, translated peptide, and mRNA; additions of  $Mg^{2+}$  ions into the translation system stabilize the complex. These ternary complexes are incubated with surface-immobilized targets for affinity selection. The unbound complexes are washed away, mRNA of the complexes displaying binding polypeptides are recovered. Recovered mRNAs are purified and subjected to a reverse transcription-polymerase chain reaction for amplification into DNA library. These DNAs are subsequently employed in the next round of the selection process. The selection process is repeated to enrich the highest affinity sequences. On average, from 5 to 15 rounds of selection is sufficient to obtain high-affinity aptamers.

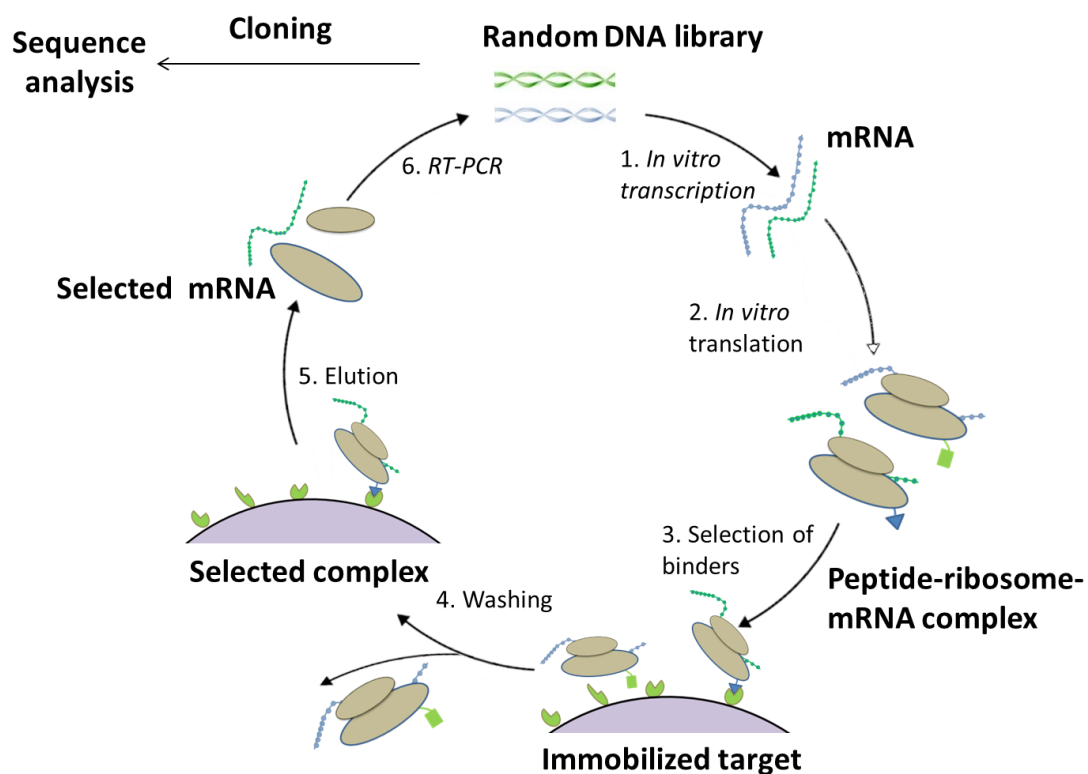


**Figure 1-9.** *In vitro* selection of functional peptide aptamer using ribosomal display technique.

### 3. APPLICATIONS OF APTAMERS

Aptamers are a strong and versatile alternative to antibodies due to that they are smaller in size, exhibit strong binding affinity and can be easily modified for conjugations and labeling features. Moreover, aptamers are low-immunogenic and low-toxic materials which made them potential molecules for medical applications, such as diagnosis and treatment of disease. The target molecules for aptamers are theoretically unlimited, and the selection techniques have become powerful with the novel technologies. Thus, the aptamers have a potential for a wider range of applications.

### 3.1 Diagnosis Application

Mono- and polyclonal antibodies have been used for the diagnosis of various diseases. After the advancement of aptamer development, antibodies are sometimes successfully replaced by aptamers, when highly selective and effective binding to a target is required.<sup>59, 60</sup> Some aptamer-based enzyme-linked immunosorbent assay (ELISA) and Western blotting type analysis also showed more sensitive and effective than antibodies.<sup>61-64</sup> Moreover, aptamers possess the advantages of easy chemical modification, which enables them to be applied for novel techniques, such as flowcytometry, microfluidic cell separation, endogenous nucleic acid analysis, fluorescence imaging, nanoparticles-based sensing, and electropolymerization, to maximize their diagnostic functions. The first aptamer used as a diagnostic tool was developed by Bruno et al.<sup>65</sup> in 1999 to detect anthrax spores. Now, aptamers have been widely applied for the diagnosis of cancer, viral infection, cardiac diseases, and ophthalmology. For example, Li et al. selected high-affinity aptamer against metastatic colon cancer cells and further modified the aptamer with fluorescence to image cancer tissues.<sup>66</sup> Lian et al. reported the aptamer-based sensor which can detect *S. aureus* rapidly and specifically within 60 minutes.<sup>67</sup> Parekh et al. selected aptamers against Vaccinia virus; the selected aptamer was highly specific towards virus-encoded hemagglutinin expressed on the surface of infected cells.<sup>68</sup> There are numerous aptamers selected recently to facilitate the detection of various diseases, and some representative aptamers are listed in Table 1-1.

*Table 1-1: Some examples of the aptamers selected for diagnosis applications.*

<b>Aptamers Name</b>	<b>Target</b>	<b>Application</b>	<b>References</b>
Myo040-7-27	Myoglobin	Diagnosis – cardiovascular disease	69

---

2008s	Plasmodium falciparum lactate dehydrogenase	Diagnosis – infectious	70
HeA2_1 /HeA2_3	Human epidermal growth factor receptor 2(HER2)	Diagnosis and therapy of HER2 positive breast cancer	71
XL-33	Metastatic colon cancer cells (SW620)	Diagnosis- metastatic cancer recognition and imaging	66
yl19	Cholangiocarcino ma cells (QBC- 939)	Diagnosis	72
XL-33	Metastatic colon cancer cells (SW620)	Diagnosis- cancer	66
LXL-1	Metastatic breast cancer cells (MDA-MB-231)	Diagnosis- cancer	73
SYL3-C	Epithelial Cell Adhesion Molecule (EpCAM)	Diagnosis- cancer cell imaging and capture	74
Myo040-7-27	Myoglobin	Diagnosis -cardiovascular diseases	69
n/d	Tat protein	Detection- HIV-1 virus	75

---

PP3	Hemagglutinin	Detection-vaccinia	68
PA-1 and PA-3	Intrinsically disordered proteins (IDPs)	To understand functional interactions or molecular mechanism	76
VT4	Verotoxin	Detection -verotoxin	77
n/d	Cathepsin E (CatE)	Detection of CatE in serum for cancer	78

The developed medical biosensor should be highly specific and extremely sensitive for proper recognition and efficient signal transduction. Thus, the aptamer seems to be a promising agent due to their smaller size which can be arranged with a higher density on the biosensor surface to develop portable and extremely sensitive kits.<sup>63,79</sup>

### 3.2 Therapeutic Application

One of the most promising applications is the therapeutic application due to their specificity to the designated target. In this approach, aptamers are developed for either a therapeutic agent or a carrier for drug delivery. The first aptamer drug was Macugen approved by U.S. Food and Drug Administration (USFDA) in 2004, an anti-vascular endothelial growth factor (VEGF) aptamer that recognizes the majority of human VEGF-A isoforms for the treatment of age-related macular degeneration and diabetic macular edema.<sup>80-82</sup> Macugen is the most successful example of aptamer-based therapeutics in both clinical application and commercial viability with the first annual sales exceeding 200 million U.S dollars. There are several aptamers based therapeutic agent that have undergone clinical trials<sup>83,84</sup> (Table 1-2).

**Table1-2: Clinical trial of therapeutic aptamers**

<b>Aptamer Name</b>	<b>Target</b>	<b>Medical Condition</b>	<b>Phase</b>
Pegaptanib	Vascular endothelial growth factor (VEGF)-165	Ischaemic diabetic macular oedema	Phase IV completed
E10030	Platelet-derived growth factor (PDGF)	Age-related macular degeneration	Phase III
REG1 (RB006 and RB007)	Coagulation factor IXa	Coronary artery disease	Phase III
ARC1905	C5 (Complement component 5)	Age-related macular degeneration	Phase III
ARC1779	A1 domain of von Willebrand factor	Von Willebranddisease thrombocytopenic/purpura	Phase II
NOX-E36 and NOX-A12	Chemokine C-C motif ligand 2 (CCL2)	Chronic inflammatory diseases/type 2 diabetes /systemic lupus erythematous	Phase II
NU172	Thrombin	Heart disease	Phase II
ARC19499	Tissue factor pathway inhibitor (TFPI)	Hemophilia	Phase I
EYE001	Protein encoded in exon 7 of VEGF gene	Wet age-related macular degeneration	Phase I
NOX-H94	Hepcidin	Anemia of chronic inflammation	Phase I

Besides the aptamers undergoing clinical trial, huge numbers of potential therapeutic aptamers have been reported in the literature. Some of them are anti-cancer agents. Dassie et al. reported an RNA aptamer against a prostate-specific membrane that inhibited the migration and invasion of prostate cancer cells *in vivo*.<sup>85</sup> Simmons et al. reported a DNA aptamer that specifically binds to and inhibits up regulated in certain tumors and an *in*

*in vitro* study aptamer inhibited invasion of carcinoma cells.<sup>86</sup> Soldevilla et al. reported an RNA aptamer specifically binding to CD40 and the aptamers could develop antitumor agent in future.<sup>87</sup> Kotula et al. reported an RNA aptamer that binds to  $\beta$ -arrestin 2 and the aptamer might be useful against leukemia treatment.<sup>88</sup> Similarly, other examples of aptamers for various therapeutic activities were reported. Prodeus et al. reported DNA aptamer exhibiting immunosuppressive activity and may be useful for aiding transplantation of organ and tissue.<sup>89</sup> Ojima et al. developed a DNA aptamer useful in treating vascular injury by reducing PDGF-BB and macrophage infiltration via suppression of the glycation end products and their receptor (AGE-RAGE) mediated oxidative stress generation.<sup>90</sup> Sakai et al. reported an RNA aptamer binding to phospholamban (PLA) protein, and the aptamer may be used as a therapeutic reagent for heart failure.<sup>91</sup> Yu et al.<sup>92</sup> reported a DNA aptamer binding to the protein of the C virus, and Kwon et al.<sup>93</sup> have selected an RNA aptamer binding to the protein, these aptamers have the potential to treat the respective viruses. Butzet al. selected a peptide aptamer targeting the core protein of hepatitis B virus which blocks viral replication by interfering with capsid formation.<sup>94</sup> Liu et al. selected a peptide aptamer against the pathogenic *Aeromonas veronii* and inhibited the function of small protein B required for pathogenesis in zebrafish.<sup>95</sup> Similarly, Blum et al. developed peptide aptamers against the *Escherichia coli* having bacteriostatic and bacteriocidal properties.<sup>96</sup> Another, attractive therapeutic application of aptamer is drug carrier in targeted drug delivery (TDD), due to their chemically stable for drug conjugation. TDD is one of the best methods in clinical practice to reduce the side effect and treatment cost by reducing the amount of drug required for treatment. In this system, therapeutic molecules are directly delivered to specific cells or tissue with the help of selected aptamers. Some example of the aptamers reported as a drug carrier: Porciani et al. delivered the doxorubicin and NF- $\kappa$ B binding DNA with the help of an RNA aptamer specifically binding to tumor receptor protein and results showed greater

activity than doxorubicin only.<sup>97</sup> Zhao et al. used DNA aptamer conjugated methotrexate and found a subdued proliferation of erythroleukemia cells and lymphoma cells *in vitro*.<sup>98</sup> Chu et al. prepared an aptamer-gelonin conjugated construct for targeted delivery of gelonin into PSMA-positive prostate cancer cells and reported the activity of gelonin increased by 180-fold in target cells.<sup>99</sup> Min et al. reported the dual-aptamer complex of RNA and peptide to deliver doxorubicin into prostate cancer.<sup>100</sup>

### **3.3 Other Applications**

Due to the specificity of the aptamers toward any kind of target ligand make them ideal tool not only for diagnosis and therapeutic application but also for other applications such as bio-imaging<sup>101</sup>, western blot analysis<sup>61</sup>, aptamers affinity chromatography system<sup>102</sup>, analytical reagent<sup>103</sup>, hazard detection<sup>104</sup> food inspection<sup>105</sup> and many more.

#### 4. REFERENCES

1. Tuerk, C.;Gold, L. S. Systematic evolution of ligands by exponential enrichment: RNA ligands to bacteriophage T4 DNA polymerase.*Science***1990**, *249*, 505-510.
2. Ellington, A. D.;Szostak, J.W.In vitro selection of RNA molecules that bind specific ligands.*Nature***1990**, *346*, 818-822.
3. Mayer, G. The chemical biology of aptamers.*Angew. Chem. Int. Ed.***2009**, *48*, 2672-2689.
4. Hoppe-Seyler,F.;Crnkovic-Mertens,I.;Tomai, E.; Butz,K. Peptide aptamers: specific inhibitors of protein function.*Curr. Mol. Med.***2004**, *4*, 529-538.
5. Mascini,;Palchetti, M. I.;Tombelli, S. Nucleic acid and peptide aptamers: fundamentals and bioanalytical aspects.*Angew. Chem. Int.Ed.***2012**, *51*, 1316-1332.
6. Colas, P.; Cohen, B.; Jessen, T.; Grishina, I.; McCoy, J.; Brent, R. Genetic selection of peptide aptamers that recognize and inhibit cyclin-dependent kinase 2.*Nature***1996**,*380*,548-550.
7. Baines, I. C.; Colas, P. Peptide aptamers as guides for small-molecule drug discovery.*DrugDiscov. Today.***2006**, *11*, 334-341.
8. Colas, P. The eleven-year switch of peptide aptamers.*J. Biol.* **2008**, *7*, 2.
9. Hoppe-Seyler, F.;Butz, K. Peptide aptamers: powerful new tools for molecular medicine.*J. Mol. Med.***2000**, *78*,426-430.
10. Lee, J. F.; Stovall, G. M.; Ellington, A. D. Aptamer therapeutics advance. *Curr. Opin in Chem. Biol.***2006**, *10*, 282-289.
11. Tan, W.; Wang, H.; Chen, Y.; Zhang, X.; Zhu, H.; Yang, C.; Yang, R.; Liu, C. Molecular aptamers for drug delivery.*Trends Biotechnol.* **2011**, *29*, 634-640.
12. Keefe, A. D.;Pai, S.; Ellington, A. Aptamers as therapeutics.*Nat. Rev. Drug Discov.***2010**, *9*,537-550.

13. Jenison, R. D.; Gill, S.C;Pardi, A.; Polisky, B. High-resolution molecular discrimination by RNA. *Science***1994**, *263*, 1425-1429.
14. Geiger, A.;Burgstaller, P.; von der Eltz, H.; Roeder, A.;Famulok, M. RNA aptamers that bind L-arginine with sub-micromolar dissociation constants and high enantioselectivity.*Nucleic Acids Res.***1996**, *24*, 1029-1036.
15. Francis, K. Charles Darwin and the origin of species, Greenwood Publishing Group, London, 2007.
16. Chen, M.; Yu, Y.; Jiang, F.; Zhou, J.; Li, Y.; Liang, C.; Dang, L.;Lu, A.; Zhang, G. Development of cell-SELEX technology and its application in cancer diagnosis and therapy.*Int. J. Mol. Sci.* **2016**, *17*,2075.
17. Sun, H.; Zhu, X.; Lu, P. Y.;Rosato, R. R; Tan, W.; Zu, Y. Oligonucleotide aptamers: new tools for targeted cancer therapy.*Mol. Ther. Nucleic Acids.***2014**, *3*, e182.
18. Legiewicz, M.;Lozupone, C.; Knight, R.; Yarus, M. Size, constant sequences, and optimal selection.*RNA.* **2005**, *11*, 1701-1709.
19. Fields, S.; Song, O. A novel genetic system to detect protein-protein interactions.*Nature***1989**, *340*,245-246.
20. Crawford, M.; Woodman, R.;Ferrigno, P. K. Peptide aptamers: tools for biology and drug discovery.*Brief.Funct. Genomic Proteomic.***2003**, *2*, 72-79.
21. Bass, S.; Greene, R; Wells, J. AHormone phage: an enrichment method for variant proteins with altered binding properties.*Proteins***1990**, *8*, 309-314.
22. Scott, J. K.; Smith, G. P. Searching for peptide ligands with an epitope library.*Science***1990**, *249*, 386-390.
23. Clackson, T.;Hoogenboom, H. R.; Griffiths, A. D.; Winter, G. Making antibody fragments using phage display libraries.*Nature***1991**, *352*, 624-628.

24. Boder, E. T.;Wittrup, K. D. Yeast surface display for screening combinatorial polypeptide libraries. *Nat.Biotechnol.***1997**, *15*,553-557.
25. Bowley, D. R;Labrijn, A. F.; Zwick, M. B;. Burton, D. R Antigen selection from an HIV-1 immune antibody library displayed on yeast yields many novel antibodies compared to selection from the same library displayed on phage. *Protein Eng. Des. Sel.***2007**, *20*, 81-90.
26. Wernerus, H.;Lehtio, J.;Teeri, T.;Nygren, P.A.; Stahl, S. Generation of metal-binding staphylococci through surface display of combinatorially engineered cellulose-binding domains.*Appl. Environ.Microbiol.* **2001**, *67*, 4678-4684.
27. Hanes, J.;Pluckthun, A. In vitro selection and evolution of functional proteins by using ribosome display.*Proc. Natl. Acad. Sci., USA***1997**, *94*, 4937-4942.
28. Mattheakis, L. C.; Bhatt, R. R.; Dower, W. J. An in vitro polysome display system for identifying ligands from very large peptide libraries. *Proc. Natl. Acad. Sci. USA* **1994**, *91*, 9022-9026.
29. Shen, X.; Valencia, C.A.;Szostak, J.; Dong, B.; Liu, R. Scanning the human proteome for calmodulin-binding proteins.*Proc. Natl. Acad. Sci., USA***2005**, *102*, 5969-5974.
30. Keefe, A. D;Szostak, J. W. Functional proteins from a random-sequence library, *Nature***20014**, *10*, 715-718.
31. Seelig, B.;Szostak, J. W. Selection and evolution of enzymes from a partially randomized non-catalytic scaffold.*Nature* **2007**, *448*, 828-831
32. Roberts, R. W.;Szostak, J. W. RNA-peptide fusions for the in vitro selection of peptides and proteins.*Proc. Natl. Acad. Sci., USA***1997**, *94*,12297-12302.
33. Yamaguchi, J.;Naimuddin, M.;Biyani, M.; Sasaki, T.; Machida, M.; Kubo, T.;Funatsu, T.;Husimi, Y. Nemoto, N. cDNA display: a novel screening method for

- functional disulfide-rich peptides by solid-phase synthesis and stabilization of mRNA–protein fusions.*Nucleic Acids Res.***2009**, *37*,e108.
34. Murray, C. J.;Baliga, R. Cell-free translation of peptides and proteins: from high throughput screening to clinical production.*Curr. Opin. Chem. Biol.***2013**, *17*, 420-426.
  35. Mochizuki, Y.;Nemoto, N. Evolution of disulfide-rich peptide aptamers using cDNA display.*Methods Mol. Biol.* **2012**, *805*, 237-250.
  36. Ueno, S.;Nemoto, N. cDNA display: rapid stabilization of mRNA display, *Methods Mol. Biol.***2012**, *805*,113-135.
  37. Tawfik, D. S.; Griffiths, A. D. Man-made cell-like compartments for molecular evolution.*Nat. Biotechnol.* **1998**, *16*, 652-656.
  38. Kaltenbach, M.;Hollfelder, F. SNAP display: in vitro protein evolution in microdroplets.*Methods Mol. Biol.***2012**, *805*, 101-111.
  39. Keppler, A.;Gendreizig, S.;Gronemeyer, T.; Pick, H.; Vogel, H.;Johnsson, K. A general method for the covalent labeling of fusion proteins with small molecules in vivo.*Nat. Biotech.***2003**, *21*,86-89
  40. Leemhuis, H.; Stein, V.; Griffiths, A. D.;Hollfelder, F. New genotype-phenotype linkages for directed evolution of functional proteins.*Curr.Opin.Struct. Biol.***2005**, *15*, 472-478.
  41. Smith, G. P. Filamentous fusion phage: novel expression vectors that display cloned antigens on the virion surface.*Science***1985**, *228*, 1315-1317.
  42. Brown, S. Engineered iron oxide-adhesion mutants of the Escherichia coli phage lambda receptor.*Proc. Natl. Acad. Sci., USA.* **1992**, *89*, 8651-8655.

43. Naik, R. R.;Brott, L .L;Clarson, S.J.; Stone, M. O. Silica-precipitating peptides isolated from a combinatorial phage display peptide library.*J.Nanosci.Nanotechnol.***2002**, 2, 95-100.
44. Rozinov, M. N.; Nolan, G. P. Evolution of peptides that modulate the spectral qualities of bound, small-molecule fluorophores.*Chem. Biol.* **1998**, 5, 713-728.
45. Liu, Z.; Liu, J.; Wang, K.; Li, W.;Shelver, W. L; Li, Q. X.; Li, J.; Xu, T. Selection of phage-displayed peptides for the detection of imidacloprid in water and soil. *Anal.Biochem.***2015**, 485, 28-33.
46. Aoki, S.;Morohashi, K.;Sunoki, T.;Kuramochi, K.; Kobayashi, S.; Sugawara, F. Screening of paclitaxel-binding molecules from a library of random peptides displayed on T7 phage particles using paclitaxel-photoimmobilized resin.*Bioconjug Chem.***2007**, 18, 1981-1986.
47. Whaley, S. R.; English, D. S.; Hu, E. L.; Barbara P. F.; Belcher, A. M. Selection of peptides with semiconductor binding specificity for directed nanocrystal assembly. *Nature***2000**, 405,665-668
48. Zhao, S. W.; Shen, P. P.; Zhou,Y.; Wei, Y.;Xin, X.B.; Hua, Z. C. Selecting peptide ligands of microcystin-LR from phage-displayed random libraries.*Environ. Int.***2005**, 31, 535-541.
49. Sanghvi, A. B.;Miller,K. P.; Belcher, A. M.; Schmidt, C. E. Biomaterials functionalization using a novel peptide that selectively binds to a conducting polymer.*Nat. Mater.***2005**, 4,496-502.
50. Seker,U. O.;Demir, H. V. Material binding peptides for nanotechnology, *Molecules.***2011**, 16, 1426-1451.

51. Barry, M.A.; Dower, W. J.; Johnston, S. A. Toward cell-targeting gene therapy vectors: Selection of cell-binding peptides from random peptide-presenting phage libraries. *Nat. Med.* **1996**, *2*, 299-305
52. Lo, A.; Lin, C. T.; Wu, H. C. Hepatocellular carcinoma cell-specific peptide ligand for targeted drug delivery. *Mol. Cancer Ther.* **2008**, *7*, 579-589.
53. Lee, T.Y.; Lin, C. T.; Kuo, S. Y.; Chang, D. K.; Wu, H. C. Peptide-mediated targeting to tumor blood vessels of lung cancer for drug delivery. *Cancer Res.* **2007**, *67*, 10958-10965.
54. Reverdatto, S.; Burz, D. S.; Shekhtman, A. Peptide aptamers: development and applications. *Curr. Top. Med. Chem.* **2015**, *15*, 1082-101.
55. Alberts, B.; Bray, D.; Hopkin, K.; Johnson, A.; Lewis, J.; Raff, M.; Roberts, K.; Walter, P.; Hopkin A. B.; et al. From DNA to protein: how cells read the genome. *Essential Cell Biology*, 3rd ed.; Garland Science, New York, 2010; 231-267.
56. He, M.; Taussig, M. J. Ribosome display: cell-free protein display technology. *Brief Funct. Genomic Proteomic.* **2002**, *1*, 204-212.
57. Moore, P. B.; Steitz, T. A. The involvement of RNA in ribosome function. *Nature* **2002**, *418*, 229-235.
58. Makeyev, E. V.; Kolb, V. A.; Spirin, A.S. Enzymatic activity of the ribosome-bound nascent polypeptide. *FEBS Lett.* **1996**, *378*, 166-170.
59. Hong, P.; Li, W.; Li, J. Applications of aptasensors in clinical diagnostics. *Sensors* **2012**, *12*, 1181-1193.
60. Soontornworajit, B.; Wang, Y. Nucleic acid aptamers for clinical diagnosis: cell detection and molecular imaging. *Anal. Bioanal. Chem.* **2011**, *399*, 1591-1599.

61. Shin, S.; Kim, I. H.; Kang, W.; Yang, J. K.; Hah, S. S. An alternative to western blot analysis using RNA aptamer-functionalized quantum dots. *Bioorg. Med. Chem. Lett.* **2010**, *20*, 3322-3325.
62. Lee, S.; Song, K. M.; Jeon, W.; Jo, H.; Shim, Y. B.; Ban, C. A highly sensitive aptasensor towards Plasmodium lactate dehydrogenase for the diagnosis of malaria. *Biosens Bioelectron* **2012**, *35*, 291-296.
63. Huang, Y.; Zhao, S.; Chen, Z. F.; Shi, M.; Liang, H. Amplified fluorescence polarization aptasensors based on structure-switching-triggered nanoparticles enhancement for bioassays. *Chem. Commun (Camb)*. **2012**, *48*, 7480-7482.
64. Tan, X.; Chen, W.; Lu, S.; Zhu, Z.; Chen, T.; Zhu, G.; You, M.; Tan, W. Molecular beacon aptamers for direct and universal quantitation of recombinant proteins from cell lysates. *Anal. Chem.* **2012**, *84*, 8272-8276.
65. Bruno, J. G.; Kiel, J. L. In vitro selection of DNA aptamers to anthrax spores with electrochemiluminescence detection. *Biosens Bioelectron* **1999**, *14*, 457-464.
66. Li, X.; An, Y.; Jin, J.; Zhu, Z.; Hao, L.; Liu, L.; Shi, Y.; Fan, D.; Ji, T.; Yang, C. J. Evolution of DNA aptamers through in vitro metastatic-cell-based systematic evolution of ligands by exponential enrichment for metastatic cancer recognition and imaging. *Anal. Chem.* **2015**, *87*, 4941-4948.
67. Lian, Y.; He, F.; Wang, H.; Tong, F. A new aptamer/graphene interdigitated gold electrode piezoelectric sensor for rapid and specific detection of *staphylococcus aureus*. *Biosens Bioelectron* **2015**, *65*, 314-319.
68. Parekh, P.; Tang, Z.; Turner, P. C.; Moyer, R. W.; Tan, W. Aptamers recognizing glycosylated hemagglutinin expressed on the surface of vaccinia virus-infected cells. *Anal. Chem.* **2010**, *82*, 8642-8649.

69. Wang, Q.; Liu, W.; Xing, Y.; Yang, X.; Wang, K.; Jiang, R.; Wang, P.; Zhao, Q. Screening of DNA aptamers against myoglobin using a positive and negative selection unit integrated microfluidic chip and its biosensing application. *Anal. Chem.* **2014**, *86*, 6572-6579.
70. Cheung, Y.W.; Kwok, J.; Law, A.W.; Watt, R.M.; Kotaka, M.; Tanner, J.A. Structural basis for discriminatory recognition of Plasmodium lactate dehydrogenase by a DNA aptamer. *Proc. Natl. Acad. Sci., USA.* **2013**, *110*, 15967-15972.
71. Gijs, M.; Penner, G.; Blackler, G. B.; Impens, N. R. E. N; Baatout, S.; Luxen, A.; Aerts, A. M. Improved aptamers for the diagnosis and potential treatment of HER2-positive cancer. *Pharmaceuticals (Basel)* **2016**, *9*, 29.
72. Wan, Y.; Kim, Y.; Li, N.; Cho, S. K.; Bachoo, R.; Ellington, A. D.; Iqbal, S. M. Surface-immobilized aptamers for cancer cell isolation and microscopic cytology. *Cancer Res.* **2010**, *70*, 9371-9380
73. Li, X.; Zhang, W.; Liu, L.; Zhu, Z.; Ouyang, G.; An, Y.; Zhao, C.; Yang, C. J. In vitro selection of DNA aptamers for metastatic breast cancer cell recognition and tissue imaging. *Anal. Chem.* **2014**, *86*, 6596-6603.
74. Song, Y.; Zhu, Z.; An, Y.; Zhang, W.; Zhang, H.; Liu, D.; Yu, C.; Duan, W.; Yang, C. J Selection of DNA aptamers against epithelial cell adhesion molecule for cancer cell imaging and circulating tumor cell capture. *Anal. Chem.* **2013**, *85*, 4141-4149.
75. Ruslinda, A. R.; Tanabe, K.; Ibori, S.; Wang, X.; Kawarada, H. Effects of diamond-FET-based RNA aptamer sensing for detection of real sample of HIV-1 Tat protein. *Biosens Bioelectron* **2013**, *40*, 277-282.
76. Cobbett, J.D.; DeMott, C.; Majumder, S.; Smith, E.A.; Reverdatto, S.; Burz, D. S.; McDonough, K. A.; Shekhtman, A. Caught in action: selecting peptide aptamers against intrinsically disordered proteins in live cells. *Sci. Rep.* **2015**, *5*, 9402.

77. Manandhar, Y.; K.C. T. B.; Wang, W.; Uzawa, T.; Aigaki, T.; Ito, Y. In vitro selection of a peptide aptamer that changes fluorescence in response to verotoxin. *Biotechnol Lett.***2015**, *37*, 619-625.
78. Tung, N. T.; Tue, P. T.; Lien, T. N.; Ohno, Y.; Maehashi, K.; Matsumoto, K.; Nishigaki, K.; Biyani, M.; Takamura, Y. Peptide aptamer-modified single-walled carbon nanotube-based transistors for high-performance biosensors. *Sci. Rep.***2017**, *7*, 17881.
79. Han, K.; Liang, Z.; Zhou, N. Design strategies for aptamer-based biosensors. *Sensors (Basel)***2010**, *10*, 4541-4557.
80. Ng, E. W.; Shima, D. T.; Calias, P.; Cunningham, E. T. Jr.; Guyer, D. R.; Adamis, A. P. Pegaptanib, a targeted anti-VEGF aptamer for ocular vascular disease. *Nat. Rev. Drug Discov.***2006**, *5*, 123-132.
81. Green, L. S.; Jellinek, D.; Bell, C.; Beebe, L. A.; Feistner, B. D.; Gill, S. C.; Jucker, F. M.; Janjic, N. Nuclease-resistant nucleic acid ligands to vascular permeability factor/vascular endothelial growth factor. *Chem. Biol.***1995**, *2*, 683-695.
82. Ciulla, T. A.; Rosenfeld, P. J.; Antivascular endothelial growth factor therapy for neovascular age-related macular degeneration. *Curr. Opin. Ophthalmol.***2009**, *20*, 158-165.
83. Zhuo, Z.; Yu, Y.; Wang, M.; Li, J.; Zhang, Z.; Liu, J.; Wu, X.; Lu, A.; Zhang, G.; Zhang, B. Recent advances in SELEX technology and aptamer applications in biomedicine. *Int. J. Mol. Sci.***2017**, *18*, e2142.
84. Poolsup, S.; Kim, C. Y. Therapeutic applications of synthetic nucleic acid aptamers. *Curr. Opin. Biotechnol.***2017**, *48*, 180-186.
85. Dassie, J. P.; Hernandez, L. I.; Thomas, G. S.; Long, M. E.; Rockey, W. M.; Howell, C. A.; Chen, Y.; Hernandez, F. J.; Liu, X. Y.; Wilson, M. E. Targeted inhibition of

- prostate cancer metastases with an RNA aptamer to prostate-specific membrane antigen. *Mol. Ther.* **2014**, *22*, 1910-1922.
86. Simmons, S. C.; Jamsa, H.; Silva, D.; Cortez, C. M.; McKenzie, E. A.; Bitu, C. C.; Salo, S.; Nurmenniemi, S.; Nyberg, P.; Risteli, J. Anti-heparanase aptamers as potential diagnostic and therapeutic agents for oral cancer. *PLoS One.* **2014**, *9*, e96846.
87. Soldevilla, M. M.; Villanueva, H.; Bendandi, M.; Inoges, S.; de Cerio, A. L. D.; Pastor, F. 2-fluoro-RNA oligonucleotide CD40 targeted aptamers for the control of B lymphoma and bone-marrow aplasia. *Biomaterials.* **2015**, *67*, 274-285.
88. Kotula, J. W.; Sun, J.; Li, M.; Pratico, E. D.; Fereshteh, M. P.; Ahrens, D. P.; Sullenger, B. A.; Kovacs, J. J. Targeted disruption of  $\beta$ -arrestin 2-mediated signaling pathways by aptamer chimeras leads to inhibition of leukemic cell growth. *PLoS One.* **2014**, *9*, e93441.
89. Prodeus, A.; Cydzik, M.; Abdul-Wahid, A.; Huang, E.; Khatri, I.; Gorczynski, R.; Garipey, J. Agonistic CD200R1 DNA aptamers are potent immunosuppressants that prolong allogeneic skin graft survival. *Mol. Ther. Nucleic Acids.* **2014**, *3*, e190.
90. Ojima, A.; Oda, E.; Higashimoto, Y.; Matsui, T.; Yamagishi, S. DNA aptamer raised against advanced glycation end products inhibits neointimal hyperplasia in balloon-injured rat carotid arteries. *Int. J. Cardiol.* **2014**, *171*, 443-446.
91. Sakai, H.; Ikeda, Y.; Honda, T.; Tanaka, Y.; Shiraishi, K. Inui, M. A cell-penetrating phospholamban-specific RNA aptamer enhances Ca<sup>2+</sup> transients and contractile function in cardiomyocytes. *J. Mol. Cell Cardiol.* **2014**, *76*, 177-185.
92. Yu, X.; Gao, Y.; Xue, B.; Wang, X.; Yang, D.; Qin, Y.; Yu, R.; Liu, N.; Xu, L.; Fang, X. Inhibition of hepatitis C virus infection by NS5A-specific aptamer. *Antiviral Res.* **2014**, *106*, 116-124.

93. Kwon, H. M.; Lee, K. H.; Han, B. W.; Han, M. R.; Kim, D. H.; Kim, D. E. An RNA aptamer that specifically binds to the glycosylated hemagglutinin of avian influenza virus and suppresses viral infection in cells. *PLoS One*. **2014**, *9*, e97574.
94. Butz, K.; Denk, C.; Fitscher, B.; Crnkovic-Mertens, I.; Ullmann, A.; Schroder, C. H.; Hoppe-Seyler, F. Peptide aptamers targeting the hepatitis B virus core protein: a new class of molecules with antiviral activity. *Oncogene* **2001**, *20*, 6579-6586.
95. Liu, P.; Huang, D.; Hu, X.; Tang, Y.; Ma, X.; Yan, R.; Han, Q.; Guo, J.; Zhang, Y.; Sun, Q. Targeting inhibition of SmpB by peptide aptamer attenuates the virulence to protect zebrafish against aeromonas veronii infection. *Front Microbiol.* **2017**, *8*, 1766.
96. Blum, J. H.; Dove, S. L.; Hochschild, A.; Mekalanos, J. J. Isolation of peptide aptamers that inhibit intracellular processes. *Proc. Natl. Acad. Sci., USA*. **2000**, *97*, 2241-2246.
97. Porciani, D.; Tedeschi, L.; Marchetti, L.; Citti, L.; Piazza, V.; Beltram, F.; Signore, G. Aptamer-mediated codelivery of doxorubicin and NF- $\kappa$ B decoy enhances chemosensitivity of pancreatic tumor cells. *Mol. Ther. Nucleic Acids*. **2015**, *4*, e235.
98. Zhao, N.; Pei, S. N.; Qi, J.; Zeng, Z.; Iyer, S. P.; Lin, P.; Tung, C. H.; Zu, Y. Oligonucleotide aptamer-drug conjugates for targeted therapy of acute myeloid leukemia. *Biomaterial* **2015**, *67*, 42-51.
99. Chu, T. C.; Marks, J. W.; Lavery, L. A.; Faulkner, S.; Rosenblum, M. G.; Ellington, A. D.; Levy, M. Aptamer: toxin conjugates that specifically target prostate tumor cells. *Cancer Res.* **2006**, *66*, 5989-5992.
100. Min, K.; Jo, H.; Song, K.; Cho, M.; Chun, Y. S.; Jon, S.; Kim, W. J.; Ban, C. Dual-aptamer-based delivery vehicle of doxorubicin to both PSMA (+) and PSMA (-) prostate cancers. *Biomaterial*. **2011**, *32*, 2124-2132.

101. Shangguan, D.; Li, Y.; Tang, Z.; Cao, Z. C.; Chen, H. W.; Mallikaratchy, P.; Sefah, K.; Yang, C. J.; Tan, W. Aptamers evolved from live cells as effective molecular probes for cancer study. *Proc. Natl. Acad. Sci., USA*. **2006**, *103*, 11838-11843.
102. Romig, T.S.; Bell, C.; Drolet, D. W. Aptamer affinity chromatography: combinatorial chemistry applied to protein purification. *J. Chromatogr B. Biomed Sci. Appl.* **1999**, *731*, 275-284.
103. Tombelli, S.; Minunni, M.; Mascini, M.; Analytical applications of aptamers. *Biosens Bioelectron.* **2005**, *20*, 2424-2434.
104. Hayat, A.; Marty, J. L. Aptamer based electrochemical sensors for emerging environmental pollutants. *Front Chem.* **2014**, *2*, 41.
105. Dong, Y.; Xu, Y.; Yong, W.; Chu, X.; Wang, D. Aptamer and its potential applications for food safety. *Crit. Rev. Food Sci. Nutr.* **2014**, *54*, 1548-1561.

**CHAPTER 2: WASH-FREE AND SELECTIVE  
IMAGING OF EPITHELIAL CELL ADHESION  
MOLECULE (EPCAM) EXPRESSING CELLS  
WITH FLUOROGENIC PEPTIDE LIGANDS**

## 1. INTRODUCTION

Cancer is the second leading cause of death worldwide.<sup>1-3</sup> More than 90% of cancer-related mortalities are due to metastasis.<sup>4-6</sup> In 1869 Thomas Ashworth proposed that the cause of cancer metastasis could be circulating tumor cells (CTCs).<sup>7</sup> CTCs are the cells detached from a primary tumor, actively circulate in the peripheral blood and invade other distant organs to establish secondary tumor sites.<sup>8-10</sup> After the correlations between the numbers of CTCs and prognosis were found from patients of some cancers, United State Food and Drug Administration (USFDA) approved a CTC-based diagnosis for breast cancer in 2004, in which the number of the CTC is used as diagnostic information. Although CTCs are extremely rare cells in peripheral blood (about 1 CTC /10<sup>7</sup> blood cells)<sup>10-12</sup>, recent technical developments to isolate CTCs have made it possible that genetic information can be obtained from a single CTC level, maximizing the diagnostic information of CTCs.<sup>12-15</sup>

In the current CTC-based diagnosis, an epithelial cell adhesion molecule (EpCAM) is used as a hallmark of CTCs.<sup>16, 17</sup> The USFDA-approved Cell Search™ technique separates EpCAM-positive cells from other cells in blood using magnetic ferrofluid modified with anti-EpCAM antibodies.<sup>18</sup> However, the cost to produce antibodies is not low, and some cumbersome processes including washing steps are required to eliminate unbound antibodies from CTC-bound antibodies as well as fixation, which possibly hinders single-cell based genetic analyses (Figure 2-1).

To overcome such problems related to the use of antibodies, fluorogenic detection using ligands has been recently developed for convenient detection of biological components. For example, Venkatraman et al.<sup>19</sup> and Sainlos et al.<sup>20</sup> reported fluorogenic peptide ligands to understand the protein-mediated interaction. Walkup et al.<sup>21</sup> and Ma et al.<sup>22</sup> reported a fluorogenic peptidyl chemosensor and fluorescence-switching molecular probes, respectively, to sense small molecules. Zhuang et al. reported a fluorescence turn-on probe to detect both

enzymes and non-enzymatic proteins.<sup>23</sup> We also generated peptide ligands to fluorescently detect proteins of interest; by virtue of an environment-sensitive fluorophore incorporated in the peptide ligands, the fluorescence intensity was either enhanced<sup>24-26</sup> or suppressed<sup>27</sup> due to the change of microenvironment of the fluorophore when the peptide ligands bind the proteins of interest.

In this study, I generate new fluorogenic ligands to detect the EpCAM by modifying an EpCAM-binding peptide (Figure 2-1). So far, a few EpCAM-binding peptides have been reported. For example, Bai et al. created an EpCAM-binding peptide from de novo designed peptides and found that even inexpensive peptide exhibited strong binding affinity to the EpCAM (Kd = 1.98nM) and the peptide was applicable to capture CTCs.<sup>28</sup> Iwasaki et al. generated an artificial macrocyclic peptide using an *in vitro* evolution system.<sup>29</sup> Co-authors of this study, Shiba et al. also selected an EpCAM-binding peptide, Ep114, using phage display<sup>30</sup> and demonstrated that the Ep114 captures EpCAM-expressing vesicles.<sup>31</sup> Because Ep114 is composed of the 12 canonical amino acids, we here functionalize Ep114 by replacing its amino acids (Table 2-1) to an aminophenylalanine modified with environmentally sensitive 7-nitro-2,1,3-benzoxadiazole (NBD-amPhe). I demonstrate that two of the synthesized peptide ligands can mark EpCAM-positive cells by just adding the peptide ligand into the cell cultivation medium.

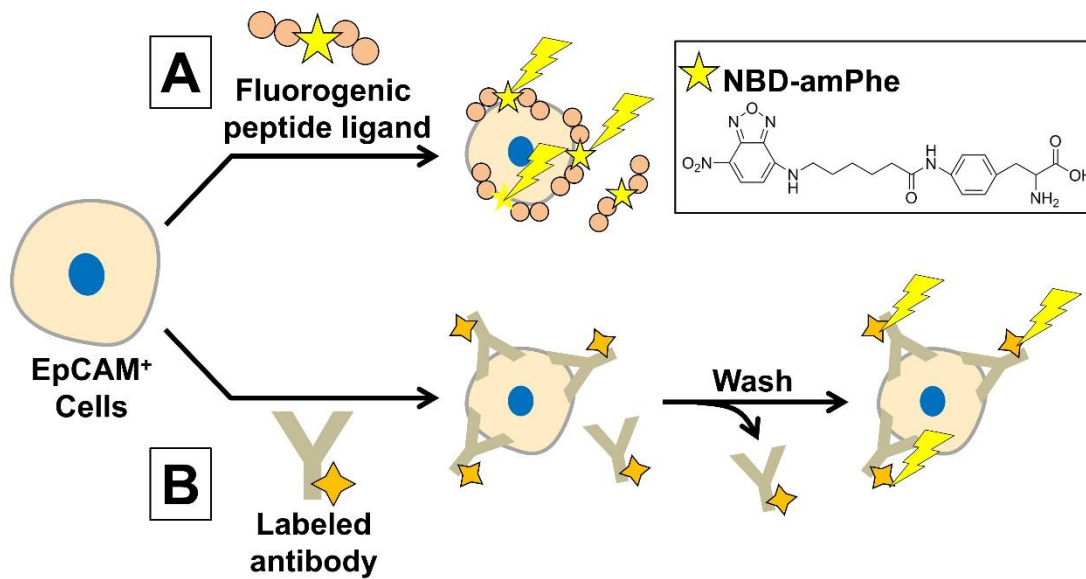


**Figure 2-1.** Approaches to detect an EpCAM-positive cell. (A) In this approach, a fluorogenic peptide ligand can mark the EpCAM-positive cell by just adding the peptide ligand in the cultivation medium. (B) In a widely-used conventional approach, cumbersome processes including washing steps are required to eliminate unbound antibodies from CTC-bound antibodies.

**Table 2-1:** Experimental design to functionalize the EpCAM-binding peptide (Ep114)

Peptides name	Residual number											
	1	2	3	4	5	6	7	8	9	10	11	12
Ep114	K	<b>H</b>	<b>L</b>	Q	<b>C</b>	V	R	N	I	<b>C</b>	<b>W</b>	S
K1X	<b>X</b>	<b>H</b>	<b>L</b>	Q	<b>C</b>	V	R	N	I	<b>C</b>	<b>W</b>	S
Q4X	K	<b>H</b>	<b>L</b>	<b>X</b>	<b>C</b>	V	R	N	I	<b>C</b>	<b>W</b>	S
V6X	K	<b>H</b>	<b>L</b>	Q	<b>C</b>	<b>X</b>	R	N	I	<b>C</b>	<b>W</b>	S
R7X	K	<b>H</b>	<b>L</b>	Q	<b>C</b>	V	<b>X</b>	N	I	<b>C</b>	<b>W</b>	S
N8X	K	<b>H</b>	<b>L</b>	Q	<b>C</b>	V	R	<b>X</b>	I	<b>C</b>	<b>W</b>	S
I9X	K	<b>H</b>	<b>L</b>	Q	<b>C</b>	V	R	N	<b>X</b>	<b>C</b>	<b>W</b>	S
S12X	K	<b>H</b>	<b>L</b>	Q	<b>C</b>	V	R	N	I	<b>C</b>	<b>W</b>	<b>X</b>

**Note:** I incorporated NBD-amPhe (X) into seven positions in Ep114. The five amino acids written in bold are expected to be important to bind the EpCAM<sup>30</sup>

## 2. MATERIALS AND METHODS

### 2.1 Chemical Synthesis

#### 2.1.1 Preparation of functional amino acid.

An aminophenylalanine carrying NBD was prepared as shown in Figure 2. Briefly, the starting material 4-chloro-7-nitro-2,1,3-benzoxadiazole (Tokyo Chemical Industry, Tokyo, Japan), was conjugated with a linker 6-aminohexanoic acid (Wako Pure Chem. Ind. Ltd., Japan) in an equal molar ratio in the presence of three times excess molar concentration of sodium bicarbonate in the solvent system of methanol and water (1:1 volume). The mixture was stirred at 0°C for 30min, and then the reaction was performed at room

temperature for 2 hours followed by another 2 hours at 50°C. After cooled down the solution to room temperature, carefully acidified the solution using 0.1 M HCl till pH reached 5. Methanol was removed by evaporation, and the obtained NBD-hexanoic acid was transferred to an organic phase by washing with ethyl acetate and dehydrated using magnesium sulfate. The dried NBD-hexanoic acid was activated by 1-(3-Dimethylaminopropyl) -3-ethylcarbodiimide hydrochloride (Tokyo Chemical Industry, Tokyo, Japan) and N-Hydroxysuccinimide (Wako Pure Chem. Ind. Ltd., Japan) in dimethylformamide by overnight incubation at room temperature. The activated NBD-hexanoic acid was extracted with ethyl acetate in the presence of 1N HCl, subsequently washed with saturated sodium bicarbonate solvent, and dehydrated by magnesium sulfate. The obtained NBD-linker-NHS ester was conjugated with Fmoc-4-amino-L-phenylalanine (AnaSpec Inc., USA) at the molar ratio of 1.2:1 for overnight incubation at 37°C in a solvent system of pyridine-HCl (pH 5) and dimethyl sulfoxide (1:1 volume). After the incubation, ethyl acetate was added to transfer the product into the organic phase and washed with saturated citric acid followed by ultrapure water. After dehydration using magnesium sulfate, ethyl acetate was evaporated under reduced pressure. The obtained, product was purified the by flash chromatography on silica gel (CH<sub>2</sub>Cl<sub>2</sub>: CH<sub>3</sub>OH, 100:1 to 50:1, v/v).

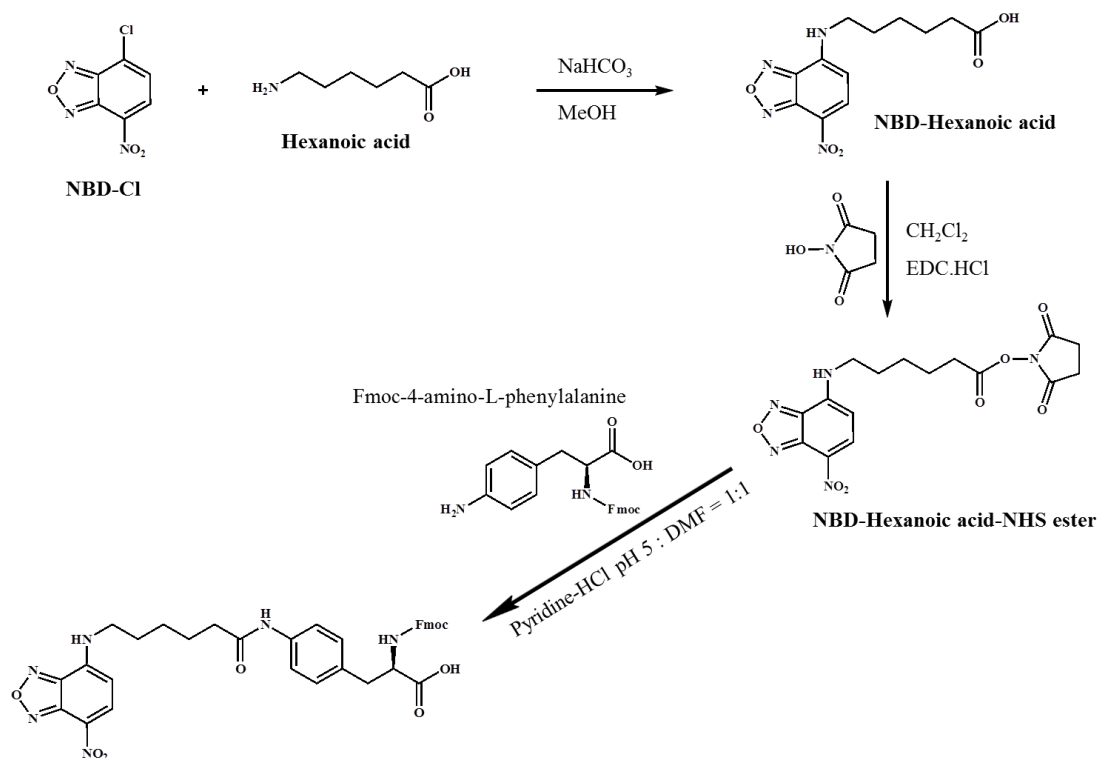


**Figure 2-2.** A scheme to prepare NBD- aminophenylalanine

Finally, the resultant NBD-amPhe was characterized by  $^1\text{H}$  NMR (Appendix 1) and MALDI-TOF MS (Microflex, Bruker, USA) (found  $m/z = 701.208$ , calc.  $m/z = 701.24$  monoisotopic mass  $[\text{M}+\text{Na}]^+$ ) and HPLC (JASCO, Tokyo, Japan) before used for peptide synthesis (Appendix 2).

### 2.1.2 Preparation of peptides by solid phase synthesis

All peptides used in this study were synthesized on Rink Amide MBHA resin (Novabiochem, China) in 0.1mmol scale. The coupling and deprotection reactions were performed by following a standard CEM protocol using the reagents N-ethyl-diisopropylamine (Wako Pure Chem. Ind. Ltd., Japan) and 1-[bis(dimethylamino)methylene]-1H-1,2,3-triazolo[4,5-b]pyridinium 3-oxid hexafluorophosphate (AnaSpec Inc., USA) and 20% piperidine (Wako Pure Chem. Ind. Ltd., Japan) in N-Methyl-2-pyrrolidone, NMP (Wako Pure Chem. Ind. Ltd., Japan). For the

coupling reaction of NBD-amPhe; we used an optimized condition for the coupling reaction of NBD-amPhe (17.5 minutes at  $50 \pm 5^\circ\text{C}$ , 20W of power). After coupling all the amino acids, synthesized peptides were cleaved from the resin after 2 and 1.5 hours incubation on ice and room temperature, respectively. Cleavage cocktail consisting of 81.5:5:5:5:2.5:1 (v/v) mixture of trifluoroacetic acid (Wako Pure Chem. Ind. Ltd., Japan), thioanisole (Tokyo Chemical Industry, Japan), phenol (Wako Pure Chem. Ind. Ltd., Japan), ultrapure water (Milli-Q), 1,2-ethanedithiol (Tokyo Chemical Industry, Japan) and tri-isopropylsilane (Tokyo Chemical Industry, Japan). The collected peptides were purified using the Extrema HPLC (JASCO, Japan) equipped with the C18 column (COSMOSIL AR-II, NacalaiTesqueInc, Japan) in a linear gradient of acetonitrile (Sigma-Aldrich, USA) and water solvent system containing 0.1% TFA. Purity was characterized by HPLC using C18 column (5C18-AR-II /4.6mm ID x 250 mm, NacalaiTesqueInc, Japan) and MALDI-TOFMS (Appendix 3).

### **2.3 Solubility Test**

Synthesized peptide candidates were dissolved in water, and then concentration was calculated using the extinction coefficient of NBD ( $25,000\text{M}^{-1}\text{cm}^{-1}$  at 480nm).<sup>32</sup> For solubility measurement, 10 $\mu\text{M}$  concentration of peptides solution was prepared in water and centrifuged at 10,000 revolutions per minute (rpm) / (9,100g) for 10 minutes. Peptide absorbance was measured before and after centrifuge as well as sedimentation was observed.

### **2.4 Preparation of Cells for Imaging**

Two cell lines of an EpCAM-positive human colon adenocarcinoma (HT-29) and an EpCAM-negative human fibrosarcoma (HT1080) were purchased from American Type Culture Collection. The HT-29 cell line was cultured in 10% Fetal Bovine Serum (Thermo Fisher Scientific, New York, USA) supplemented with Dulbecco's Modified Eagle Medium

(Invitrogen, New York, USA) using a poly-L-lysine coated glass-bottom dish (Matsunami Glass, Osaka, Japan). For the HT1080 cell line, RPMI1640 medium (Thermo Fisher Scientific, New York, USA) was used. I incubated the cells together with the peptide ligands (5 $\mu$ M) for 1 hour at room temperature and observed their brightfield and fluorescence images using a microscope (FV1000, Olympus, Japan) equipped with a 60X objective lens (PlanApo N, NA. 1.40, Olympus, Japan). Then I analyzed the obtained fluorescence images to estimate the fluorescence intensity of the cell membrane.

## **2.5 Image Analysis to Obtain Fluorescence Intensity**

The purpose of this image analysis is to obtain the intensity of fluorescence from the cell surface (membrane), based on the fluorescence images taken by the confocal microscopy. Due to the following features of the fluorescence images, analysis was not straightforward even though the cell membranes were clearly visualized.

- a) The extracellular cultivation medium presents relatively high fluorescence.
- b) The intracellular area present lower fluorescence.
- c) Thickness of the cell membrane (< 10nm) is much smaller than the pixel size (~ 400nm).
- d) There are two cell membranes at the border between two cells, while there is one membrane at the cell border exposed to the extracellular cultivation medium. Indeed, the images show higher fluorescence intensity at the intercellular membranes than that at the cell membranes exposed to the external cultivation medium.

From (c), we can assume that most of the pixel area is occupied by the extracellular or intracellular area, and the area of the cell membrane(s) is only a few percentages or less of the pixel area. To obtain the intensity of fluorescence from the cell membrane(s), therefore, the intensity of the extracellular or intracellular area must be subtracted as the background. More concretely, for the pixels at the intercellular membranes, the intensity at the intracellular area

is subtracted as the background, while for the pixels at the cell membranes exposed to the extracellular medium, the weighted average of the intensities at the extracellular medium and at the intracellular area. In the latter case, we can expect that, in average, the extracellular area and the intracellular one occupies each 50% of the pixel area, so that we can use a simple average as the background. After subtraction of the background, we divide the intensity of fluorescence from the intercellular membranes by 2, based on d). Then the fluorescence intensity was averaged over the pixels of membrane of each cell, and finally the average and standard deviation of the intensity was calculated over the cells of interest.

Image analysis was performed using ImageJ software (National Institute of Health, USA). More concrete procedure is as follows:

- 1) The color fluorescence images were separated into red(R), green(G), and blue(B) components, and only G component was converted into 256-level grey-scale image.
- 2) Averaged intensities at the extracellular medium  $I_{\text{ext}}$  and intracellular area  $I_{\text{int}}$  were obtained.
- 3) 10 cells in each image were randomly selected. There are two images for each concentration of Q4X, and thus 20 cells were used for analysis at each concentration.
- 4) Pixels at the cell membranes were traced as the region of interest (ROI) for each cell. In each cell, averaged intensity over the ROI for the single membrane exposed to the extracellular medium  $I_{\text{me}}$  and that for the intercellular double membranes  $I_{\text{mi}}$  were obtained.
- 5) For each cell,  $\{ I_{\text{me}} - (I_{\text{ext}} + I_{\text{int}}) / 2 \}$  for the single membrane and  $( I_{\text{mi}} - I_{\text{int}}) / 2$  for the double membrane were calculated, and averaged with the weight of number of pixels. This is the intensity of fluorescence from the membrane of cell # $i$   $I_{\text{cell-}i}$ .
- 6) Average and standard deviation of  $I_{\text{cell-}i}$  ( $i=1, \dots, 20$ , for each concentration) was obtained and shown in Figure 2-5b.

### 3. RESULTS AND DISCUSSION

#### 3.1 Fluorogenic Functionalization of an EpCAM-Binding Peptide.

To establish an easy-to-use and inexpensive method to detect the EpCAM, I here designed and synthesized a series of fluorogenic peptides. Specifically, I functionalized Ep114 that was previously selected using phage display.<sup>30</sup> Because Ep114 is composed of the 12 canonical amino acids, I functionalized Ep114 by replacing its amino acid to the aminophenylalanine modified with environmentally sensitive NBD-amPhe (Figure 2-1). I chose seven amino acids to be replaced with NBD-amPhe (Table 2-1) because these were expected to be less important for the binding of Ep114 to the EpCAM from alanine scanning results.<sup>30</sup> Although the synthesis of R7X met failure presumably due to the poor solubility, I synthesized the other six peptides by solid phase chemistry (Table 2-2).

**Table2- 2:** Synthesized peptide sequences and their MALDI TOFMS results.

Name	Peptide sequences	Calculated ( $[M+H]^+$ )	Found ( $[M+H]^+$ )
K1X	XHLQCVRNICWS	1795.82	1795.86
Q4X	KHLXCVRNICWS	1795.86	1795.96
V6X	KHLQCXRNICWS	1824.85	1824.87
R7X	KHLQCVXNICWS	1767.44	-----
N8X	KHLQCVRXICWS	1809.87	1809.96
I9X	KHLQCVRNXCWS	1810.85	1810.94
S12X	KHLQCVRNICWX	1836.89	1837.07

*Note: X represents NBD-amPhe. R7X met failure in the synthesis.*

### 3.2 Solubility

To examine whether the synthesized peptide ligands were soluble in water, I compared two absorbance spectra for each peptide (10 $\mu$ M peptide in ultrapure water) before and after the centrifuge. I confirmed that these six peptides were soluble in ultrapure water (Figure 2-3) and used them for further experiments.

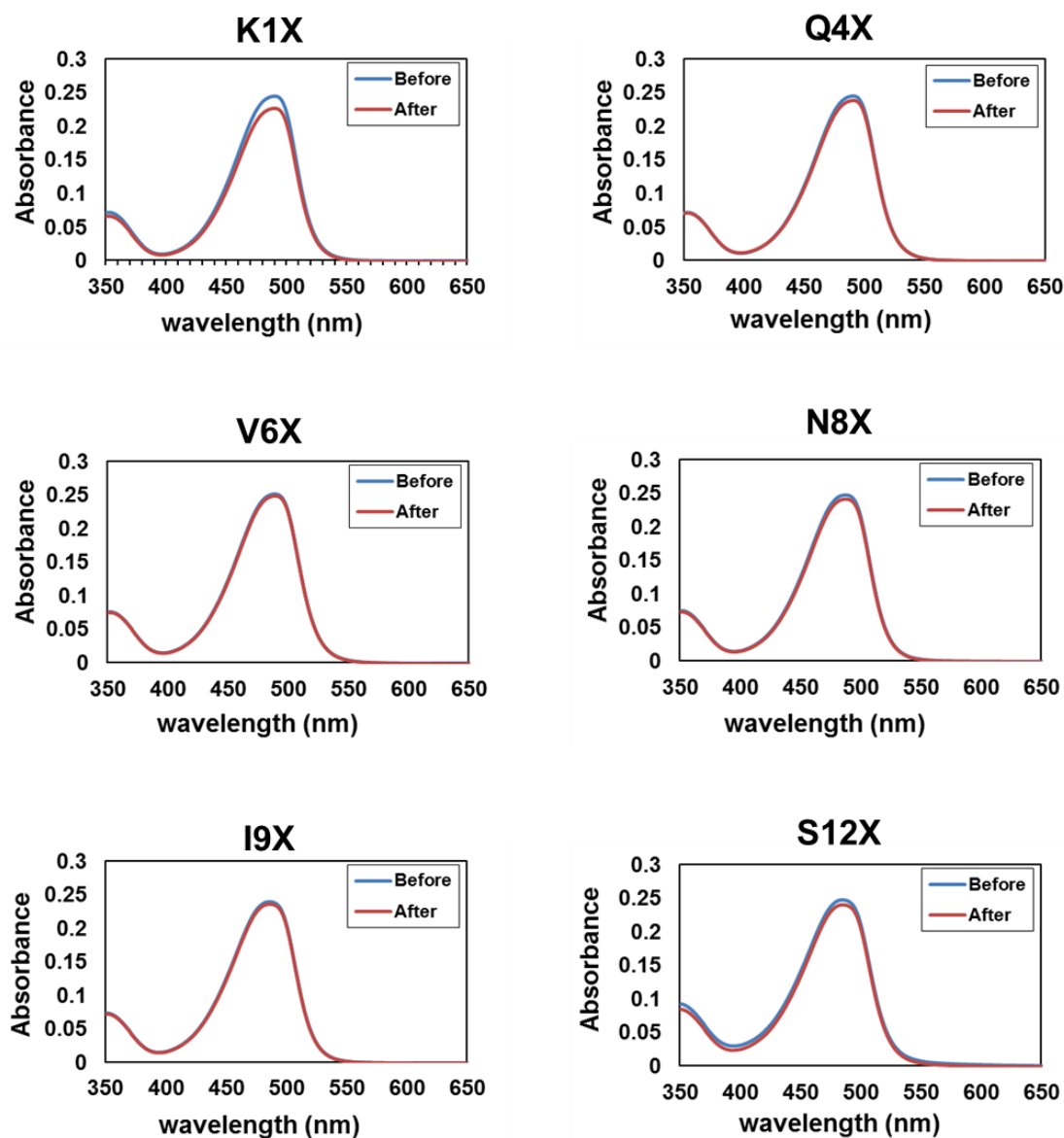


*Figure 2-3. All six peptides were soluble in ultrapure water. The absorbance spectra were effectively same as the spectra after centrifuge, implying that there were almost negligible precipitations for all peptides.*

### **3.3 Cell Imaging and Image Analysis to Obtain Fluorescence Intensity.**

To examine the fluorogenic activity of these peptides against EpCAM-positive cells, I added each peptide to the cultivation media of an EpCAM-positive cell line, HT-29. The fluorescence images clearly indicate that the two peptides, Q4X and V6X, emit fluorescence on the surface of HT-29 (Figure 2-4). On the other hand, none of the peptides emit fluorescence on the surface of an EpCAM-negative cell line, HT-1080 (Figure 2-4).

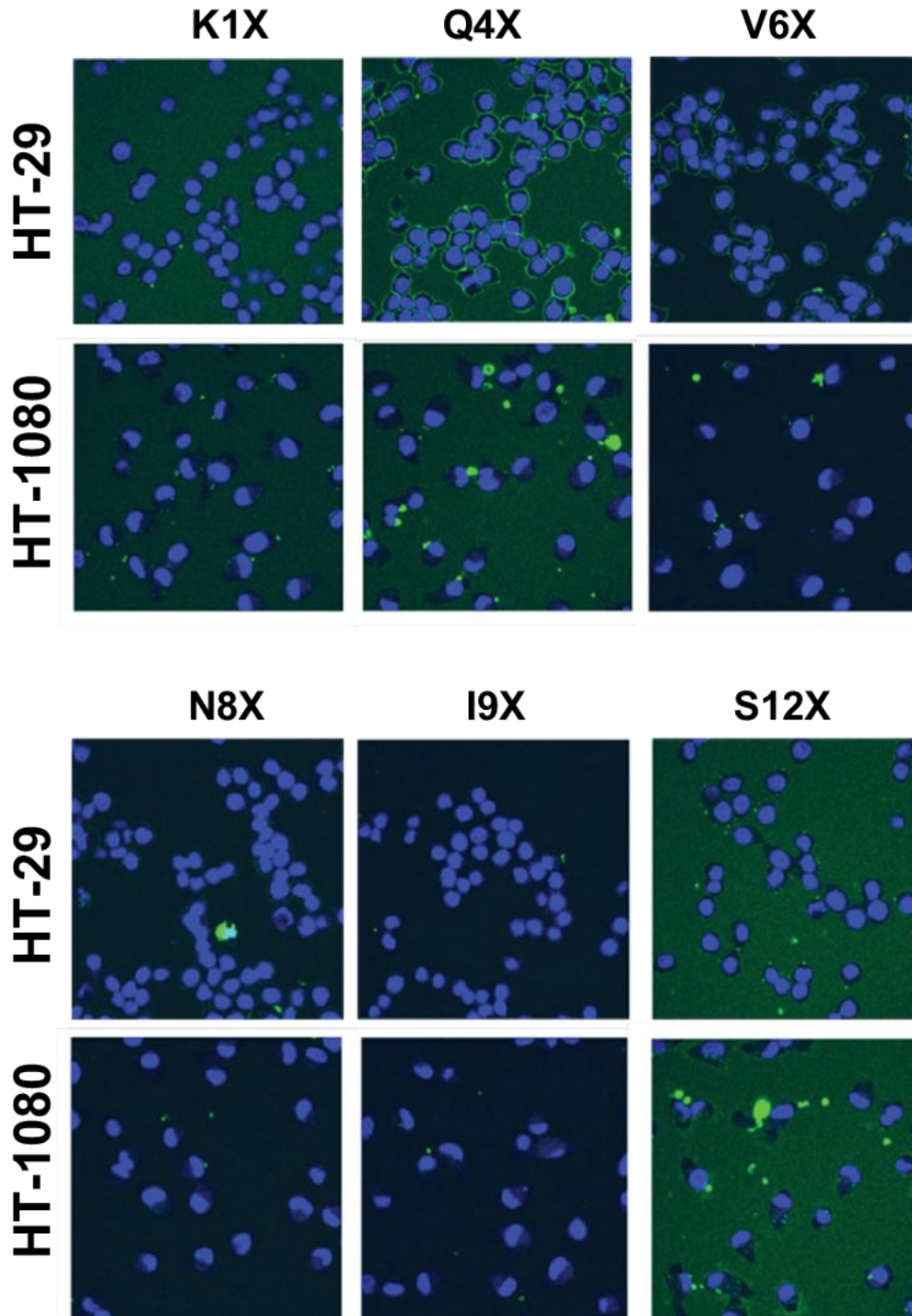


*Figure 2-4. The fluorescence images clearly indicate that the two peptides, Q4X and V6X, emit fluorescence on the surface of the EpCAM-positive cell line (HT-29). In contrast sharply, all peptides do not remarkably emit fluorescence on the surface of the EpCAM-negative cell line (HT-1080).*

Next, I examined whether the fluorescence intensity on the surface of HT29 depends on the Q4X concentration (Figure 2-5). I decided to use Q4X because Q4X exhibited a higher fluorescence signal for HT-29 than V6X. As I expect, the fluorescence intensity depends on the concentration of Q4X. I also note that even when I use Q4X at even 50 $\mu$ M, the background signal from the cultivation medium is relatively low, and the cell boundary is clearly visible. This is one of the essential features of a fluorogenic ligand to minimize the possibility of getting a false positive result.

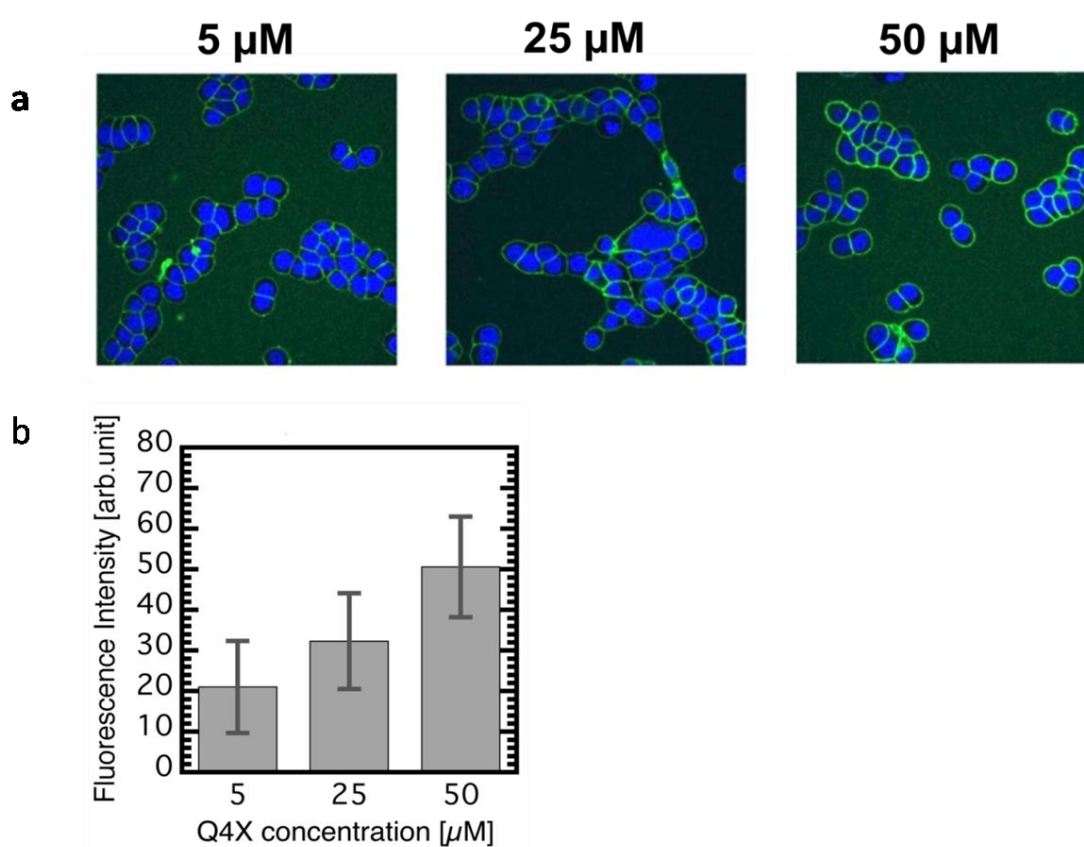


**Figure 2-5.** The fluorescence intensity on the cell membrane of HT-29 depends on the Q4X concentration. (a) Fluorescence images obtained by adding 5, 25, 50 $\mu$ M of Q4X into the cultivation media. (b) Fluorescence intensity of the cell membranes obtained from image analysis.

#### **4. CONCLUSION**

In this approach, the EpCAM binding peptide was functionalized with the environmentally sensitive fluorophore. The functionalized peptide ligand can fluorescently mark the EpCAM-positive cells by just adding the peptide ligand to the cultivation medium. Thus, wash-free fluorogenic peptide ligand would boost the development of next-generation devices for CTC diagnoses.

## 5. REFERENCES

1. Naghavi, M.; Abajobir, A. A.; Abbafati, C.; et al. Global, regional and national age-sex specific mortality for 264 causes of death, 1980–2016: a systematic analysis for the global burden of disease study 2016. *The Lancet***2017**, *390*, 1151-1210.
2. Fitzmaurice, C.; Allen, C.; Barber, R. M.; et al. Global, regional, and national cancer incidence, mortality, years of life lost, years lived with disability, and disability-adjusted life-years for 32 cancer groups, 1990 to 2015: a systematic analysis for the global burden of disease study. *JAMA Oncol.* **2017**, *3*, 524-548.
3. WHO, <http://www.who.int/mediacentre/factsheets/fs297/en/> (accessed on March 2018.)
4. Gupta, G. P.; Massague, J. Cancer metastasis: building a framework. *Cell***2006**, *127*, 679-695.
5. Chaffer, C. L.; Weinberg, R. A. A perspective on cancer cell metastasis. *Science***2011**, *331*, 1559-1564.
6. Wicha, M.S.; Hayes, D.F. Circulating tumor cells: not all detected cells are bad and not all bad cells are detected. *J. Clin. Oncol.***2011**, *29*, 1508-1511.
7. Ashworth, T. A case of cancer in which cells similar to those in the tumours were seen in the blood after death, *Aust. Med. J.***1869**, *14*, 146-149.
8. Pantel, K.; Alix-Panabieres, C.; Riethdorf, S. Cancer micrometastases. *Nat. Rev. Clin. Oncol.***2009**, *6*, 339-351.
9. Plaks, V.; Koopman, C. D.; Werb, Z. Cancer circulating tumor cells. *Science***2013**, *341*, 1186-1188.
10. Yu, M.; Stott, S.; Toner, M.; Maheswaran, S.; Haber, D.A. Circulating tumor cells: approaches to isolation and characterization. *J. Cell. Biol.* **2011**, *192*, 373-382.
11. Krebs, M. G.; Metcalf, R. L.; Carter, L.; Brady, G.; Blackhall, F. H.; Dive, C. Molecular

- analysis of circulating tumour cells-biology and biomarkers.*Nat. Rev.Clin.Oncol.***2014**, *11*, 129-144.
12. Miyamoto,D. T.;Sequist,L. V.; Lee,R.J. Circulating tumour cells-monitoring treatment response in prostate cancer.*Nat. Rev.Clin.Oncol.***2014**,*11*, 401-412.
  13. Parkinson,D. R.;Dracopoli,N.; Petty,B. G.; Compton,C.;Cristofanilli,M.;Deisseroth, A.; Hayes,D. F.;Kapke,G.; Kumar,P.; Lee,J.; Liu,M. C.; McCormack,R.; Mikulski,S.;Nagahara,L.;Pantel,K.; Pearson-White, S.;Punnoose,E. A.; Roadcap,L. T.;Schade,A.E.;Scher,H. I.;Sigman,C. C.;Kelloff,G. J. Considerations in the development of circulating tumor cell technology for clinical use. *J. Transl. Med.***2012**,*10*,138.
  14. Thege,F.I.;Lannin,T.B.;Saha,T.N.; Tsai,S.;Kochman,M.L.; Hollingsworth,M.A.;Rhim,A. D.; Kirby,B.J. Microfluidic immunocapture of circulating pancreatic cells using parallel EpCAM and MUC1 capture: characterization, optimization and downstream analysis.*Lab Chip.* **2014**, *14*, 1775-1784.
  15. Alix-Panabieres,C.;Pantel,K. Circulating tumor cells: liquid biopsy of cancer. *Clinical Chemistry.***2013**,*59*, 110-118.
  16. Nagrath,S.;Sequist,L. V.;Maheswaran,S.; Bell,D. W.;Irimia,D.;Ulkus,L.; Smith,M. R.;Kwak,E. L.;Digumarthy,S.;Muzikansky,A.; Ryan,P.;Balis,U.J.; Tompkins,R. G.; Haber,D. A.; Toner,M. Isolation of rare circulating tumour cells in cancer patients by microchip technology. *Nature***2007**,*450*, 1235-1239.
  17. Myung,J. H.;Launier,C. A.; Eddington,D. T.; Hong,S. Enhanced tumor cell isolation by a biomimetic combination of E-selectin and anti-EpCAM: implications for the effective separation of circulating tumor cells (CTCs).*Langmuir***2010**, *26*, 8589-8596.
  18. Veridex,L. CellSearch circulating tumor cell kit premarket notification-expanded

indications for use—metastatic prostate cancer, **2008**.

([www.accessdata.fda.gov/cdrh\\_docs/pdf7/K073338](http://www.accessdata.fda.gov/cdrh_docs/pdf7/K073338)).

19. Venkatraman,P.; Nguyen,T. T.;Sainlos,M.;Bilsel,O.;Chitta,S.;Imperiali,B.; Stern,L.J. Fluorogenic probes for monitoring peptide binding to class II MHC proteins in living cells. *Nat. Chem. Biol.***2007**,*3*, 222-228.
20. Sainlos,M.;Iskenderian,W. S.;Imperiali,B. A general screening strategy for peptide-based fluorogenic ligands: probes for dynamic studies of PDZ domain-mediated interactions.*J. Am. Chem. Soc.***2009**,*131*, 6680-6682.
21. Walkup,G. K.;Imperiali,B. Fluorescent chemosensors for divalent zinc based on zinc finger domains enhanced oxidative stability, metal binding affinity, and structural and functional characterization.*J. Am. Chem. Soc.***1997**, *119*, 3443-3450.
22. Ma,S.; Fang,D.C.; Ning,B.; Li,M.; He,L.; Gong,B. The rational design of a highly sensitive and selective fluorogenic probe for detecting nitric oxide.*Chem. Commun.***2014**, *50*, 6475-6478.
23. Zhuang,Y. D.; Chiang,P. Y.; Wang,C. W.; Tan,K. T. Environment-sensitive fluorescent turn-on probes targeting hydrophobic ligand-binding domains for selective protein detection.*Angew. Chem. Int. Ed.***2013**,*52*, 8124-8128.
24. Wang,W.;Uzawa,T.;Tochio,N.;Hamatsu,J.; Hirano,Y.; Tada,S.;Saneyoshi,H;Kigawa,T.; Hayashi,N.; Ito,Y.;Taiji,M.;Aigaki,T.; Ito,Y. A fluorogenic peptide probe developed by in vitro selection using tRNA carrying a fluorogenic amino acid.*Chem. Commun.* **2014**,*50*, 2962-2964.
25. Manandhar,Y.; Wang,W.; Inoue,J.; Hayashi,N.;Uzawa,T.; Ito,Y.;Aigaki,T.; Ito, Y. Interactions of in vitro selected fluorogenic peptide aptamers with calmodulin.*Biotechnol Lett.***2017**,*39*, 375-382.
26. Wang,W.; Zhu,L.; Hirano,Y.;Kariminavargani,M.; Tada,S.;

- Zhang,G.;Uzawa,T.;Zhang,D.; Hirose,T.;Taiji,M.; Ito,Y. Fluorogenic enhancement of an in vitro-selected peptide ligand by replacement of a fluorescent group.*Anal. Chem.***2016**,*88*, 7991-7997.
27. Manandhar,Y.; K.C., T. B.; Wang,W.;Uzawa,T.;Aigaki,T.; Ito,Y. In vitro selection of a peptide aptamer that changes fluorescence in response to verotoxin.*Biotechnol Lett.***2015**,*37*, 619-625.
28. Bai,L.; Du,Y.; Peng,J.; Liu,Y.; Wang,Y.; Yang,Y.; Wang,C. Peptide-based isolation of circulating tumor cells by magnetic nanoparticles.*J. Mater. Chem. B*, **2014**, *2*, 4080-4088.
29. Iwasaki,K.;Goto,Y.;Kato,T.; Yamashita,T.; Kaneko,S.;Suga,H. A fluorescent imaging probe based on a macrocyclic scaffold that binds to cellular EpCAM.*J. Mol.Evol.***2015**,*81*, 210-217.
30. Shiba,K.;Kokubun,K.;Suga,K. Peptides that bind to epithelial cell adhesion molecule, US9815866 B2, 2017.11.14.
31. Yoshida,M.; Hibino,K.; Yamamoto,S.; Matsumura,S.;Yajima,Y.;Shiba,K. Preferential capture of EpCAM-expressing extracellular vesicles on solid surfaces coated with an aptamer-conjugated zwitterionic polymer.*BiotechnolBioeng.***2018**, *115*, 536-544.
32. Ladokhin,A. S.;Isas,J. M.;Haigler,H. T.; White,S.H. Determining the membrane topology of proteins: insertion pathway of a transmembrane helix of annexin 12.*Biochemistry***2002**, *41*, 13617-13626.

# **CHAPTER 3: IN VITRO SELECTION OF ELECTROCHEMICAL PEPTIDE PROBES USING BIOORTHOGONAL tRNA FOR INFLUENZA VIRUS DETECTION**

## **1. INTRODUCTION**

The preparation of molecular-recognition ligands is important for basic research, as well as for clinical applications. To prepare a ligand for an arbitrary target, antibodies are

most commonly used.<sup>1</sup> However, some inherent characteristics related to antibody properties and production limits the usefulness and clinical efficacy of this approach. The generation of antibodies depends on animal immunization, which rules out some targets, and requires laborious and expensive biological processes. To overcome these problems, during the last three decades it has become possible to select a peptide *in vitro* from a library of random sequences.<sup>2,3</sup> The selected peptides, consisting of 5–20 amino acids, are called peptide aptamers and can specifically bind to arbitrary targets.

Progress in bioorthogonal approaches<sup>4,5</sup> has enabled the selection of peptides from a library containing non-natural amino acids that do not appear in the standard codon table.<sup>6</sup> For example, by incorporating a ligand onto a peptide or macrocyclic molecule, the binding affinity of the peptide aptamer can be enhanced.<sup>7-13</sup> The addition of p-boronphenylalanine<sup>14</sup>, or 3,4-dihydroxyphenylalanine<sup>15</sup> has been reported to enhance the specific binding affinity to glycans and metal oxides, respectively. In addition to these enhancements in affinity, other functions can be introduced to the peptide aptamers. For example, incorporation of an azobenzene moiety produced a photo-switching function.<sup>16-19</sup> Incorporation of environment-sensitive fluorescent groups produced a fluorogenic function in *in vitro*-selected peptide probes.<sup>20-22</sup>

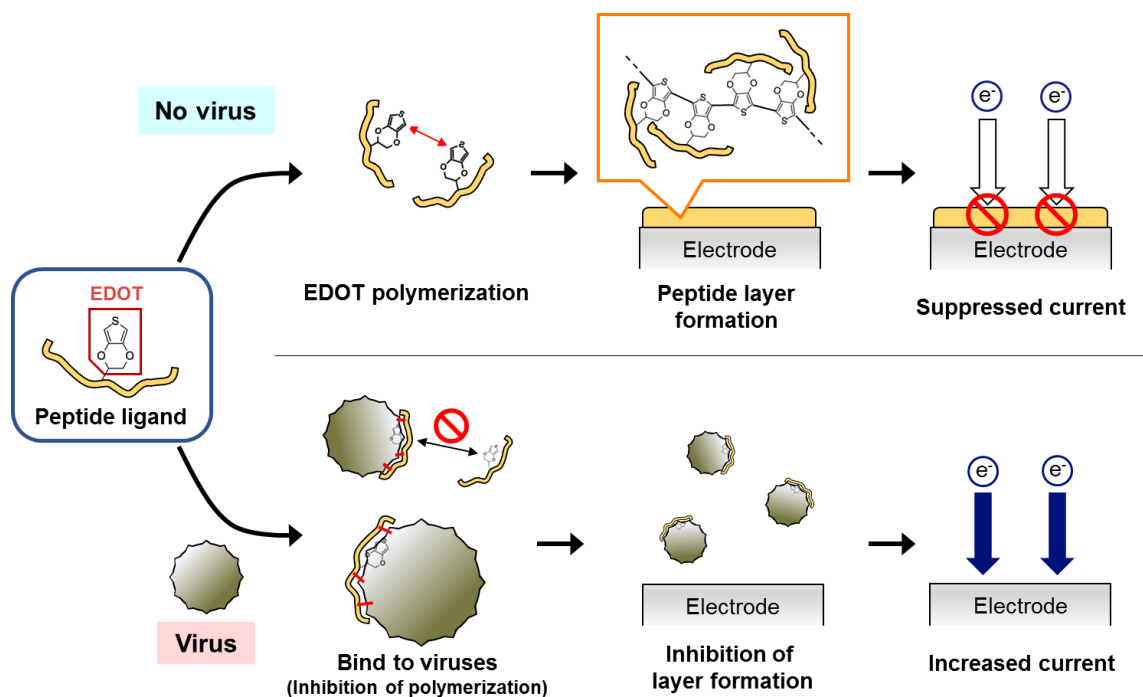


**Figure 3-1.** Basic strategy for detection of influenza virus using an electro-sensitive peptide ligand.

Here, I have developed a new sensing mechanism for detecting the influenza virus by incorporating an electrochemically sensitive 3,4-ethylenedioxythiophene (EDOT) moiety into a peptide ligand. The EDOT molecule has been widely employed as a conducting substrate for various biosensing platforms either in its monomeric form or as the polymer PEDOT, mainly because it has good biocompatibility and stability in biological buffers. The target molecules have ranged from small molecules, including gases<sup>23</sup>, ions<sup>24</sup>, and a neurotransmitter<sup>25</sup> to large biomolecules, including DNA<sup>26,27</sup> and proteins.<sup>28-30</sup> For most of these studies, the sensing mechanism was based on monitoring changes in the PEDOT conductivity or surface charge, after the targeted molecules were captured. The use of amperometric biosensors<sup>31, 32</sup> and electrochemical transistors<sup>33, 34</sup> were also reported in previous researches. Here I present a new detection system. While in most electrochemical biosensors the probes are immobilized on substrates, in our detection system the selected peptide ligands are dispersed in biological buffers to capture the virus. This homogeneous

capture process is theoretically favorable for efficient and selective capture. As shown in Figure 3-1, this system works by monitoring the electropolymerization of the peptide ligand. During the procedure, if no influenza virus is present after mixing a sample with a solution containing the peptide ligand, the peptide ligands become electropolymerized and are deposited as a polymer layer on the electrode surface. This peptide deposition on the electrode reduces the electron transfer between the redox molecules and the electrode. In contrast, if the influenza virus is present in a sample, some of the peptide ligands bind to the virus and are unavailable for the electropolymerization of EDOT. In this case, the overall electron transfer to the electrode increases, depending on the amount of influenza virus present in the original sample. Therefore, an amplified "turn-on" signal should be observed with this sensing platform.

## **2. MATERIALS AND METHODS**

### **2.1 Synthesis of EDOT-Aminophenylalanyl-tRNA**

EDOT-aminophenylalanine-tRNA was prepared as shown in Figure 3-2. tBoc- $\epsilon$ -aminophenylalanine was coupled to 5'-O-phosphoryl-2'-deoxycytidylyl-(3'-5') adenosine (pdCpA) to give the corresponding aminophenylalanine-pdCpA, (AF-pdCpA). Then, a DMSO solution of EDOT-succinimidyl ester was treated with a DMSO solution of AF-pdCpA (5mM, 40 $\mu$ L) in aqueous pyridine-HCl (5M, pH 5.0, 80 $\mu$ L), and the resulting mixture was incubated at 37°C for three hour. The EDOT-AF-pdCpA product was purified by reversed-phase HPLC using an XTerra C18 column (4.6  $\times$  20mm, 2.5 $\mu$ m particle size; Waters, Milford, MA, USA), which was eluted at a flow rate of 1.5mL min<sup>-1</sup> with a linear gradient of 0–100% acetonitrile in 0.1% trifluoroacetic acid over a period of 10min. The identity of the product was confirmed by matrix-assisted laser desorption/ionization time-of-flight mass spectrometry (Voyager, Applied Biosystems, Foster City, CA, USA). The

resulting EDOT-AF-pdCpA was ligated to an amber-suppressor tRNA, which was derived from *Mycoplasma capricolum* Trp1tRNA without the 3' dinucleotide, using a previously reported chemical ligation method.<sup>35</sup> The purified EDOT-AF-tRNA molecules were lyophilized and stored at  $-80^{\circ}\text{C}$ .

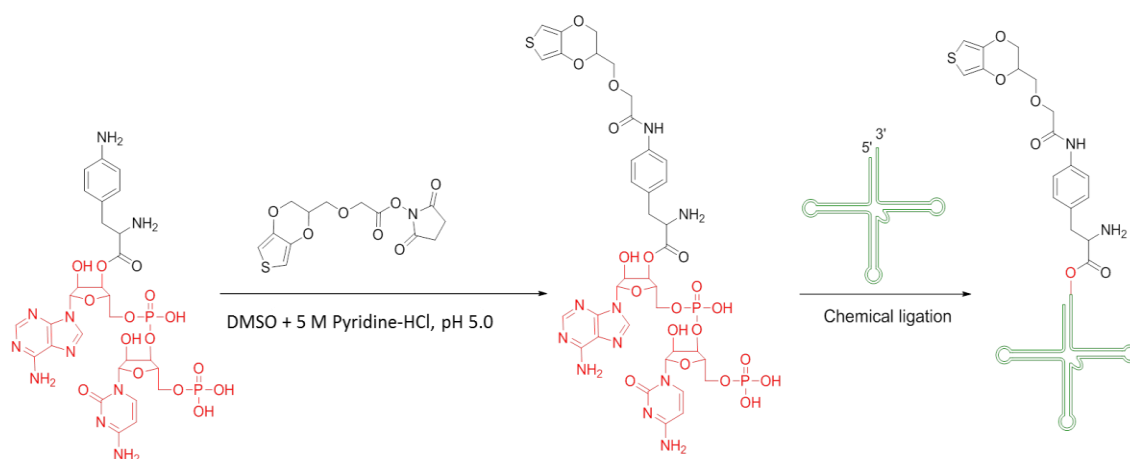


**Figure 3-2.** Scheme for the preparation of EDOT-aminophenylalanyl-tRNA

## 2.2 *In Vitro* Selection of an Electrosensitive Peptide Ligand

The selection protocol is shown schematically in Figure 3-3. A 13Trx plasmid was employed in the current study carrying a promoter sequence for the T7 RNA polymerase, an *Escherichia coli* ribosome-binding sequence, an *SfiI* restriction enzyme sequence, a protein-linker sequence, and a ribosome-arrest sequence. Random double-stranded DNA (dsDNA) was also prepared in parallel. The library sequences were obtained from Eurofins Genomics (Tokyo, Japan). These sequences were based on the general sequence 5'-ATATGGCCATGCAGGCC (VVN)3TAG(VVN)7GGCCAGCTAGGCCAGTT-3', where V represents G, C, or A; and N represents G, C, T, or A. The VVN sequence covers only 10 of the naturally-occurring amino acids, and was selected to exclude hydrophobic amino acids, such as leucine, valine, and tryptophan, and stop codons (e.g., TAG, TAA, and TGA). This design strategy was selected for peptides with high solubility in an aqueous buffer, and to

allow for the incorporation of one EDOT molecule at the same position in each library sequence, whilst avoiding the unintentional incorporation of additional EDOT molecules.

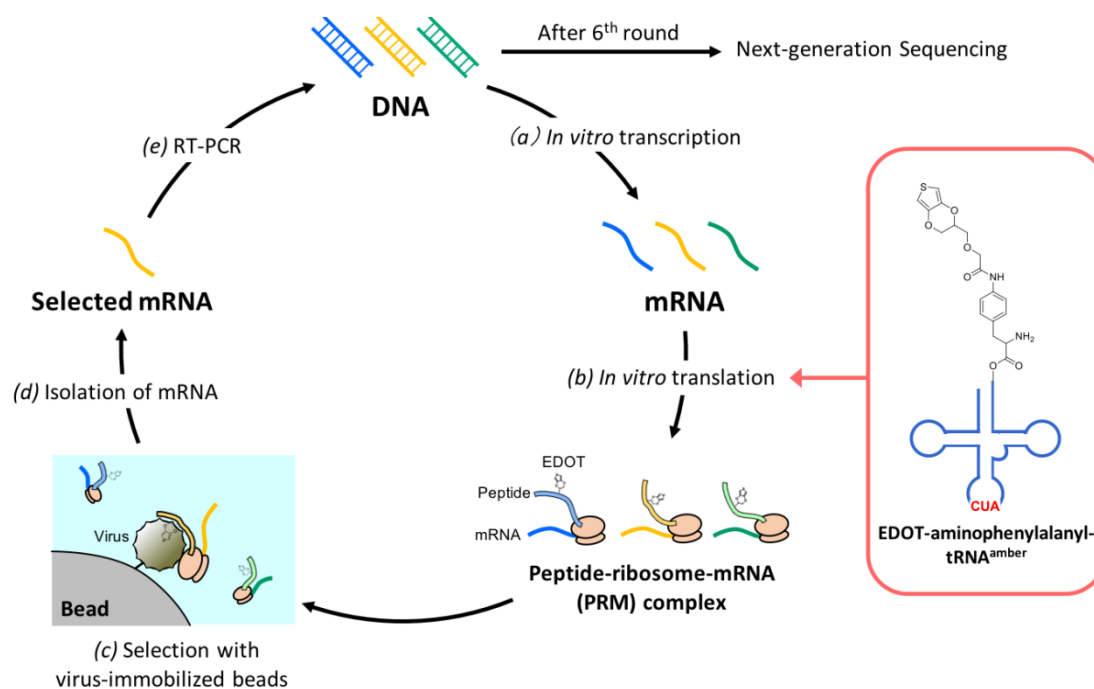


**Figure 3-3.** Basic principles of the *in vitro* selection process using ribosome display and misacylated tRNA. A DNA library was transcribed into an mRNA library. The mRNA library and EDOT-AF-tRNA (tRNA carrying EDOT-coupled aminophenylalanine) were then introduced into a cell-free translation system, resulting in the production of an EDOT-modified peptide, which was displayed on the surface of the ribosome. After an affinity selection process, the eluted complexes were collected and subsequently dissociated. The mRNA responsible for encoding the peptide sequence was recovered and used for the next round of selection after RT-PCR.

To run selection, dsDNA was prepared by one cycle of a polymerase chain reaction (PCR) using Takara Ex taq DNA polymerase (Takara Bio Inc., Otsu, Shiga, Japan), and the crude material was purified with a QIAquick PCR Purification kit (Qiagen, Valencia, CA, USA). The resulting dsDNA and 13Trx plasmid were digested with a restriction enzyme (SfiI; New England Biolabs, Ipswich, MA, USA) and fused (DNA Ligation Kit; Takara Bio).

Finally, a dsDNA library was prepared by PCR with new primers (New-T7-fp-rec-1: 5'-GTAATACGACTCACTATAGGCCGCGTCGACAATAA-3' and New-rp-fp-M13-NS: 5'-GATTACGCCAAGCTGAGTGAGA-3'). Transcription was performed at 37°C for three h, and the product was then treated with DNase. The mRNA was purified using an RNeasy kit (Qiagen). *In vitro* translation was performed using a PURESYSTEM Classic II kit (Wako Pure Chemical Industries Ltd., Osaka, Japan) with EDOT-AF-tRNAs. Given that the mRNA did not contain any stop codons, it was not possible for the ribosome to release the mRNA or the translated peptide, and the mRNA, ribosome, and peptide became coupled as a ternary complex (the PRM complex, see Figure 3-3). The reaction was stopped by placing the mixture on ice for 10 min. The translated solution was then incubated with inactivated influenza virus A/California/07/2009 (H1N1, kindly provided as a gift from Denka Seiken Co., Ltd., Tokyo, Japan), which was immobilized on silica affinity beads (Sumitomo Bakelite Co., Ltd., Tokyo, Japan) in the selection buffer (0.1% Tween 20, 50mM Tris-acetate, 150 mMNaCl, 50 mM magnesium acetate, pH 7.4) at 4°C for 1h. The virus-immobilized beads were collected by centrifugation at 10,000×g for 5 min and washed with buffer (50mM Tris-acetate, 150mM NaCl, 50mM magnesium acetate, pH 7.4) at 4°C to remove any free mRNA-ribosome-peptide complexes. The mRNA was recovered from the bound mRNA-ribosome-peptide complex following a 30min period of incubation with ethylenediaminetetraacetic acid at room temperature, which allowed for the removal of the Mg<sup>2+</sup> ions and resulted in the detachment of the ribosomes from the mRNA. The isolated mRNA was purified using an RNeasy kit. Preparative PCR was performed to amplify the reverse transcription products, and the DNA product was purified using a QIAquick PCR purification kit (Qiagen). The isolated DNA was used as the template for the next round of selection.

After six rounds, the sequences of the selected DNAs were analyzed by the Next-Generation Sequencing (NGS) service provided by Takara-bio (Otsu, Japan) using a

MiSeqsequencer (Illumina, San Diego, CA, USA). The obtained sequences (approximately 200,000) were trimmed to use only the random library sequences and converted from nucleotide sequences to amino acid sequences. The trimmed and translated reads were aggregated, and those with 90% sequence identity were clustered using Cd-hit.<sup>36</sup> The clusters representing singletons (with a multiplicity of one) were discarded, and the remaining clusters were ranked based on the sum of multiplicities within each cluster. Representative sequences, which are defined as the reads with highest multiplicities, were determined for the clusters. Representative sequences and multiplicities for each cluster were tabulated, and the top 100 clusters were identified as the enriched sequences mediated by the selection process (Appendix 4).

### **2.3 Preparation of EDOT Aminophenylalanine**

To add electrochemical functionality into synthesized peptides. A non-natural amino acid, Fmoc-aminophenylalanyl EDOT (EDOTaa), was prepared according to the scheme shown in Figure 3-4 and product was confirmed by NMR analysis in each step (Appendix 5 and 6).

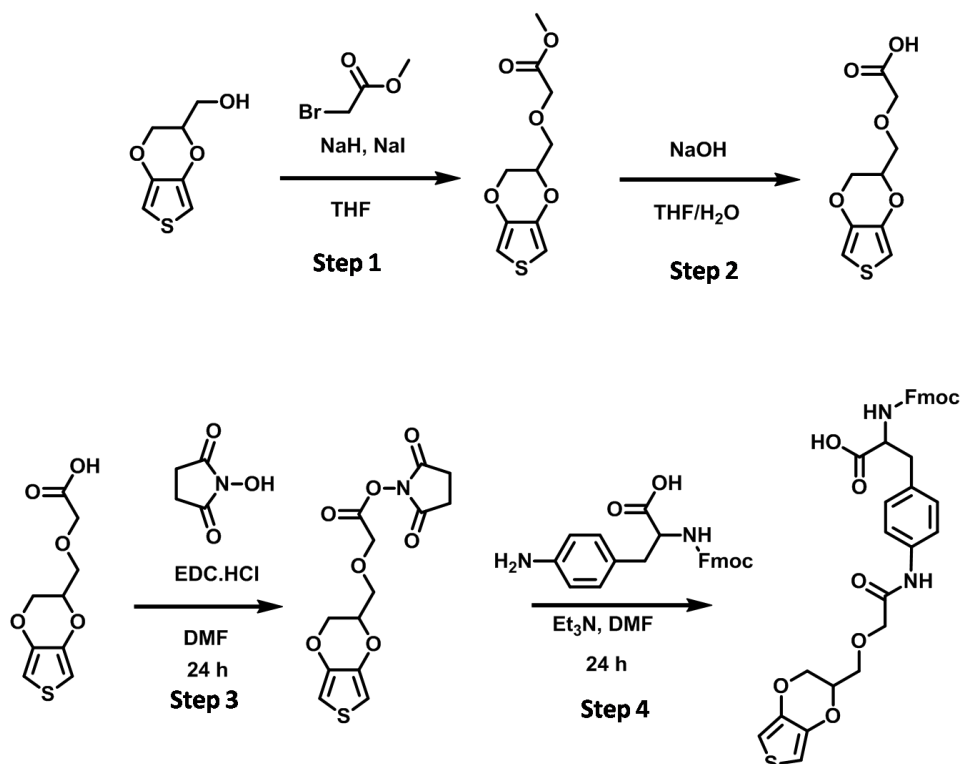


**Figure 3-4.** The synthesis scheme of Fmoc protected EDOT-coupled aminophenylalanine

**Step 1:** Synthesis of methyl 2-((2,3-dihydrothieno[3,4-b][1,4]dioxin-2-yl)methoxy)acetate (1). A 100mL round-bottom flask was charged hydroxymethyl EDOT (430mg, 2.62mmol), sodium iodide (NaI, 7.5mg, 0.5mmol) and sodium hydride (NaH, 60% suspension in mineral oil, 120mg, and 3.0mmol). The flask was backfilled with argon gas (3 times). Then, dehydrated tetrahydrofuran (10mL) was introduced, and the suspension was stirred for 15 min at room temperature (r.t.) before cooled in an ice bath. To this, added dropwise methyl bromoacetate (0.28mL, 0.46 g, 3.0mmol), and the reaction mixture was stirred for 46 h in an ice bath. The solvent was removed with a rotary evaporator and added water to the reaction mixture. The crude product was extracted with ethyl acetate three times, and combined organic layers were washed with brine before drying on  $MgSO_4$ , filtered, and the filtrate was evaporated. The residue was purified with a size exclusion chromatography (Yield 62 %).

**Step 2:** Synthesis of 2-((2,3-dihydrothieno[3,4-b][1,4]dioxin-2-yl)methoxy)acetic acid (2).

To methyl 2-((2,3-dihydrothieno[3,4-b][1,4]dioxin-2-yl) methoxy) acetate (Compound 1, 400 mg, 1.63mmol) was dissolved in tetrahydrofuran (10mL) in a 100mL round-bottom flask, and freshly prepared aqueous NaOH solution (2M, 11mL) was added. The reaction mixture was stirred vigorously overnight until the starting material was completely consumed which was confirmed by thin layer chromatography (TLC). Then, the mixture was acidified to pH <3 using diluted HCl aqueous solution and then extracted with ethyl acetate (5 times). The combined organic layers were washed with water (until a neutral pH obtained) over ten times before drying over MgSO<sub>4</sub>, filtered and the filtrate was evaporated. The compound 2 was obtained as thick, colorless oil that solidified upon standing overnight (White solid, Yield: 69%).

**Step 3:** Synthesis of 2,5-dioxopyrrolidin-1-yl 2-((2,3-dihydrothieno[3,4-b][1,4]dioxin-2-yl)methoxy)acetate (3). A mixture of 2-((2,3-dihydrothieno[3,4-b][1,4]dioxin-2-yl)methoxy)acetic acid (Compound 2, 175 mg, 0.71 mmol), 1-(3-dimethyl-aminopropyl)-3-ethylcarbodiimide hydrochloride (EDC HCl, 190mg, 0.99mmol), and N-hydroxysuccinimide (98mg, 0.86mmol, 1.2 eq) in 5mL of anhydrous DMF was stirred under argon atmosphere at room temperature for 24 h. After completion of the reaction, acetone (10mL) and water (10 mL) were added, and the mixture was extracted (3X30mL) with a solvent mixture of diethyl ether and ethylacetate (2/1 vol/vol). The combined organic layers were washed with water before drying over MgSO<sub>4</sub>, filtered, and the filtrate was evaporated. The obtained crude product was then purified through column chromatography using a solvent ratio of 5:95 methanol and dichloromethane, and then further purified by size exclusion chromatography (yield: 75 %).

**Step 4:** Synthesis of EDOT-Fmoc-Phenylalanine (4). 2,5-dioxopyrrolidin-1-yl 2-((2,3-dihydrothieno[3,4-b][1,4]dioxin-2-yl) methoxy)acetate (200mg, 0.61mmol) and Fmoc-Phe-(4-NH<sub>2</sub>)-OH ( 245mg, 0.61mmol) were dissolved in a 5ml dehydrated dimethylsulfoxide.

Pyridine-HCl (5M, pH= 5) was separately prepared by mixing 5ml of Hydrochloric acid, 4.75ml pyridine and 1.95ml of water at 0°C. A freshly prepared pyridine-HCl solution was then injected to the reaction mixture and stirred at 37°C for 24h. After completion of the reaction, ethyl acetate was added to the reaction mixture and the organic layer was washed with citric acid aqueous solution for three times before drying over MgSO<sub>4</sub>, filtered, evaporated the solvent to obtain the crude product (yield: 46%).

### **2.3 Synthesis and Purification of Peptide Sequences.**

Selected peptides sequences from the NGS analysis were synthesized using a conventional Fmoc-solid phase peptide synthesis method on preloaded Wang resin (Watanabe Chemical Industries, Hiroshima, Japan). Peptide coupling and deprotection reactions were performed with a Discover microwave (CEM Corporation, Matthews, NC, USA) using standard CEM protocols, with mild N<sub>2</sub> bubbling, at a 0.1mmol scale (at 70°C, 5 and 3min for coupling and deprotection, respectively). EDOTaa was attached using optimized conditions for coupling (10min at 25°C and 25 min at 50°C) and deprotection (5 min at 50°C). After coupling EDOTaa, elongation with other amino acids was also carried out at reduced temperature but for prolonged times (at 50°C, 7 and 5min for coupling and deprotection, respectively) to prevent the degradation of the non-natural amino acid. The elongation of the peptide sequence was confirmed by checking the MALDI MS at various steps, and after final cleavage from the resin. For cleavage, a ΔTIS cocktail consisting of an 85:5:4:4:2 (v/v) mixture of trifluoroacetic acid: phenol: thioanisole: ddH<sub>2</sub>O: ethanedithiol was used to avoid reducing the thiophene moiety. The cleaved peptides were precipitated via chilled diethyl ether and centrifuged, and the peptide pellet was washed and lyophilized for further purification. For the peptide-binding assay, the N-terminal primary amine group of the peptide was modified with fluorescein at the RIKEN Brain Science Institute, Japan. The fluorescein-labeled reaction was carried out on a solid support using a fluorescein-NHS ester

(Thermo Fisher Scientific Inc., Rockford, IL, USA). After confirming the reaction, the resin was thoroughly washed, and the peptide was cleaved as described above.

Peptide purification and analysis were performed using an Extrema HPLC (JASCO, Tokyo, Japan). Purification was performed with a linear gradient using 0.1% trifluoroacetic acid in water, and acetonitrile in a COSMOSIL 5C18-AR-II column (NacalaiTesque, Kyoto, Japan). Finally, the prepared peptides were characterized by HPLC, as well as MALDI-TOF MS before the interaction analysis.

#### **2.4 Evaluation of Peptide Binding Affinity**

To determine the binding affinity using immobilized microbeads, first, the inactivated influenza virus (1 $\mu$ g) was immobilized on 20mg of silica microbeads (Sumitomo Bakelite, Tokyo, Japan) following the manufacturer's protocol. Then, the peptides labeled with fluorescein were incubated with 300 $\mu$ g of the virus-immobilized silica microbeads containing approximately 15ng of inactivated influenza viral particles, maintaining the volume at 200 $\mu$ L in the selection buffer at 25°C for one hour. During the incubation process, the beads and peptide solution were continuously mixed using a microtube mixer (ThermoMixer C; Eppendorf, Hamburg, Germany) at 1000rpm. After incubation, the beads and peptide solution were centrifuged at 10,000rpm for 5min, and the solution containing unbound peptide was discarded. The peptide-bound beads were washed three times with 300 $\mu$ L washing buffer (50mM Tris-acetate, 150mMNaCl, 50mM magnesium acetate, pH7.4) and were protected from light during the experiment. For the fluorescence measurements, the bead volume was adjusted to 100 $\mu$ L, and the suspension was transferred to a 96-well black microplate (PerkinElmer, Waltham, MA, USA), and the fluorescence intensities were quantified at 530 nm using a microplate reader (Enspire 2300; PerkinElmer, Hamburg, Germany). All data are presented as the mean values  $\pm$  SD (n = 3).

## 2.5 Biological Specificity

The biological specificity of the binding of the Sequence 2 peptide to the influenza virus was studied using a dot blot analysis. A polyvinylidene fluoride (PVDF) membrane (Immobilon-P Transfer Membrane, pore size: 0.2 $\mu$ m; Millipore, Bedford, MA, USA) was immersed in methanol followed by blotting with a buffer solution [25mM Tris, 192mM glycine, 20% (v/v) methanol]. The membrane was then placed on wet filter paper to avoid excessive drying. A 2 $\mu$ L portion of 1 mg mL<sup>-1</sup> inactivated influenza virus in PBS buffer was then dropped onto the membrane. Similar samples of Epstein–Barr virus, gelatine, and bovine serum albumin (Sigma-Aldrich) were also dropped onto the membrane as negative controls. After it had dried out, the membrane was immersed in methanol, followed by the blotting buffer. The membrane was then immersed in a blocking buffer (5% w/v of ECL Advance blocking agent) and a TBS-T buffer (50mM Tris, 150mM NaCl, 0.05% Tween 20, pH 7.4), and incubated for one hour at room temperature to block any nonspecific binding. The membrane was briefly washed with TBS-T buffer and put on parafilm to keep it wet. Fluorescein-labeled Sequence 2 peptide (500nM) was dropped on to the membrane to cover the entire area. After being incubated for 1h at room temperature in the dark, the membrane was washed three times with TBS-T buffer for 10min each time, and an image of the surface of the membrane was recorded using a Molecular Imager FX system (Bio-Rad Laboratories, Hercules, CA, USA) at the RIKEN Brain Science Institute, Japan. The image was analyzed using the ImageJ64 software package to find the integrated densities of the spots.

## 2.6 Electropolymerization of EDOT-Conjugated Peptide Ligand

Electrochemical experiments were carried out using an Autolabpotentiostat system (ALS/CH, electrochemical analyzer, 700C, CH Instruments Inc. Austin, TX, USA). A gold electrode (ALS Au 6 X 3.0 mm; ALS Co., Ltd., Tokyo, Japan) was used as the working

electrode, and a platinum wire and an Ag/AgCl electrode (RE-1S, ALS Co., Ltd., Tokyo, Japan) were used as the counter and reference electrodes, respectively (Figure 3-5). After setup, the distance between the counter/reference electrodes and the working electrode was kept at 1mm. Twelve microliters of the Sequence 2 peptide solution were dropped onto the working electrode, ensuring that the counter and reference electrodes were submerged in the solution. Cyclic voltammetry (CV) ( $-0.6$  to  $0.95\text{V}$  vs. Ag/AgCl, scanning at  $0.1\text{Vs}^{-1}$ ) was conducted during the polymerization reaction in  $0.1\text{M}$  Tris-HCl buffer (pH 7.0) supporting electrolyte. After the polymerization reaction, the gold electrode was gently washed with Milli-Q water to remove unpolymerized peptide. For the optimization of the electropolymerizing conditions, Sequence 2 peptide polymerization was performed at various oxidative potentials ( $-0.6$  and  $+0.70$  to  $+1.4\text{V}$ ). At lower potentials (below  $+0.75\text{V}$ ) the peptide did not polymerize, because no current inhibition was detected on the gold electrode even after 15 cycles of polymerization. At higher potentials, the peptide polymerized after fewer cycles and started to be destroyed. Thus, I selected the parameters of  $-0.6$  to  $0.95\text{V}$  at  $0.1\text{Vs}^{-1}$  scanning speed for 12 cycles for further analysis.

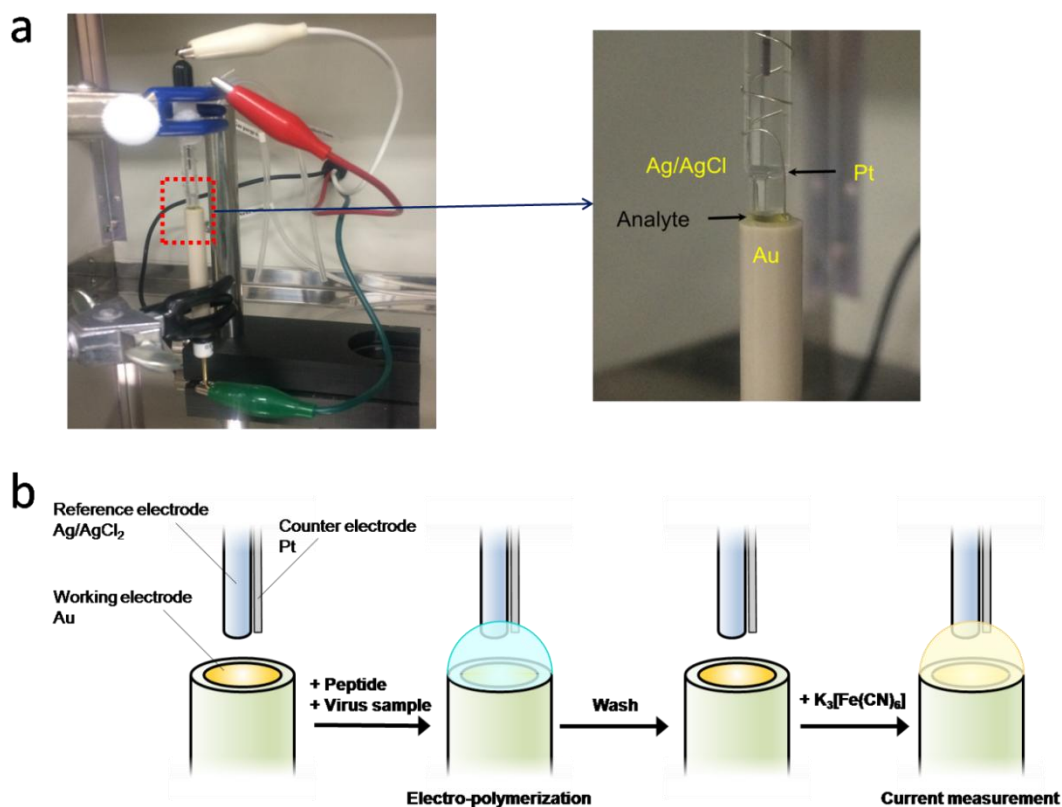


**Figure 3-5.** Electrochemical Analysis (a) Laboratory experimental setup (b) Process of electrochemical measurement.

For the Fourier transform infrared (FT-IR) measurements, electropolymerization of the peptide was performed on a gold-coated chip (5 x 10 mm) cut from a gold-coated silicon wafer (Sigma-Aldrich). The experimental setup was similar to the peptide electropolymerization experiment described above, but a gold-coated silicon chip was used instead of the gold working electrode. A 20 $\mu$ L portion of a 2mg mL<sup>-1</sup> solution of Sequence 2 peptide in 0.1M Tris-HCl buffer (pH 7.0) was dropped onto the gold-coated silicon chip, and cyclic voltammetry (-0.6 to 0.95V vs. Ag/AgCl, at a scanning speed of 0.1Vs<sup>-1</sup> for 12 cycles) was performed using a potentiostat system. The gold-coated chip was dipped in Milli-Q water to remove any unpolymerized peptide. After drying, the sample was analyzed by FT-IR spectroscopy using an FT-IR 4100 system (Jasco, Tokyo, Japan). The FT-IR spectra were recorded in the range of 4500–600cm<sup>-1</sup> using an average of 80 scans to increase the signal to

noise ratio, and the spectral resolution was  $4\text{cm}^{-1}$ . The FT-IR spectrum of the Sequence 2 peptide monomer was also measured for comparison.

## 2.7 Electrochemical Detection of Influenza Virus

Three electrodes were set up as described above for the peptide polymerization (Figure 3-5). First, the effective concentration of the peptide was determined by running the polymerization reaction on the gold electrode ( $-0.6$  to  $0.95\text{V}$  vs.  $\text{Ag}/\text{AgCl}$ , at a scanning speed of  $0.1\text{Vs}^{-1}$  for 12 cycles) using various concentrations, and then the current was measured. The cathodic current was effectively suppressed at  $0.1\text{mg mL}^{-1}$  of the peptide (Appendix 8), so this concentration of peptide was used. For the detection system,  $12\mu\text{L}$  of Sequence 2 peptide was dropped on to the gold electrode, ensuring that the entire surface of the electrode was covered. Cyclic voltammetry was performed for the polymerization reaction, as described above. After cleaning, the working electrodes were set up in the same manner as before, and  $12\mu\text{L}$  of  $10\text{mM}$  potassium ferricyanide/ $\text{K}_3[\text{Fe}(\text{CN})_6]$  was dropped onto the surface of the gold electrode. Then, cyclic voltammetry ( $-0.3$  to  $0.65\text{V}$  vs.  $\text{Ag}/\text{AgCl}$ , at  $0.1\text{Vs}^{-1}$ ) was performed, and the current at the gold electrode was recorded. In the same way,  $12\mu\text{L}$  of the mixture of Sequence 2 peptide (final concentration,  $0.1\text{mg mL}^{-1}$ ) and various concentrations of influenza virus were applied to the detection system, and the current at the gold electrode was recorded as a function of the influenza virus concentration. The spectrum of the second cycle is shown in the figures because the spectra stabilized after the second cycle. To determine the limit of detection (LOD) of the system, the anodic current obtained after the electrochemical analysis of inactivated influenza virus at different concentrations in the presence of a fixed amount of Sequence 2 Peptide was analyzed statistically at the 95% confidence interval. The p-values of the different concentrations were calculated by

comparing the results with those recorded in the absence of influenza virus using Student's t-test.

## **2.8 Interference of Microorganism on Electrochemical Detection System.**

The interference of the common microorganism in an electrochemical detection system was examined using *Staphylococcus aureus* and *Streptococcus pneumoniae*. They were kindly provided by Dr. Suresh Panthee at Teikyo University Institute of Medical Mycology, Japan, after heat treatment at 121°C for 15min by an autoclave. For this measurement, we used the much higher number of the microorganisms ( $1 \times 10^6$  colony-forming unit (CFU)  $\text{mL}^{-1}$ ), than the number of staphylococci species in saliva ( $10^2$ – $10^4$  CFU  $\text{mL}^{-1}$ ).<sup>37</sup> Specifically, all three electrodes were set up as described above for the peptide polymerization and then the current on clean working electrode was recorded by cyclic voltammetry ( $-0.3$  to  $0.65\text{V}$  vs. Ag/AgCl, at  $0.1\text{Vs}^{-1}$ ) measurement using  $12\mu\text{L}$  of  $10\text{mM}$   $\text{K}_3[\text{Fe}(\text{CN})_6]$  in  $0.1\text{M}$  Tris-HCl buffer (pH 7.0). Cyclic voltammetry was performed along the polymerization cycle ( $-0.6$  to  $0.95\text{V}$  vs. Ag/AgCl, at a scanning speed of  $0.1\text{Vs}^{-1}$  for 12 cycles) using  $12\mu\text{L}$  of Sequence 2 peptide ( $0.1\text{mg mL}^{-1}$ ) in presence of  $1 \times 10^6$  CFU  $\text{mL}^{-1}$  of microorganism, only Sequence 2 peptide ( $0.1\text{mg mL}^{-1}$ ) and only the microorganism  $1 \times 10^6$  CFU  $\text{mL}^{-1}$  in  $0.1\text{M}$  Tris-HCl buffer (pH 7.0). Then the current at the gold electrode was re-recorded, as described above, and the obtained cyclic voltammograms were compared.

## **3. RESULTS AND DISCUSSION**

### **3.1 Selection of Electrosensitive Peptides**

#### **3.1.1 *In vitro* selection using ribosomal display**

I designed a random peptide library composed of 11 amino acids with the sequence, (VVN)3TAG(VVN)7, where V = G, C, or A; and N = G, C, T, or A. The VVN sequence was

selected to exclude stop codons and minimize the possibility of incorporation of hydrophobic amino acids. I introduced an EDOT moiety into a random peptide library using a bioorthogonal tRNA-bearing EDOT-conjugated aminophenylalanine (EDOT-amPhe) to add an electrochemical functionality into the selected peptide ligands. I incorporated EDOT-amPhe at the TAG codon in the middle of the peptides in the library. I avoided the incorporation of EDOT at the terminus of peptides in the library because I expected an effective inhibition of electropolymerization after the peptide binds to the target. I performed an *in vitro* selection of a peptide aptamer against inactivated influenza virus (A/California/07/2009, H1N1) using ribosome display (Figure 3-3) to select an aptamer, which not only binds to the influenza virus but also generates a quantitative electrochemical-signal. At the end of the sixth round of selection, I analyzed the obtained DNA library using NGS. I arranged the 200,000 obtained sequences based on repetition numbers and 100 sequences tabulated (Appendix 4). The analysis indicated the enrichment of selected peptide sequences against the influenza virus, and the three peptide sequences with the highest enrichment top three were selected for interaction analysis (Table3-1).

**Table 3-1:** Nominated peptide sequences for the interaction analysis.

Peptide Name	Amino acid sequences <sup>[a]</sup>	Ratio <sup>[b]</sup>
Sequence 1	AAPBKAGKGAP	2.65
Sequence 2	ARRBGHRKPRR	2.52
Sequence 3	AGRBRRGAHDT	1.93

[a] B stands for EDOT-coupled aminophenylalanine, which is a non-natural amino acid. [b] Sequence repetition percentage out of the total number of sequences.

### 3.1.2 Preparation of selected peptides

Three peptide sequences with the highest enrichment were selected for interaction analysis (Table 3-1). For the incorporation of EDOT into the synthesized peptide sequences, a non-natural amino acid, Fmoc-aminophenylalanyl EDOT (EDOTaa), was prepared according to the scheme shown in Figure 3-4. Before electrochemical analysis, binding affinity was performed by fluorescence titration for that peptide sequences prepared with Fluorescein on N terminal. But the Sequence 2 peptide also prepared without EDOT amino acid to know the role of introduced non-natural amino acid during interaction (Table 3-2). Finally, synthesized peptides characterized MALDI-TOF MS and HPLC (Table 3-2 and Appendix 7) before interaction analysis.

**Table 3-2:** Synthesized peptide sequences by SPPS method for interaction analysis.

Peptide Name	Calculate(M+H)	Found (M+H)
Sequence 1	1241.67	1241.81
Sequence 2	1663.95	1664.04
Sequence 3	1470.96	1471.11
Sequence 2 ( $\Delta$ EDOT)	1436.85	1436.90

*Note:* All three peptides were prepared without and with fluorescein on N terminal to perform the binding analysis. Sequence 2 peptide also prepared without EDOT-coupled aminophenylalanine as a sequence ARRF~~G~~HRKPRR. F indicates phenylalanine which was used in place of B to synthesize the Sequence 2 peptide without EDOT ( $\Delta$ EDOT).

## 3.2 Affinity and Selectivity Analysis

### 3.2.1 Binding affinity

I examined the affinities of the individual peptide ligands for the influenza virus using these three peptides coupled with fluorescein at the N-termini. I incubated the fluorescein-

labeled peptides with the influenza virus immobilized on silica microbeads. After the unbound peptides were washed out, the fluorescence intensity from the bound peptides was measured using a microplate reader. Even though the presence of the fluorescein might interfere with the binding of the peptides to the virus, the Sequence 2 peptide exhibited the highest binding affinity among the three peptides (Figure 3-6). The binding affinity was estimated by calculating the half-maximal effective concentration (EC<sub>50</sub>) and was  $9.6 \pm 2.3\mu\text{M}$  for the Sequence 2 peptide. To evaluate the effect of EDOT on the interaction between the Sequence 2 peptide and the influenza virus, I synthesized the Sequence 2 peptide without EDOT. The affinity measurements indicated that Sequence 2 ( $\Delta\text{EDOT}$ ) did not bind to the influenza virus immobilized on beads as well as the original Sequence 2 peptide (Figure 3-7), suggesting that EDOT contributes to the interaction between the Sequence 2 peptide and the influenza virus particles.

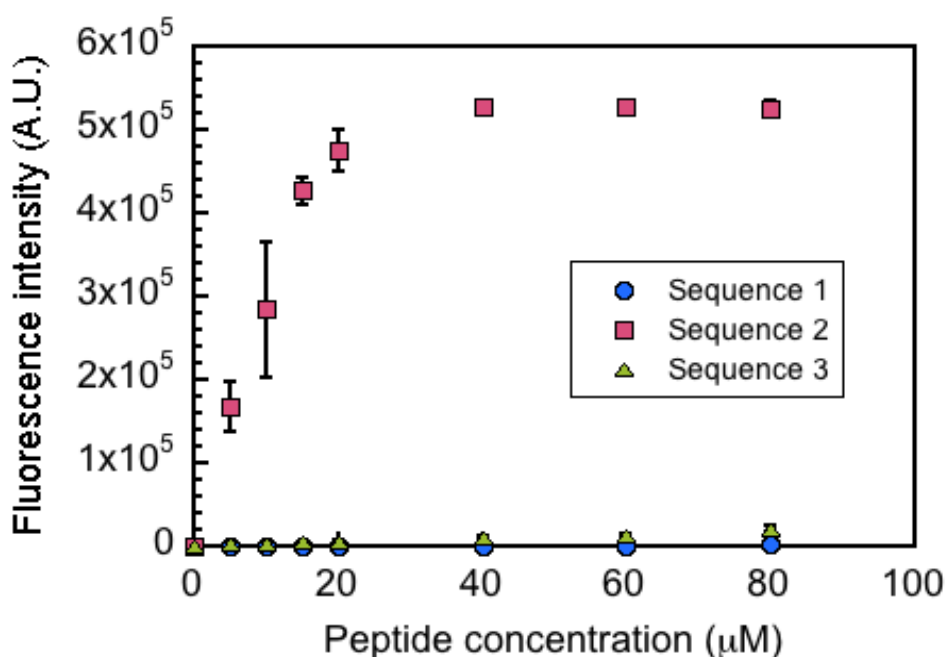


**Figure 3-6.** Comparison of affinities of the selected peptide sequences. The fluorescein-labelled peptides were incubated with inactivated influenza virus-immobilised on silica beads and the fluorescence intensities of the bound peptides were measured.

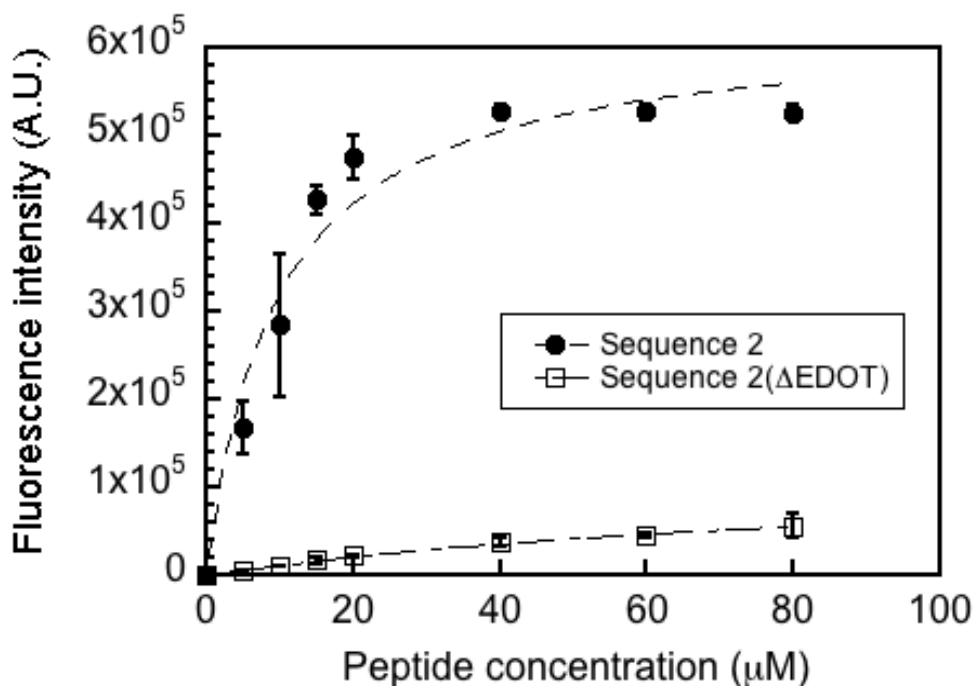


*Figure 3-7. Comparison of binding affinity of Sequence 2 peptide and Sequence 2 (ΔEDOT) peptides to the influenza virus immobilised on microbeads.*

### 3.2.2 Target selectivity

The biological specificity of the Sequence 2 peptide, in terms of its binding to the influenza virus, was confirmed using a dot blot analysis. The fluorescence image of the membrane indicated that the Sequence 2 peptide specifically bound to the influenza virus (Figure 3-8). Therefore, the Sequence 2 peptide was used for the electrochemical experiments.

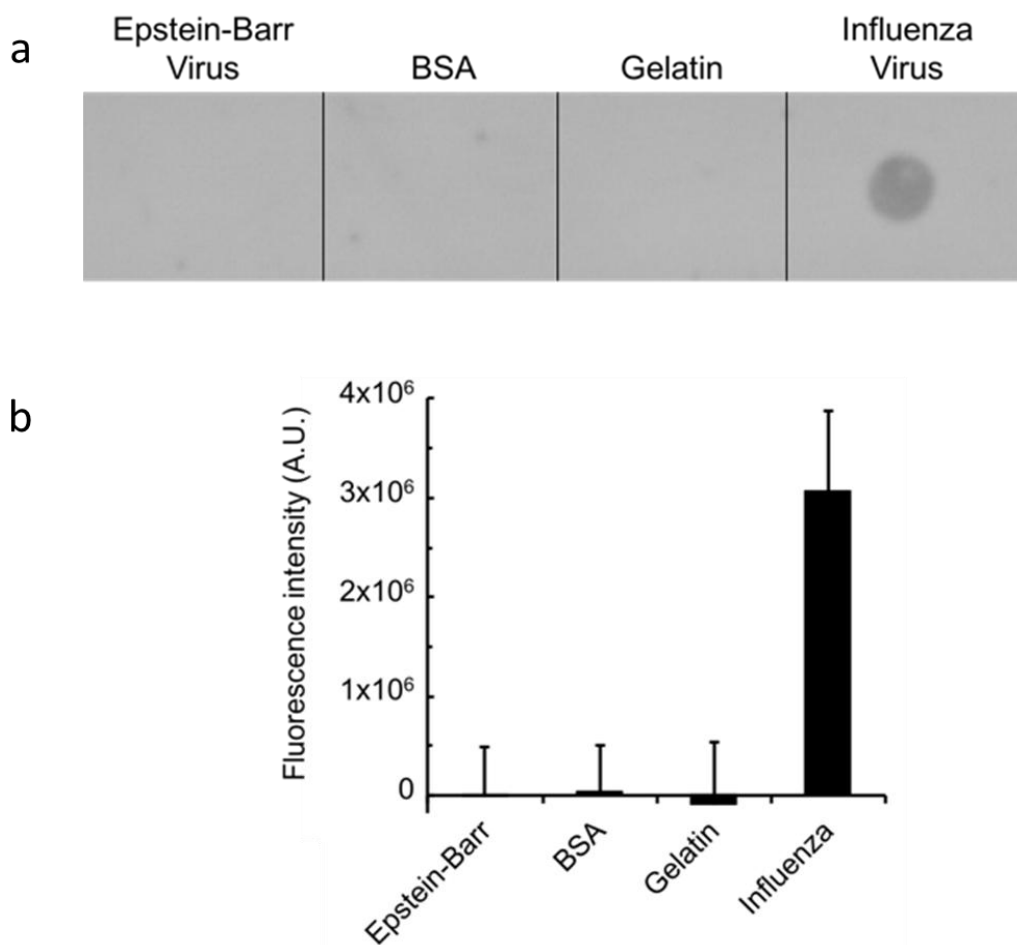


**Figure 3-8.** Biological specificity of the Sequence 2 peptide ligand. (a) A dot blot analysis result. The targets Influenza virus, Epstein–Barr virus, BSA, and Gelatine were dropped (2 $\mu$ L portion of 1 mg mL<sup>-1</sup>) on the PVDF membrane and detected with fluorescein-labeled Sequence 2 peptide. (b) Integrated density of the fluorescence after the dot blots analysis. Data are presented as the mean values  $\pm$  SD ( $n = 3$ ).

### 3.3 Electrochemical Analysis

#### 3.3.1 Electrochemical polymerization of EDOT-conjugated peptide.

For the electrochemical polymerization measurements using the EDOT-conjugated peptide, a gold electrode was used as the working electrode, and platinum wire and an Ag/AgCl electrode were used as the counter and reference electrodes, respectively. After

setting a 1-mm distance between the gold and Ag/AgCl electrodes, a solution containing the peptide was dropped onto the working electrode, and an optimized CV sequence was run (–0.6 to 0.95V vs. Ag/AgCl, scanning at 0.1 V s<sup>-1</sup> for 12 cycles) in 0.1M Tris-HCl buffer (pH 7.0). The cyclic voltammogram suggested that the electrochemical reaction occurred at the working electrode (Figure 3-9) because the observed phenomenon was similar to a reported EDOT polymerization.<sup>38</sup> To confirm the decrease in current at the working gold electrode because of deposition of the peptide polymer on its surface, I subsequently performed CV using a 10mM K<sub>3</sub>[Fe(CN)<sub>6</sub>] solution (Figure 3-10). After electropolymerization, the current of the cyclic voltammogram was remarkably decreased.

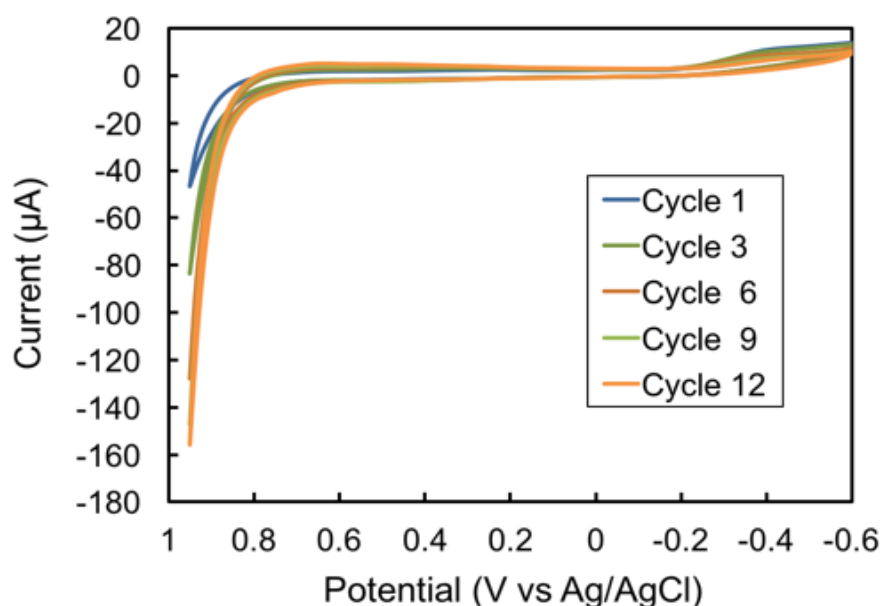


**Figure 3-9.** Cyclic voltammograms of Sequence 2 peptide polymerisation on gold electrode using a potentiostat system.

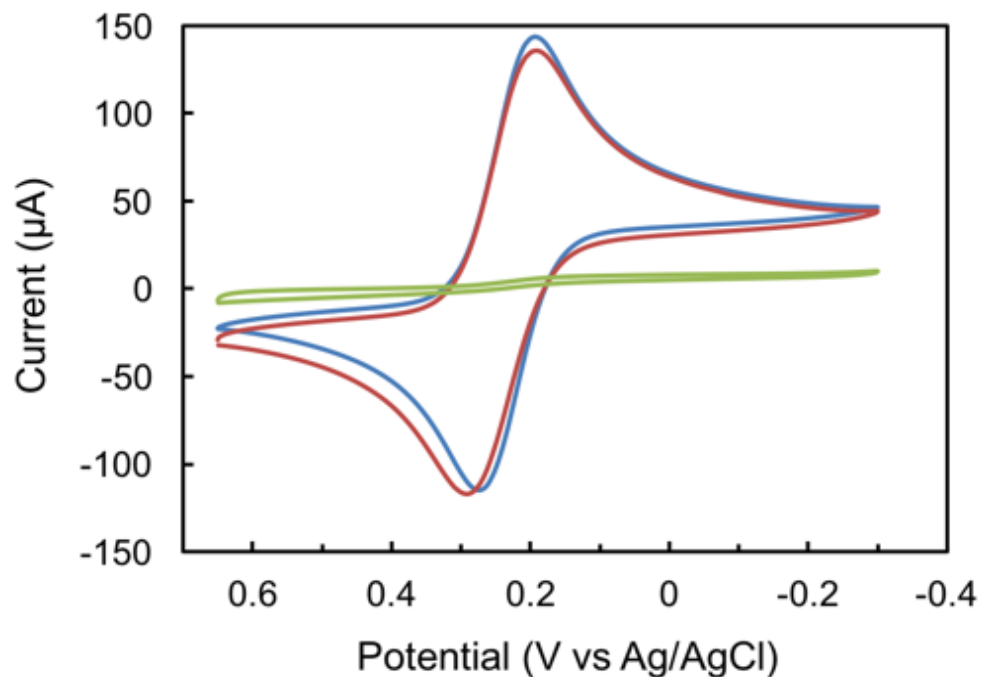


**Figure 3-10.** Cyclic voltammograms measured on a gold electrode. Before polymerisation reaction on clean gold electrode (blue), after polymerisation of  $0.1\text{mg mL}^{-1}$  (green) and  $0\text{mg mL}^{-1}$  (red) of Sequence 2 peptide, respectively.

FT-IR measurements further confirmed the peptide deposition on the electrode surface. For an FT-IR sample measurement,  $2\text{mg mL}^{-1}$  of the peptide was polymerized compared with that of the unpolymerized peptide powder. The FT-IR spectra (Figure 3-11) contained two peaks at  $1652$  and  $1540\text{cm}^{-1}$ , which were attributed to the stretching vibrations of the carbonyl (C=O) group of amide I, and the amine (N-H) bending mode of amide II, respectively. These peaks indicated the presence of a peptide backbone and demonstrated that deposition of the peptide occurred on the electrode surface. Moreover, other differences were observed in the spectra at  $1100\text{--}1250$  and  $600\text{--}900\text{cm}^{-1}$ . These differences provided further confirmation that the peptide monomer underwent the desired polymerization reaction under the electrochemical conditions.

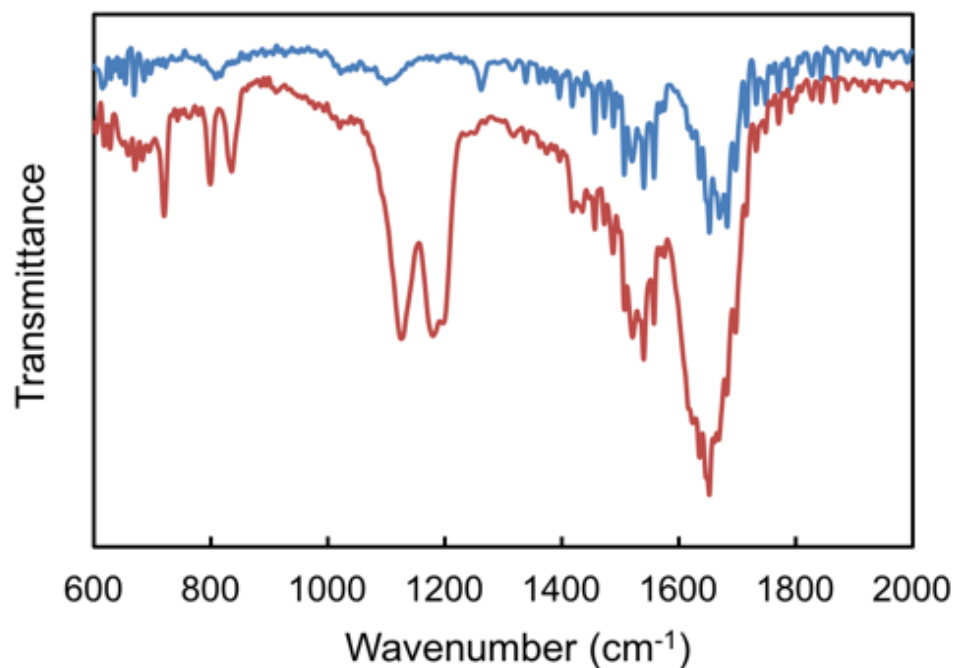


**Figure 3-11.** FT-IR spectra of Sequence 2 peptide after electrochemical polymerisation (blue) and unpolymerised powder (red) on the surface of the gold-coated silicon chip.

### 3.3.2 Electrochemical sensing of the influenza virus.

To establish a protocol to quantify the amount of influenza virus in a sample, first determined the effective peptide concentration,  $0.1 \text{ mg mL}^{-1}$ , (Appendix 8) for the electrochemical polymerization. Then, I incubated  $0.1 \text{ mg mL}^{-1}$  peptide solution with different concentrations of inactivated influenza virus. The concentration of influenza virus was determined from the total amount of protein, as measured by the Bicinchoninic Acid Protein Assay. Then the analyte was polymerized on a working electrode, and CV was subsequently performed using the  $\text{K}_3[\text{Fe}(\text{CN})_6]$  solution. The CV current increased with an increase in the concentration of influenza virus (Figure 3-12a), presumably because polymerization on the electrode was suppressed because of binding of the influenza virus to the peptide ligand. The cathodic peak current at the highest concentration of the influenza virus ( $100 \mu\text{A}$  at  $150 \mu\text{g mL}^{-1}$  influenza virus, Figure 3-12b) was not same as the current

obtained from a clean gold electrode (150 $\mu$ A, Fig. 3-12a). This current saturation arose from adsorption of the influenza virus on the working electrode (Appendix 9). Below 150 $\mu$ g mL<sup>-1</sup> of influenza virus, this system exhibited a wide linear detection range from 12.5 to 100 $\mu$ g mL<sup>-1</sup> (R<sup>2</sup> = 0.986, Figure3-13). The LOD was found to be 12.5 $\mu$ g mL<sup>-1</sup>[statistical significance ( $p < 0.05$ , Appendix 10), Figure 3-13] by comparing the results with those recorded in the absence of influenza virus using the Student's t-test. I further evaluated the specificity of this system using the Epstein-Barr virus and BSA. In these control experiments, the current measured from the electrode remained constant (Figure 3-12b).

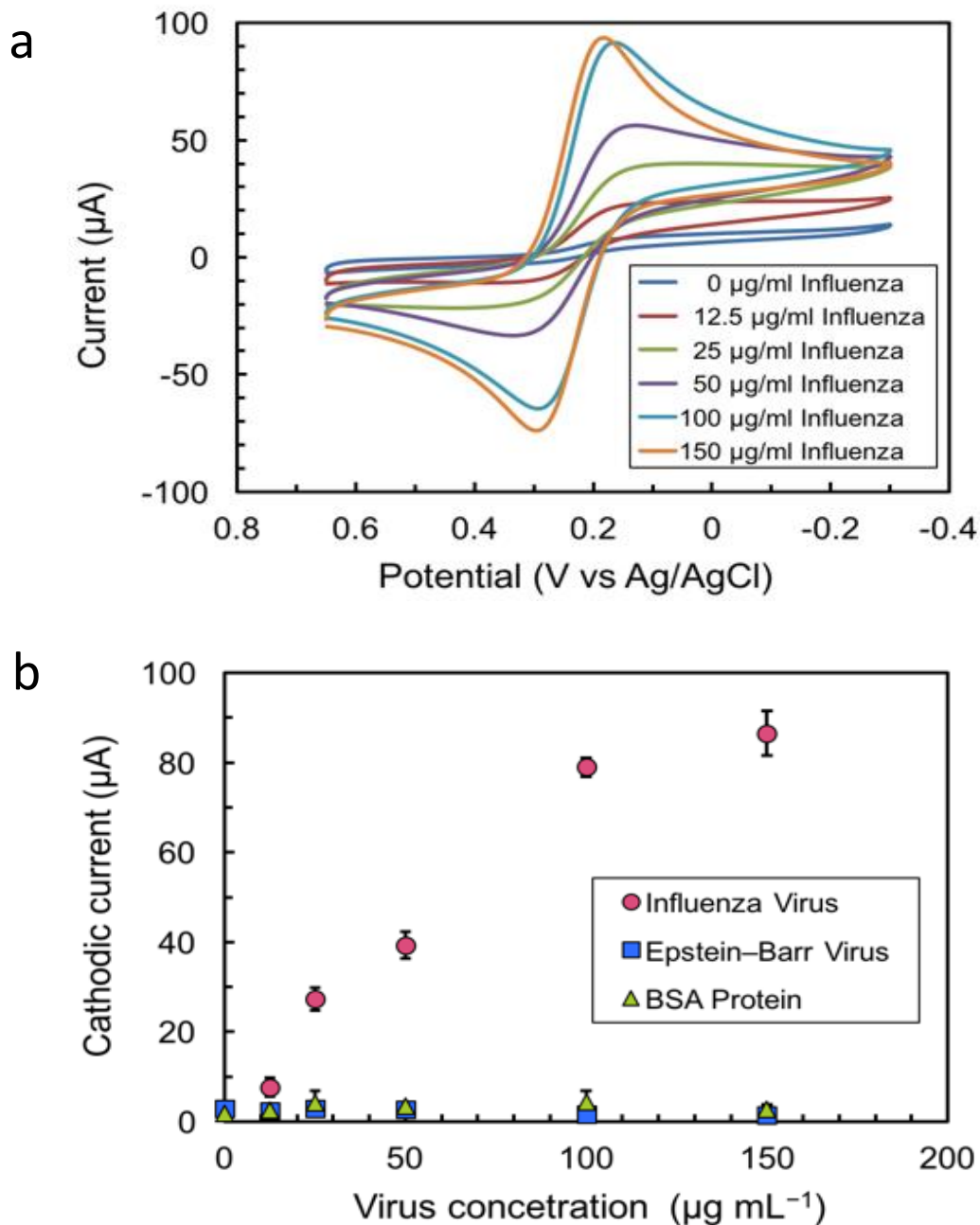


**Figure 3-12.** Electrochemical detection and specificity of detection (a) Detection of the inactivated influenza virus using the electropolymerisation technique (b) Averaged cathodic peak currents on the surface of the working gold electrode with respect to the targeted molecule influenza virus and control samples (Epstein Barr virus and BSA) after the interaction analysis using the electrochemical technique.

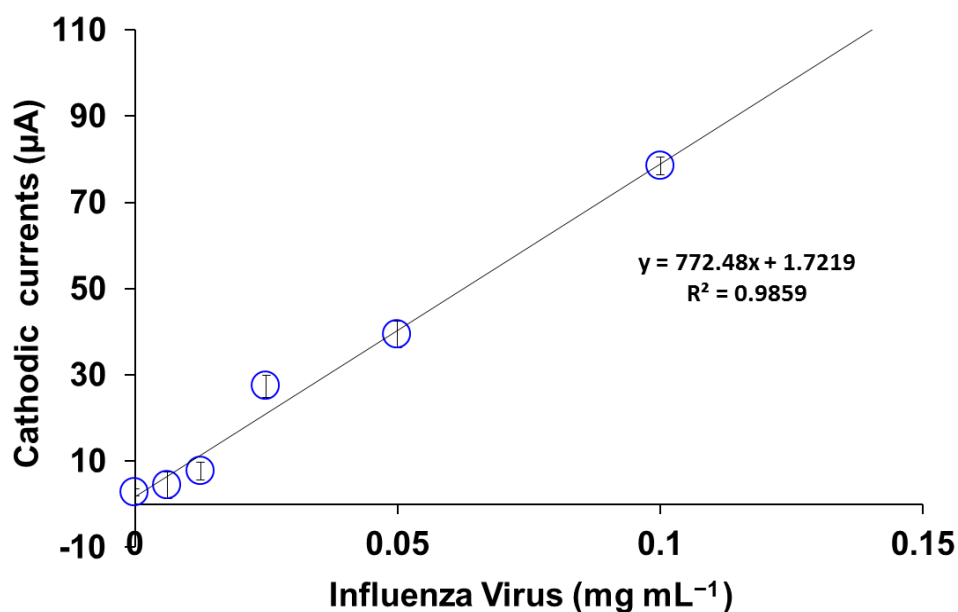


*Figure 3-13. Limits of detection analysis averaged cathodic peak currents on the surface of the working gold electrode with respect to the target influenza virus molecule and control samples.*

### **3.3.3 Interference of common microorganism on detection system.**

During clinical measurement, we can expect the presence of other common microorganisms in clinical samples. To tackle such issues, interference of the other microorganism in electrochemical detection system also examined using commonly found bacteria in the oral cavity (*Staphylococcus aureus* and *Streptococcus pneumoniae*). The result showed that microorganisms did not interfere with this influenza detection system. Both microorganisms neither remarkably suppressed the CV current measured after the polymerization cycle (blue and red lines in Figure 3-14) nor did their presence affect the peptide polymerization (green and purple in Figure 3-14). These results indicated that the peptide specifically binds to the target influenza virus.

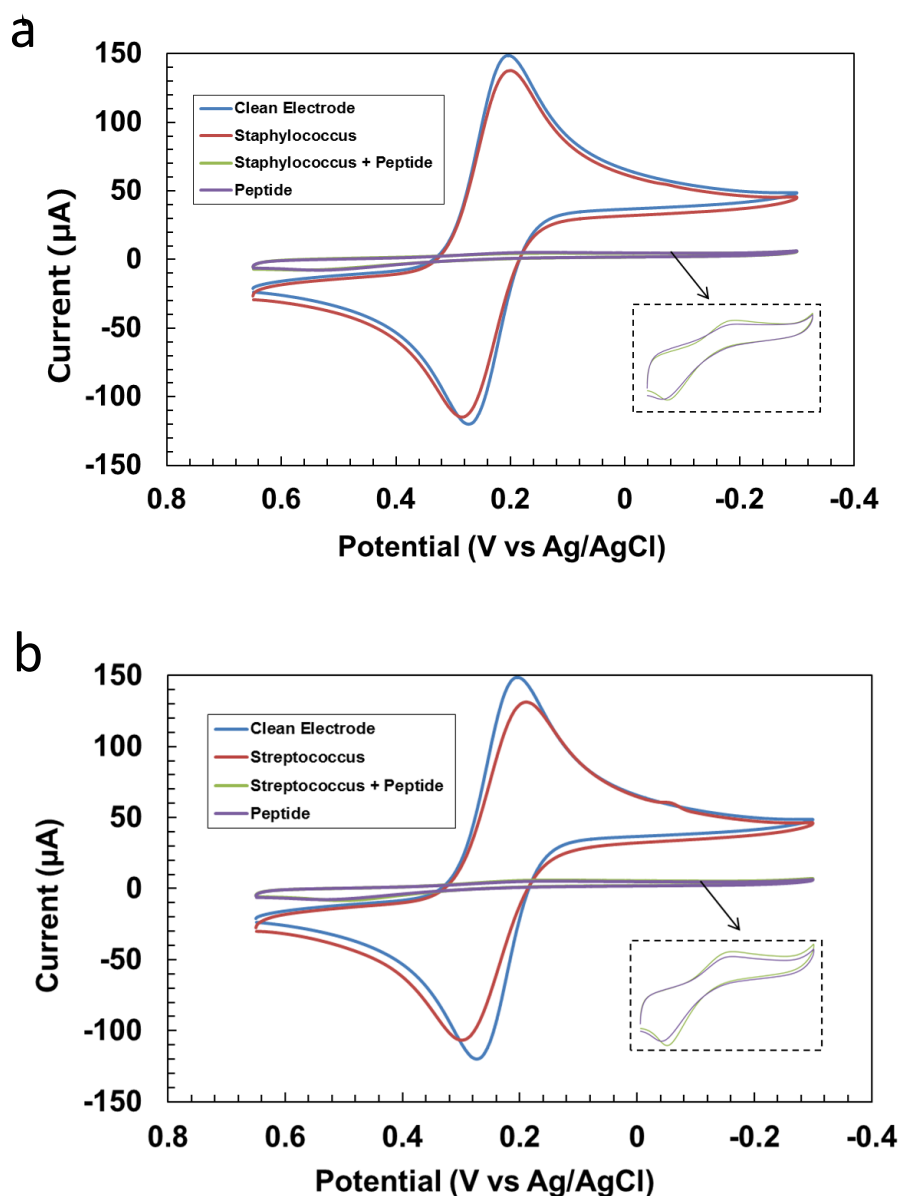


**Figure 3-14.** Comparison of cyclic voltammogram (CV) current on a working electrode. CV current on clean electrode (blue), after polymerization of Sequence 2 peptide in presence of microorganism (green), only microorganism (red) and only Sequence 2 peptide (purple). (a) *Staphylococcus aureus* and (b) *Streptococcus pneumoniae*.

Here I became able to obtain peptide ligands that specifically bind to the influenza virus, using an artificially introduced EDOT molecule. Modification of target-recognition probes with a signaling molecule, such as a fluorophore, sometimes leads to loss of affinity to a target, or too weak signaling, because the modification may hinder access to the target-

recognizing domain, or cause an unintended conformational change of the probe molecule. However, in the case of our peptide probe, the binding affinity was not reduced even with the EDOT moiety, in fact, EDOT itself contributed to the binding with the target (Figure 3-7). This involvement of EDOT in the binding affinity was realized by pre-incorporation of EDOT in the random peptide library for the *in vitro* selection of the probes. The selection method may exclude burden to work with some peptides that might intrinsically possess high affinity but lose that affinity after post-modification of functional groups.

The developed influenza detection system using an electrochemical technique may be a good choice for a diagnosis method compared with the current methods, such as reverse transcriptase polymerase chain reaction, ELISA, and immunochromatography. For point-of-care testing, detection systems should be easy to run, low-cost, portable, and sensitive. The obtained LOD of this system was found to be comparable with the fluorescent immunochromatographic strip test ( $10\mu\text{g mL}^{-1}$ ), which is 2.5-fold more sensitive than the dot blot immune assay or conventional rapid diagnosis test.<sup>39</sup> In previously reported electrochemical detection systems<sup>40, 41</sup> redox probes were immobilized on an electrode, and binding with the target induced a current decrease at the working electrode. In contrast, our detection system provides a current increase in the presence of the influenza virus, which is a form of "turn-on detection" that does not require a negative control measurement for practical analysis. In this measurement, as the concentration of the influenza virus increased, increasing amounts of the peptide became bound to the influenza virus, and less of the peptide was available for the polymerization. Because EDOT is an essential component of the polymerization reaction, binding with the virus decreases the polymer yield. Thus, by increasing the viral concentration, progressively thinner layers of peptide polymers were deposited on the working electrode, allowing more current to flow at this electrode (Figure 3-12 a and b).

#### 4. CONCLUSION

I have successfully developed a new type of electrochemical biosensor for detecting the influenza virus using a peptide ligand selected from a random peptide library containing the electro-sensitive EDOT molecule. To my knowledge, this is the first reported example of the direct *in vitro* evolution of an electrochemically sensitive peptide ligand for electrochemical analysis. It is envisaged that the strategy described in this study could also be used for the *in vitro* selection of sensing peptide ligands toward a variety of other target molecules.

## 5. REFERENCES

1. Hardiman, G. Next-generation antibody discovery platforms, *Proc. Natl. Acad. Sci. USA*. **2012**, *109*, 18245-18246.
2. Nimijee, S. M.; Rusconi, C. P.; Sullenger, B. A. Aptamers: an emerging class of therapeutics. *Annu. Rev. Med.* **2005**, *56*, 555-583.
3. Reverdatto, S.; Burz, D. S.; Shekhtman, A. Peptide aptamers: development and applications. *Curr. Top. Med. Chem.* **2015**, *15*, 1082-1101.
4. Sletten, E.M.; Bertozzi, C.R. Bioorthogonal chemistry: fishing for selectivity in a sea of functionality. *Angew. Chem. Int. Ed.* **2009**, *48*, 6974-6998
5. Johnson, J. A.; Lu, Y. Y.; Van Deventer, J. A.; Tirrell, D. A. Residue-specific incorporation of non-canonical amino acids into proteins: recent developments and applications. *Curr. Opin. Chem. Biol.* **2010**, *14*, 774-780.
6. Uzawa, T.; Tada, S.; Wang, W.; Ito, Y. Expansion of aptamer library from “natural soup” to “unnatural soup”. *Chem. Commun.* **2013**, *49*, 1786-1795.
7. Li, S.; Roberts, R. W. Novel strategy for *in vitro* selection of peptide-drug conjugates. *Chem. Biol.* **2003**, *10*, 233-239.
8. Liu, C. C.; Mack, A. V.; Tsao, M. L.; Mills, J. H.; Lee, H. S.; Choe, H.; Farzan, M.; Schultz, P. G.; Smider, V. V. Protein evolution with an expanded genetic code. *Proc. Natl. Acad. Sci. USA*. **2008**, *105*, 17688-17693.
9. Schlippe, Y. V.; Hartman, M.C.; Josephson, K.; Szostak, J. W. *In vitro* selection of highly modified cyclic peptides that act as tight binding inhibitors. *J. Am. Chem. Soc.* **2012**, *134*, 10469-10477.
10. Morimoto, J.; Hayashi, Y.; Suga, H. Discovery of macrocyclic peptides armed with a mechanism-based warhead: isoform-selective inhibition of human deacetylase SIRT2. *Angew. Chem. Int. Ed.* **2012**, *51*, 3423-3427.

11. Wang, W., Hirano, Y.; Uzawa, T.; Liu, M.; Taiji, M.; Ito, Y. *In vitro* selection of a peptide aptamer that potentiates inhibition of cyclin-dependent kinase 2 by purvalanol. *Med. Chem. Commun.* **2014**, *5*, 1400-1403.
12. Wang, W., Hirano, Y., Uzawa, T.; Taiji, M.; Ito, Y. Assisted enhancement of inhibitory effects of small molecular inhibitors for kinases. *Bull. Chem. Soc. Jpn.* **2016**, *89*, 444-446.
13. Kawamura, A.; Munzel, M.; Kojima, T.; Yapp, C.; Bhushan, B.; Goto, Y.; Tumber, A.; Katoh, T.; King, O. N.; Passioura, T.; Walport, L. J.; Hatch, S. B.; Madden, S.; Muller, S.; Brennan, P. E.; Chowdhury, R.; Hopkinson, R. J.; Suga, H.; Schofield, C. J. Highly selective inhibition of histone demethylases by *de novo* macrocyclic peptides. *Nat. Commun.* **2017**, *8*, 14773.
14. Liu, C. C.; Mack, A. V.; Brustad, E. M.; Mills, J. H.; Groff, D.; Smider, V. V.; Schultz, P. G. Evolution of proteins with genetically encoded “chemical warheads”. *J. Am. Chem. Soc.* **2009**, *131*, 9616-9617.
15. Wilke, P.; Helfricht, N.; Mark, A.; Papastavrou, G.; Faivre, D.; Borner, H. G. A direct biocombinatorial strategy toward next generation, mussel-glue inspired saltwater adhesives. *J. Am. Chem. Soc.* **2014**, *136*, 12667-12674.
16. Liu, M.; Tada, S.; Ito, M.; Abe, H.; Ito, Y. *In vitro* selection of a photo-responsive peptide aptamer by ribosome display. *Chem. Commun.* **2012**, *48*, 11871-11873.
17. Jafari, M. R.; Deng, L.; Kitov, P. I.; Ng, S.; Matochko, W. L.; Tjhung, K. F.; Zeberoff, A.; Elias, A.; Klassen, J. S.; Derda, R. Discovery of light-responsive ligands through screening of a light-responsive genetically encoded library. *ACS Chem. Biol.* **2014**, *9*, 443-450.
18. Bellotto, S.; Chen, S.; Rebollo, I. R.; Wegner, H. A.; Heinis, C. Phage selection of photoswitchable peptide ligands. *J. Am. Chem. Soc.* **2014**, *136*, 5880-5883.

19. Tada, S.; Zang, Q.; Wang, W.; Kawamoto, M.; Liu, M.; Iwashita, M.; Uzawa, T.; Kiga, D.; Yamamura, M.; Ito, Y. *In vitro* selection of a photoresponsive peptide aptamer to glutathione-immobilized microbeads. *J. Biosci. Bioeng.* **2015**, *119*, 137-139.
20. Wang, W.; Uzawa, T.; Tochio, N.; Hamatsu, J.; Hirano, Y.; Tada, S.; Saneyoshi, H.; Kigawa, T.; Hayashi, N.; Taiji, M.; Aigaki, T.; Ito, Y. A fluorogenic peptide probe developed by *in vitro* selection using tRNA carrying a fluorogenic amino acid. *Chem. Commun.* **2014**, *50*, 2962-2964.
21. Manandhar, Y.; KC, T. B.; Wang, W.; Uzawa, T.; Aigaki, T.; Ito, Y. *In vitro* selection of a peptide aptamer that changes fluorescence in response to verotoxin. *Biotechnol. Lett.* **2015**, *37*, 619-625.
22. Wang, W.; Zhu, L.; Hirano, Y.; Kariminavargani, M.; Tada, S.; Zhang, G.; Uzawa, T.; Zhang, D.; Hirose, T.; Taiji, M.; Ito, Y. Fluorogenic enhancement of an *in vitro* selected peptide ligand by replacement of a fluorescent group. *Anal. Chem.* **2016**, *88*, 7991-7997.
23. Ouay, B. L.; Boudot, M.; Kitao, T.; Yanagida, T.; Kitagawa, S.; Uemura, T. Nanostructuring of PEDOT in porous coordination polymers for tunable porosity and conductivity. *J. Am. Chem. Soc.* **2016**, *138*, 10088-10091.
24. Lin, P.; Yan, F.; Chan, H. L. Ion-sensitive properties of organic electrochemical transistors. *ACS Appl. Mater. Interfaces.* **2010**, *2*, 1637-1641.
25. Chen, C. H.; Luo, S. C. Tuning surface charge and morphology for the efficient detection of dopamine under the interferences of uric acid, ascorbic acid, and protein adsorption. *ACS Appl. Mater. Interface.* **2015**, *7*, 21931-21938.

26. Krishnamoorthy, K.; Gokhale, R. S.; Contractor, A. Q.; Kumar, A. Novel label-free DNA sensors based on poly(3,4-ethylenedioxythiophene). *Chem. Commun.***2004**, 7, 820-821.
27. Luo, S. C.; Xie, H.; Chen, N. Y.; Yu, H. H. Trinity DNA detection platform by ultrasmooth and functionalized PEDOT biointerfaces. *ACS Appl. Mater. Interfaces.* **2009**, 1, 1414-1419.
28. Mohan, K.; Donavan, K. C.; Arter, J. A.; Penner, R. M.; Weiss, G. A. Sub-nanomolar detection of prostate-specific membrane antigen in synthetic urine by synergistic, dual-ligand phage. *J. Am. Chem. Soc.***2013**, 135, 7761-7767.
29. Arter, J. A.; Taggart, D. K.; McIntire, T. M.; Penner, R. M.; Weiss, G. A. Virus-PEDOT nanowires for biosensing. *Nano Lett.***2010**, 10, 4858-4862.
30. Goda, T.; Toya, M.; Matsumoto, A.; Miyahara, Y. Poly(3,4-ethylenedioxythiophene) bearing phosphorylcholine groups for metal-free, antibody-free, and low-impedance biosensors specific for C-reactive protein. *ACS Appl. Mater. Interface.* **2015**, 7, 27440-27448.
31. Kindra, L. R.; Eggers, C. J.; Liu, A. T.; Mendoza, K.; Mendoza, J.; Myers, A. R. K.; Penner, R. M. Lithographically patterned PEDOT nanowires for the detection of Iron(III) with nanomolar sensitivity. *Anal. Chem.***2015**, 87, 11492-11500.
32. Zanardi, C.; Terzi, F.; Seeber, R. Polythiophenes and polythiophene-based composites in amperometric sensing. *Anal. Bioanal. Chem.***2013**, 405, 509-531.
33. Kergoat, L.; Piro, B.; Simon, D. T.; Pham, M. C.; Noel, V.; Berggren, M. Detection of glutamate and acetylcholine with organic electrochemical transistors based on conducting polymer/platinum nanoparticle composites. *Adv. Mater.***2014**, 26, 5658-5664.

34. Tang, H.; Lin, P.; Chan, H. L. W.; Yan, F. Highly sensitive dopamine biosensors based on organic electrochemical transistors. *Biosens. Bioelectron.* **2011**, *26*, 4559-4563.
35. Taira, H.; Matsushita, Y.; Kojima, K.; Shiraga, K.; Hoshida, T. Comprehensive screening of amber suppressor tRNAs suitable for incorporation of non-natural amino acids in a cell-free translation system. *Biochem. Biophys. Res. Commun.* **2008**, *374*, 304-308.
36. Li, W.; Godzik, A. Cd-hit: a fast program for clustering and comparing large sets of protein or nucleotide sequences. *Bioinformatics* **2006**, *22*, 1658-1659.
37. Ohara-Nemoto, Y.; Haraga, H.; Kimura, S.; Nemoto, T. K. Occurrence of staphylococci in the oral cavities of healthy adults and nasal-oral trafficking of the bacteria. *J. Med. Microbiol.* **2008**, *57*, 95-99
38. Vasanth, V. S.; Thangamuthu, R.; Chen, S. M. Electrochemical polymerization of 3,4-ethylenedioxythiophene from aqueous solution containing hydroxypropyl- $\beta$ -cyclodextrin and the electrocatalytic behavior of modified electrode towards oxidation of sulfuroxanions and nitrite. *Electroanalysis* **2008**, *20*, 1754-1749.
39. Yeo, S. J.; Huong, D. T.; Hong, N. N.; Li, C. Y.; Choi, K.; Yu, K.; Choi, D. Y.; Chong, C. K.; Choi, H. S.; Mallik, S. K.; Kim, H. S.; Sung, H. W.; Park, H. Rapid and quantitative detection of zoonotic influenza A virus infection utilizing coumarin-derived dendrimer-based fluorescent immunochromatographic strip test (FICT), *Theranostics* **2014**, *4*, 1239-1249.
40. Puiu, M.; Idili, A.; Moscone, D.; Ricci, F.; Bala, C. A modular electrochemical peptide-based sensor for antibody detection. *Chem. Commun.* **2014**, *50*, 8962-8965.
41. Chung, D. J.; Kim, K. C.; Choi, S. H. Electrochemical DNA biosensor based on avidin-biotin conjugation for influenza virus (type A) detection. *Appl. Surf. Sci.* **2011**, *257*, 9390-9396.



## **CHAPTER 4: CONCLUSION**

## CONCLUSION

The works presented in this thesis describe the design, development, and study of peptide aptamer-based biosensors for diagnostic applications. To get the desired applications of the peptide aptamers, two techniques were used. In the first one, an environment sensitive fluorophore, 7-nitro-2, 1, 3-benzoxadiazole (NBD) was functionalized into selected peptide aptamer preparing non-natural amino acid, and in the second approach, an electroreactive molecule 3,4-ethylenedioxythiophene (EDOT) was introduced into a pool of random peptide library to get the desired function of selected aptamer.

**Chapter One.** It gives general overviews about the concept of aptamer development, their advantages, the present scenario of aptamer-based researches and their scope in biomedical and other applications with some examples. It also describes the idea of the research work carried out: functionalization of sensing molecules into peptide aptamers.

**Chapter Two.** In this research, the post selection modification of the peptide aptamer was successfully carried out to add the molecular functionality. I generated new fluorogenic ligands to detect circulating tumor cells (CTC) by modifying a previously reported EP114 peptide aptamer binding to a glycoprotein, epithelial cell adhesion molecule (EpCAM) hallmark of CTC. The functional modification was done with an environmentally sensitive fluorophore NBD preparing in a non-natural amino acid form. One of the functionalized peptide ligands, Q4X can specifically detect the EpCAM-positive cells with an enhanced fluorescence by just adding the peptide ligand to the cultivation medium.

I hope the developed method could be used to capture CTC without damage the cell viability for the phenotype identification and the molecular analysis to reach an ultimate goal, which is difficult from the current cell search technique. Indeed, the functionalized fluorogenic peptide ligand has a potential to develop the third generation CTC detection tool

which will enable a more comprehensive picture of the cancer diagnosis, prognosis and lead towards the personalized medication.

**Chapter Three.** In this research, a new strategy has been developed to detect influenza virus using an electrochemical technique, which works based on simple Cyclic Voltammetry measurement. For that, electrochemically sensitive peptide ligands were selected by ribosome display method against the influenza virus from a pool of random peptide library incorporating electroreactive non-natural amino acid using the bioorthogonal tRNA-bearing EDOT-conjugated aminophenylalanine. One of the selected peptide ligands, Sequence 2 specifically binds to influenza virus with a binding affinity ( $EC_{50} = 9.6 \pm 2.3 \mu M$ ) and detected influenza virus lower to  $12.5 \mu g mL^{-1}$  ( $p < 0.05$ ) concentration based on the total protein measurement. To my knowledge, this is the first reported electrochemical peptide ligands selected from a combinatorial library.

I believe that the electropolymerizable peptide ligand developed in this research has the potential to develop a promising point-of-care testing tool to detect influenza virus in primary care to address the current expensive and time consuming diagnosis method. In addition to, the approach used in this strategy can also be applied to other variety of target molecules to develop the desired biosensors.

In the end, the studies carried out in this thesis disclose the importance of functional non-natural amino acid incorporation into peptide ligands using various techniques. The optimizations of the functionality of the developed peptide ligands have the potential to develop a point-of-care testing tool to capture CTC and detection of influenza virus in primary care setting, which are highly desirable.

## ACKNOWLEDGMENTS

Foremost, I owe my deepest gratitude to my supervisor Professor Yoshihiro Ito for welcoming me to Emergent Bioengineering Materials Research Team, Center for Emergent Matter Science, RIKEN. Without his guidance, encouragement and persistent support this thesis would not have been possible. I also express my heartfelt gratitude to my other supervisor Professor Toshiro Aigaki at Tokyo Metropolitan University, an optimistic and friendly supervisor who guided research, supported and helped during my Ph.D. course.

I thank and express my gratitude to Dr. Takanori Uzawa, my mentor in lab for his guidance, encouragement, time, intellect input, scientific support and constructive criticism in my research work. Special thanks to Dr. Seiichi Tada for being extremely generous and best guidelines in the research. I also like to thank members of the selection group for their valuable suggestions in research discussion and everyone with whom I worked in RIKEN.

I would like to express my gratitude for the financial support by Junior Research Associate (JRA) program for graduate students from the research personnel support section, Global Relation Office, RIKEN.

I would like to thank and appreciate to my beloved wife Dr. Yasodha Manandhar for her support, patience, endless encouragement through this process. Who have never given up on me even when I wanted and spent sleepless nights to keep me sane even in the time of stress when there was no one to answer my queries. I am extremely thankful to my little princess Lisa Kunwar whose smile gives me positive energy and vibration all the time.

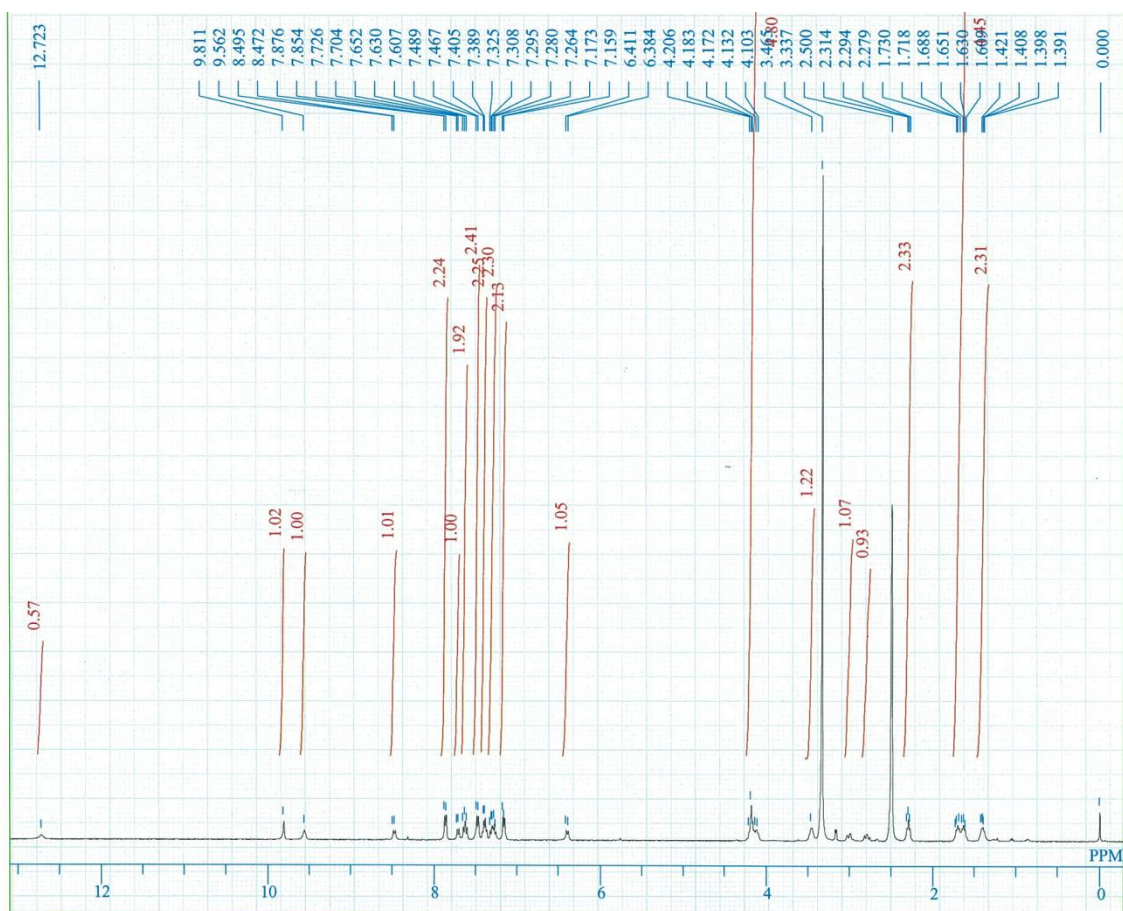
A special thanks to my family members. Words cannot express how grateful I am to my parents; Gopal Bahadur Kunwar (father) and Jamuna Devi Kuwmar (mother) for all of the sacrifices that have made to fulfill my wishes. Special gratitude to my brothers Rajendra Kunwar and Man Bahadur K.C. (Suman) whose immense support, encouragement

helped me grown up this. I am also grateful to father-in-law and mother-in-law for their enmorous love, encouragement, and assistance to take care of baby Lisa.

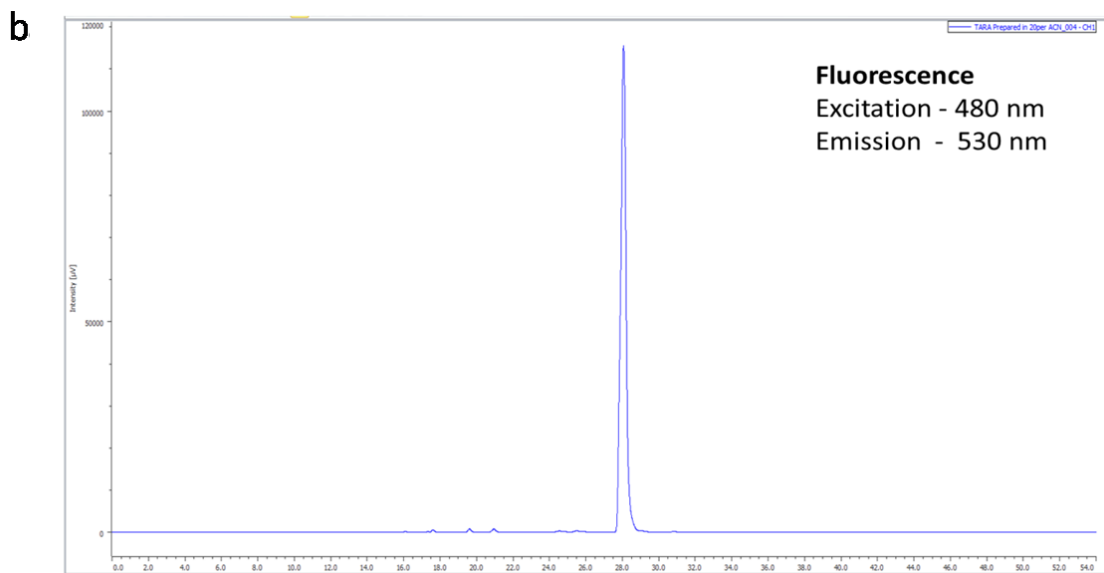
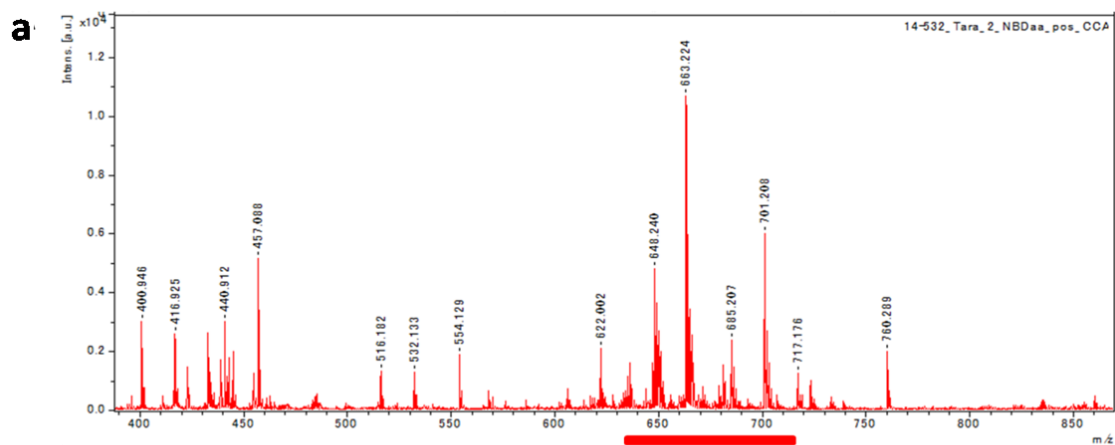
Last but not the least, I am thankful to my friends Dr. Suresh Panthee, Dr. Govinda Sharma, Jagat Shrestha, Dr. Siva Kumar, Dr. Nanda Kumar, Dr. KrishnacharySalikolimi, Dr. Rajan Shrestha, Dr. Ronak Shrestha, Dr. Amit Subedi and all other who helped me directly and indirectly.

# **APPENDIX**

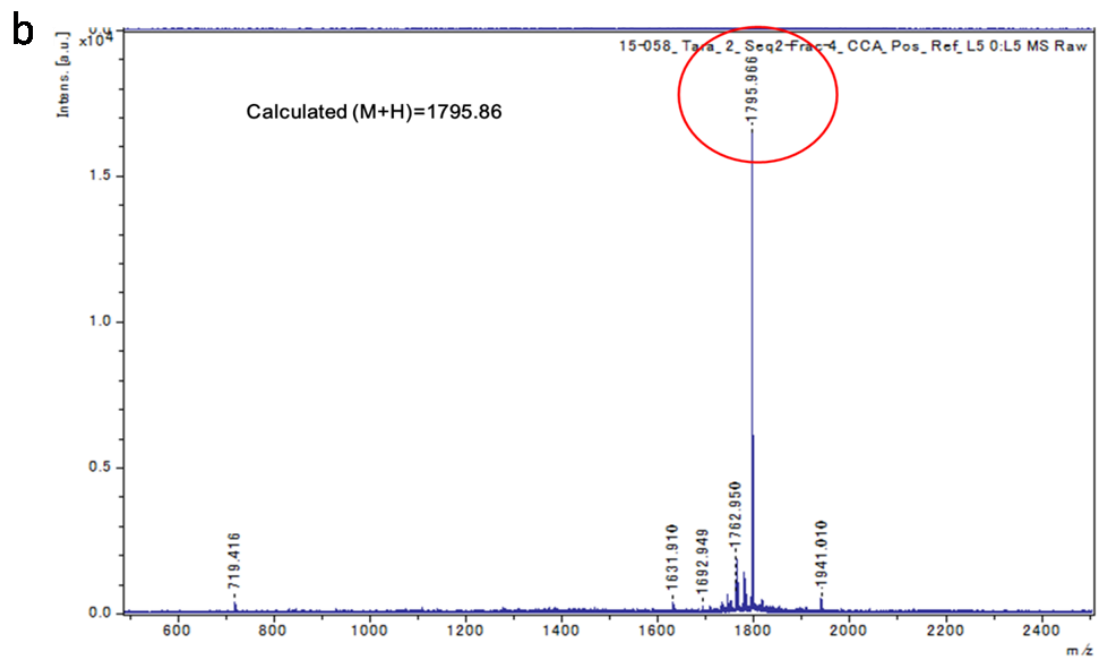
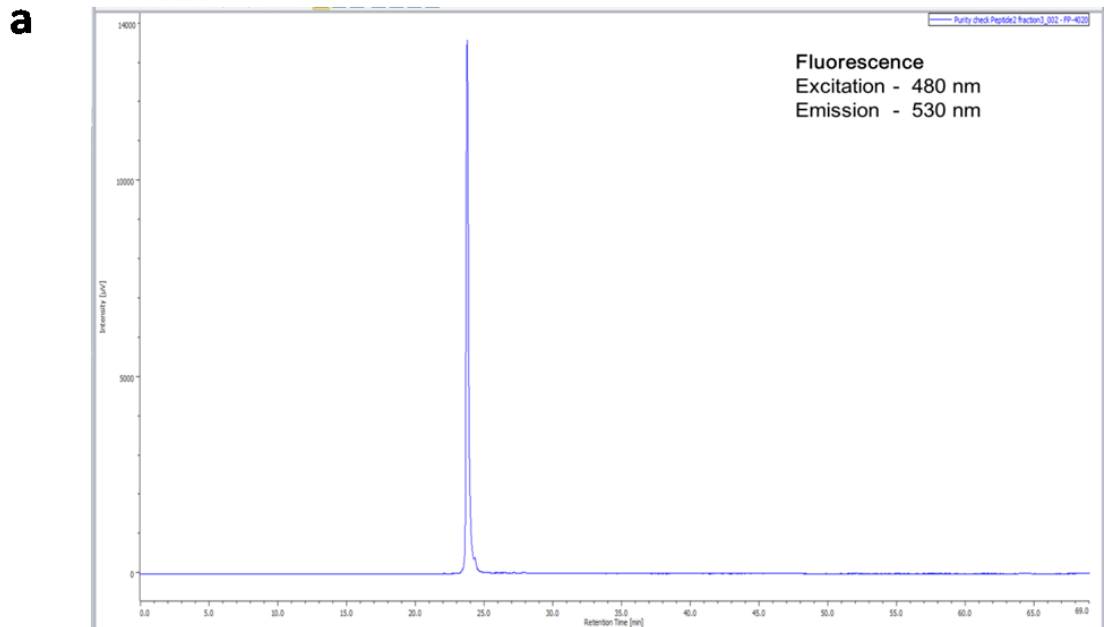
# Appendix 1. H-NMR analysis of the synthesized NBD-amPhe



**Appendix 2.**Characterization of non-canonical amino acid (A) MALDI MS analysis of NBD conjugated phenylalanine, where calculated ( $M+H=678.24$ ) and found spectra were  $M+Na=701.2$ , as well  $M+H-16= 663.22$  and  $M+H-32=646.24$ , due to  $NO_2$ ). (B) HPLC analysis of non-canonical amino acid (NBD-amPhe) for purity, fluorescence spectra was measured.



**Appendix 3.** Characterization of synthesized peptides (A) HPLC results of the purified Q4X indicated that Q4X was well-purified. All other peptides also exhibited similar HPLC charts. (B) MALDI MS analysis of Q4X peptide for product confirmation and purity.



## Appendix 4. Sequences list of the selected peptides from the NGS analysis.

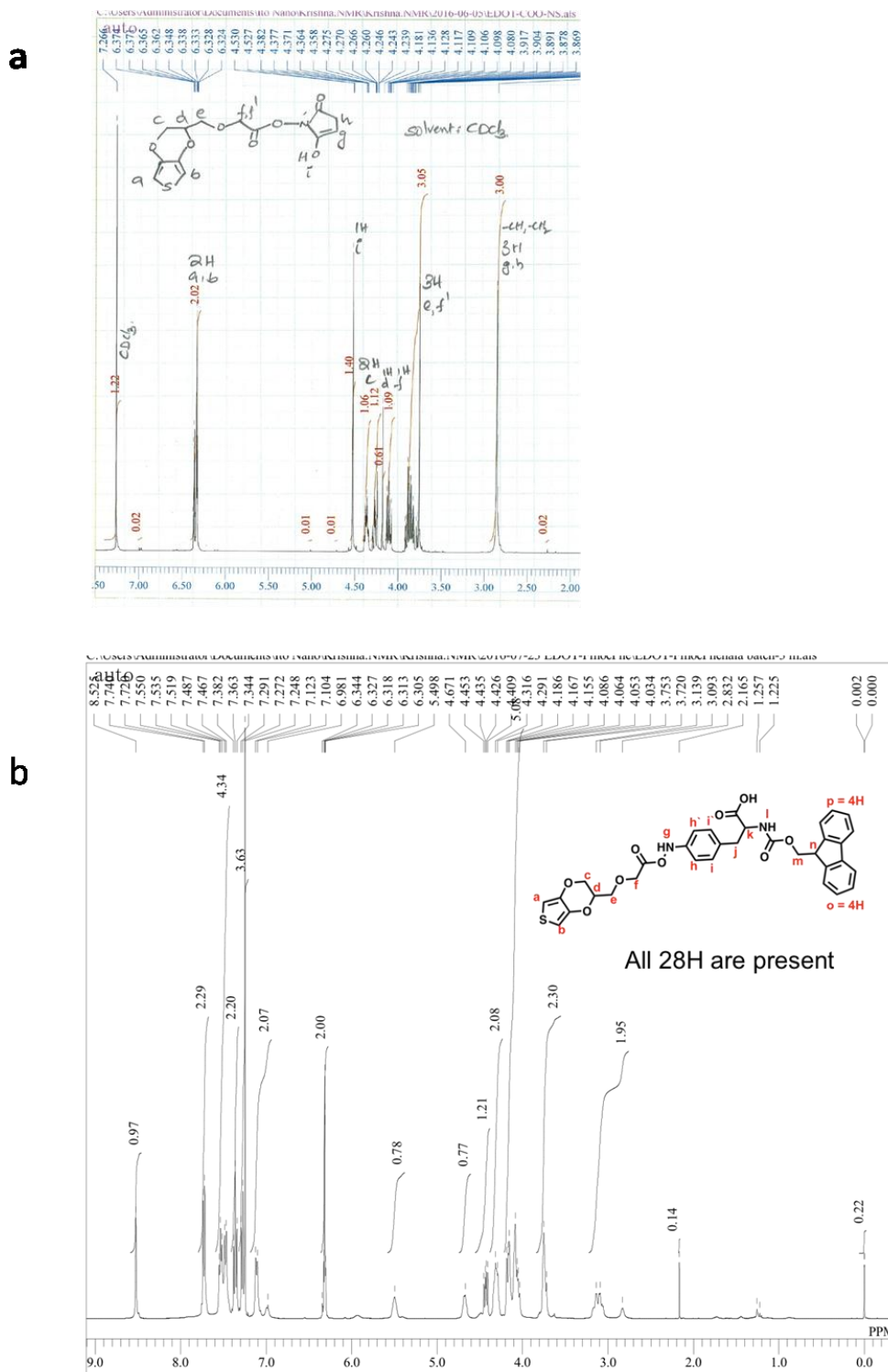
Peptide Sequences	Amino Acids	Identical /209177	Peptide Sequence	Amino Acids	Identical /209177
1	AAPBKAGKAP	5546	51	QRBADSPKKP	536
2	ARRBGHRKPRR	5278	52	TQRGGGTGAPK	523
3	AGRBRRAHDT	4042	53	ERDBEPRPQRR	517
4	GPRBTAAANRR	3045	54	GGGBSPQGAGG	521
5	AAABTGENPTT	2692	55	TGGBFGEATTP	508
6	RTPBNGPRADA	2518	56	GRPBRNGARQT	506
7	NRABGDPTGNR	2499	57	PGGBRDDHRDQ	497
8	NERBSADAGAH	2413	58	HRTBDHSPPPDR	486
9	EDPBGANTGR	2480	59	SRTBHFAQKDS	501
10	HAABHATPTSG	2116	60	RGQBADREHDT	505
11	TEPBGDRSRRR	2106	61	TEHBKKGNGTR	497
12	TSDBSRPRQDE	1970	62	TQTPPERAAGR	487
13	TRTBDTKNTTT	1810	63	DGHBDDGAEPAR	486
14	AREBPAAAGEQG	1689	64	AQRBRGATQEN	457
15	NPRBGRQQREG	1682	65	APRBHPGPADK	464
16	EAHBKPSPPHE	1478	66	AREBAANGKGP	452
17	GKEBTPRPEPP	1440	67	DKDBGPQRPSF	435
18	TTRBTGQEEQE	1309	68	RRRBQGGGRGH	422
19	TSRBTGANKR	1180	69	GAHBRREGGRR	415
20	GPGBAHRRGDP	1167	70	KGTBHEARTKP	425
21	NAKBGGSTRRR	1068	71	KGRBRTHPETG	402
22	TKEBERARRGQ	1043	72	RPABSHHDRGP	403
23	APNBEGEDTDP	1069	73	QQPBGAATPR	411
24	PPDBPDTRKR	1026	74	PRGBRAAGAHP	384
25	SNGBTREAOHT	1016	75	QTGBANPEPQE	409
26	SNGBEPTRKFP	949	76	ATTBAAAGTDTT	405
27	PRNBGRTGAAK	893	77	GGEBGNGADGR	393
28	SRRBARHPRRG	879	78	KPGBAPGKAGA	390
29	RERBESSRSDS	855	79	RSQBDQRNGDG	389
30	EDRBQQGARAP	830	80	GKABSRTASAG	389
31	REFBRDDATDQ	812	81	RTGBPPRNRRR	386
32	RGQBNAPQEEA	801	82	GPHBRRRAHAER	388
33	SRABPQSRKGP	796	83	AGPBKSAGPGG	380
34	DQSBGRRRARP	765	84	RRGBNGGEDGQ	383
35	GAGBPQTTRKT	750	85	PGHBKQKHST	377
36	GQEBDRARKTR	723	86	DGTBPREETAS	377
37	GPGBGGNRPRG	698	87	ERABGPGGATA	386
38	ARGBGPGGNQR	722	88	AGTBTGGTPHR	372
39	TRABGANRRAG	697	89	QGEBTGPGSHA	351
40	HGGBTGIPHERP	687	90	EGEBTPQTTTQ	367
41	GNSBQANNRTR	666	91	TDGBRGSRNRP	364
42	PDQBRAGGRAG	684	92	PSTBDRRGNPK	362
43	GQTBEENERRS	632	93	STQBGARGTAP	360
44	RGNBERRSIPT	617	94	SDRBSQDPAGG	340
45	TGABRTRATH	373	95	DRQBTAKGNRR	351
46	DRABPPRGGGA	595	96	GGPBSDGRAGA	339
47	NRGBARNAGAR	592	97	QRBGHTHTTDA	334
48	PPTBKKGAPPT	580	98	EKPBRPGDQEP	337
49	RGEBPDHTAGT	552	99	RGNBGDNRAGS	345
50	ATRBPGGKGEF	540	100	DESBAETESGD	347

Where B indicates the non-natural amino acid, EDOT conjugated aminophenylalanine residues

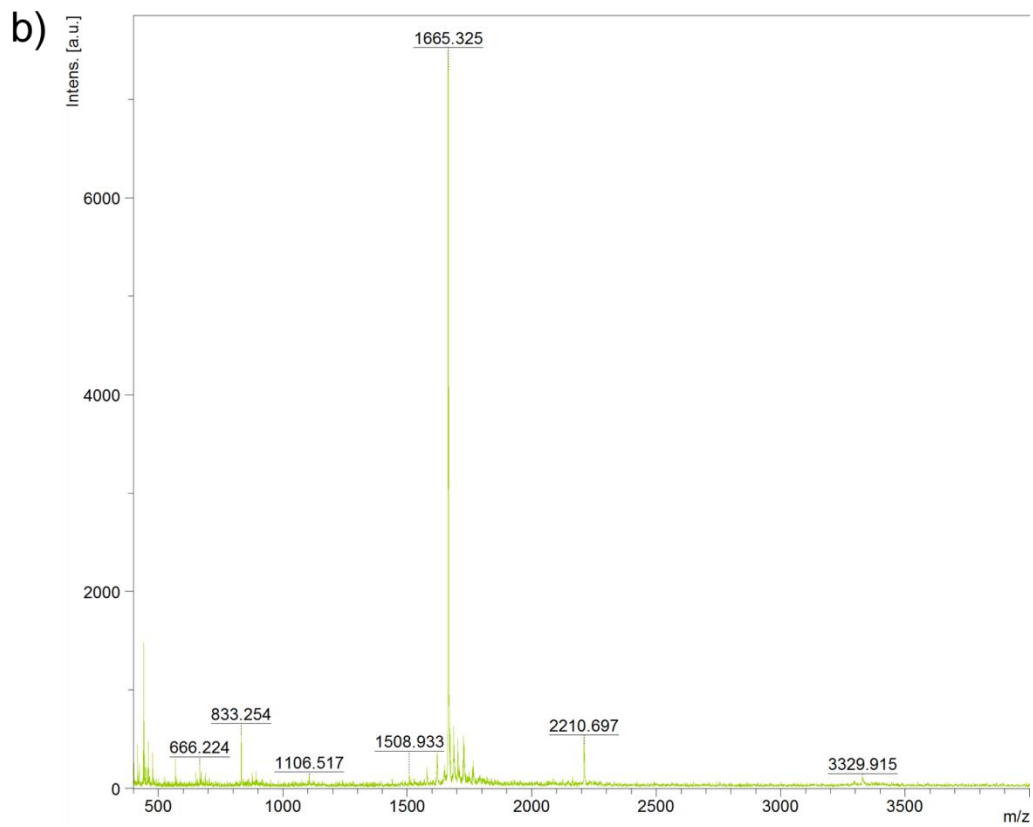
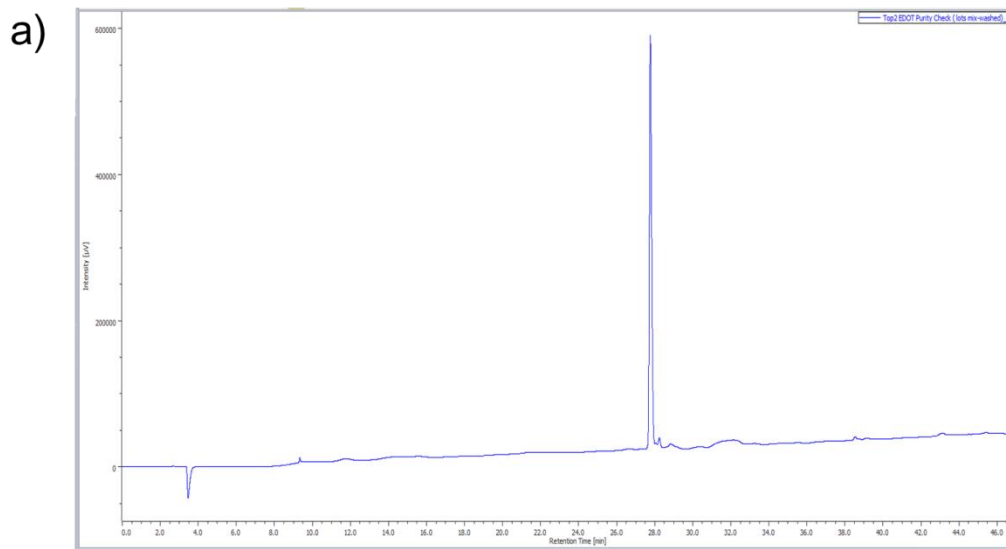


**Appendix 6.Synthesis productconfirmation by NMR analysis (a) Intermediate product (b)**

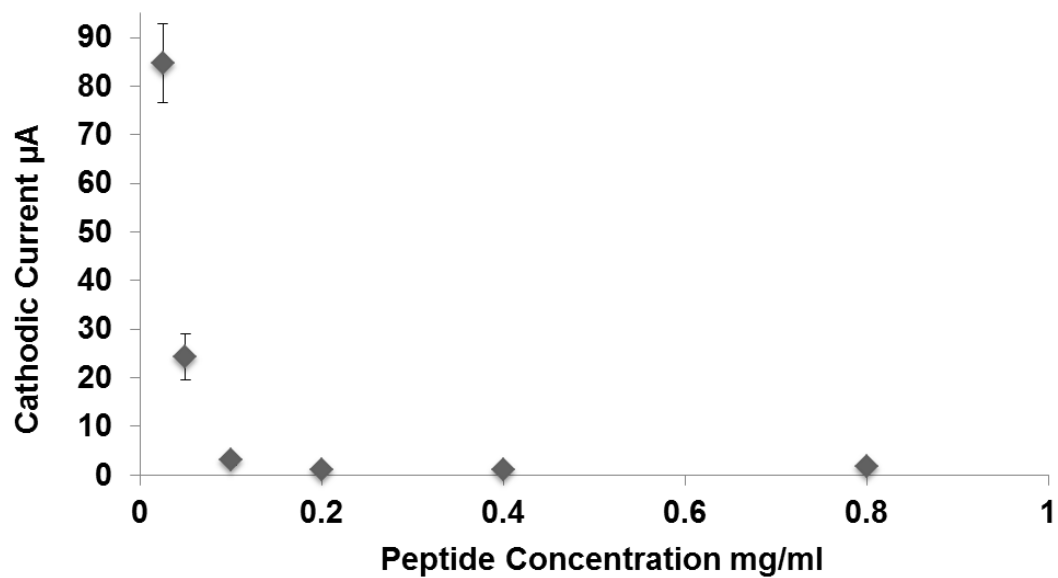
Final EDOT aa



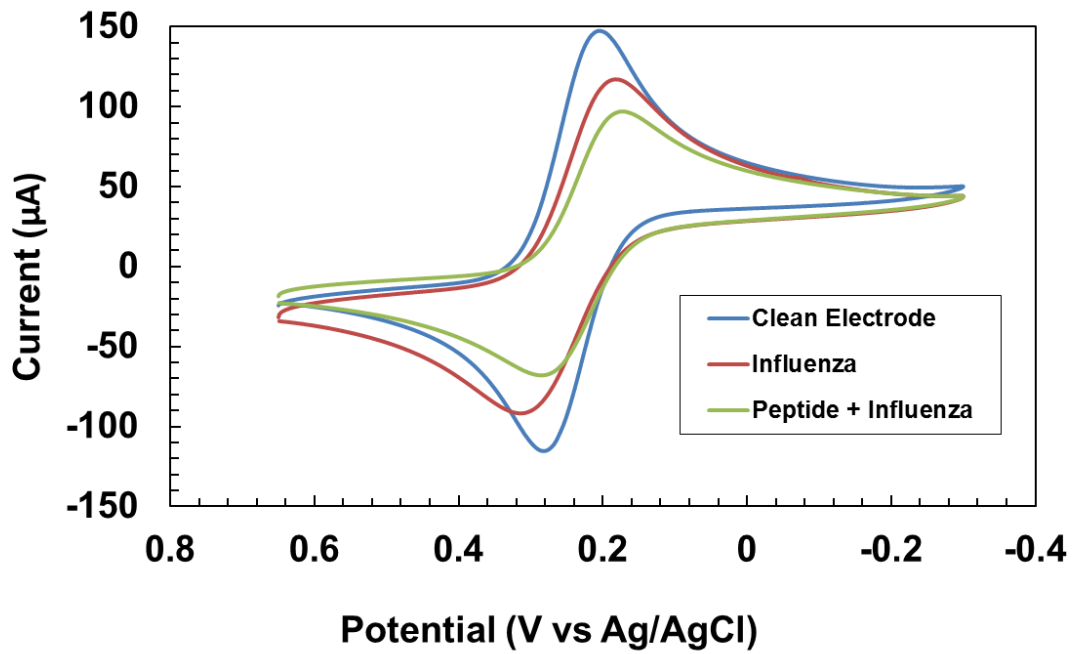
**Appendix 7.**Characterisation of Sequence 2 peptide a) HPLC analysis showing the absorbance at 220nm b) MALDI MS analysis (Calculated M+H=1663.99, experimental monoisotopic mass M+H= 1664.32). HPLC and MALDI indicate the purity of sequence 2 peptide and other peptides characterization also showed similar result.



**Appendix 8.** Averaged cathodic current after the polymerisation of various concentrations of Sequence 2 peptide on a gold electrode.



**Appendix 9.** Adsorption effect of the influenza viruses on working electrode at maximum concentration.



**Appendix 10.** P-values calculated using the Student's t-test for the detection limit of the influenza virus.

Influenza Virus ( $\mu\text{g mL}^{-1}$ )	6.25	12.5	25
P- Value	0.27	0.02	0.001

## LIST OF PUBLICATIONS

### Thesis work publication

- **Tara Bahadur K. C.**, Seiichi Tada, Liping Zhu, Takanori Uzawa, Noriko Minagawa, Shyh-Chyang Luo, Haichao Zhao, Hsiao-hua Yu, Toshiro Aigaki, Yoshihiro Ito. In vitro selection of electrochemical peptide probes using bioorthogonal RNA for influenza virus detection. *Chem. Commun.* **2018**, 54, 5201-5204.
- **Tara Bahadur K.C.**, Kanako Suga, Takashi Isoshima, Toshiro Aigaki, Yoshihiro Ito, Kiyotaka Shiba, Takanori Uzawa. Wash-free and selective imaging of epithelial cell adhesion molecule (EpCAM) expressing cells with fluorogenic peptide ligands. *Biochem. Biophys. Res. Commun.* **2018**, 500, 283-287

### Another publication during PhD course

- Yasodha Manandhar, **Tara Bahadur K.C.**, Wei Wang, Takanori Uzawa, Toshiro Aigaki, Yoshihiro Ito. *In vitro* selection of a peptide aptamer that changes fluorescence in response to verotoxin. *Biotechnology Letters*. **2015**, 37, 619-625.

### Poster presentation during PhD course

- **Tara Bahadur KC**, Yoshihiro Ito, Toshiro Aigaki and Takanori Uzawa. *Design of the system for in vitro production of single domain antibody fragment (Nanobody) from non-immunized library*. RIKEN Summer School, Tsukuba, Japan, 2016.
- **Tara Bahadur K.C.**, Hiroshi Abe, Yoshihiro Ito and Takanori Uzawa: *Selection of RNA aptamers to develop a sensor using rhodamine as a fluorogenic probe*. The 52<sup>nd</sup> Annual Meeting Biophysical Society of Japan, Hokkaido, Japan, 2014.